IDENTIFYING THE MALE MEIOTIC FUNCTIONS OF THE SPINDLE MATRIX PROTEIN MEGATOR

A thesis presented in partial fulfilment of the requirements for the degree of

Master of Science

in

Biochemistry

School of Fundamental Sciences
Massey University, Palmerston North,
New Zealand.

Daniela Bianchi

2022

Abstract

Male infertility is an emerging global concern and investigating the molecular events accountable for healthy sperm formation is crucial to the design of diagnostic assays and curative therapeutics. The work here proposed provides the first characterisation of the nucleopore protein Megator - the *Drosophila* homologue of the human Tpr - throughout the meiotic divisions responsible for sperm formation.

Megator/Tpr performs highly conserved roles at the nuclear pore complex during interphase. In somatic cells mitosis is also part of the spindle matrix, a structure that surrounds the spindle and promotes accurate chromosome segregation as a crucial component of the spindle assembly checkpoint (SAC).

Through genetic crossing, a combination of antibodies and fluorescent protein-expressing cells, Megator was found to localise in the spindle during meiosis I, consistent with forming a matrix. Moreover, Megator depletion by in vivo RNAi led to chromosome segregation defects suggesting loss of spindle assembly checkpoint function, as it has been seen in depleted mitotic cells. Remarkably, Megator was not detectable beyond background levels in meiosis II cells. Protein depletion in these cells induced abnormal chromatin masses and some cells were entirely devoid of nuclei. Examination of other spindle matrix proteins revealed that their distributions were altered by Megator depletion. These data suggest that Megator's roles in male meiosis are semi-conserved with mitosis.

Acknowledgements

First, I would like to thank my supervisor Matthew Savoian for his microscope expertise. My gratitude goes also to the Manawatu Microscopy and Imaging Centre (MMIC) for the free use of all the microscopy equipment.

I'm grateful to Dr Helen Fitzsimons for the use of her *Drosophila* Neurogenetics laboratory for the flies crossing, the donation of one of the *Drosophila* strains used in this study and, above all, for her kindness.

Thank you to the lab technicians in the MMIC: Yaniu and Raoul. Raoul, thank you for all the time you helped me in setting up the microscopes, and Yanyu... I did really enjoy our moments of laughing and "girls time". To all my friends in the statistics department whose academic achievements have been a great inspiration, thank you for your example. To my SFS colleagues, thank you for the time spent together ironically laughing over failed experiments or reassuring each other during these two tough years of research and pandemia.

I'm grateful to my family who has supported me, despite being an ocean and twelve hours distant. Last but not least, I cannot thank my lovely husband Gabriele enough for his patience, love and encouragement. I couldn't have done all of this without you.

Coronavirus statement

Due to the Covid-19 pandemic, Massey University closed from 23^{rd} March 2020 to 18^{th} May 2020 and 17^{th} August to 13^{rd} September 2021. This closure severely affected the research as not only it was not possible to produce any work during the lockdown, but any fly crossing and stock produced before the lockdown had to be destroyed. Once the university reopened, time was also lost to allow for the maintenance of the stock and the reset of the crossing needed for the experiments.

The pandemic also severely affected the supply chain for months, preventing the delivery of fundamental reagents such as transgenic flies and antibodies. When they arrived, some transgenic lines were dead or, after analysis through different microscopes, they had lost the transgene. Subsequent attempts to procure the flies were repeatedly unsuccessful. Further time was then lost when the fly stocks became ill and all experiments had to be halted until they fully recovered months later.

Finally, along with the delays, the project encountered a host of technical challenges in the live cells analysis, fundamental for the achievement of objective 3. These unexpected problems involved both the imaging conditions (radiation and cells becoming flattened) and drug efficacy (some drugs documented to be efficient in mitotic cells had no observable effect in meiotic cells).

As a result of these challenges, part of objective 1 was unable to be completed as planned and objective 3 was removed completely. Here below a detailed description of how these objectives were affected:

Objective 1: Due to both late delivery and time constraints, the examinations of the consequences of Megator depletion using additional independent RNAi strains were not performed. This was a key experiment as, despite the fly lines being previously validated, the use of additional RNAi lines would have identified if any of the observed phenotypes were due to off-target effects.

Objective 3: Following Megator depletion, the study of Megator's role in the spindle assembly checkpoint was entirely removed due to problems in the live cell imaging conditions. During the process of extraction from the testis, the spermatocyte cysts tend to disrupt upon manipulation. It has been observed that the disruption of the cyst affects the viability of the meiotic cells, resulting in low chances of cells going through both cell divisions. Also, despite the use of different culturing conditions, cells were constantly observed to flatten, resulting in the formation of aberrations in spindle morphology, making the examination of spindle and chromosome segregation defects impossible to be examined.

Table of contents

List of Figures

List of Tables

List of Abbreviations

APC/C	Anaphase-promoting complex/cyclosome
Apc2	Adenomatous Polyposis Coli tumor suppressor homolog 2
Bam	Bag-of-Marbles-protein
BDC	Bloomington *Drosophila* Center
Bub1	Budding uninhibited by benzimidazole 1
CCAN	Centromere-associated network proteins
Cdc20	Cell Division Cycle 20
Cdk	Cyclin Dependent Kinase
CENP-A	Centromere protein A
Chro	Chromator
CID	Centromeric histone H3-like protein identifier
Covid-19	Coronavirus disease
Crm1	Chromosomal maintenance 1
CySCs	Somatic cyst stem cells
DIC	Differential Interference Contrast microscopy
DNA	Deoxyribonucleic acid
dsRNA	Double Strand RNA
EGFP	Enhanced Green Fluorescence Protein
ERK	Extracellular signal-Regulated Kinase
FG-Nups	Phenylalanine-Glycine enriched nups
F1	First generation
G1	Gap 1

G2	Gap 2
GSCs	Germline Stem Cells
GTPase	Guanosine Triphosphatase
HGPS	Hutchinson-Gilford Progeria Syndrome
KD	Knock Down
kDa	Kilodalton
KMN	network Knl1/Mis12 complex/Ndc80 complex
K-fiber	Kinetochore fibres
KLP10A	Kinesin Like Protein 10A
KLP59C	Kinesin Like Protein 59C
kMTs	Kinetochore microtubules
KPNA2	Karyopherin alpha 2
Mad1	Mitotic Arrest Deficient protein 1
Mad2	Mitotic Arrest Deficient protein 2
MAPK	Mitogen-Activated Protein Kinase
MCC	Mitotic Checkpoint Complex
Mlp1	Myosin-like protein 1
Mlp2	Myosin-like protein 2
MTs	Microtubules
MTOCs	Microtubule Organizing Centers
Mtor	Megator
MI	First meiotic division
MII	Second meiotic division
NEB	Nuclear Envelope Breakdown
NLS	Nuclear Localization Signal
NPC	Nuclear Pore Complex
Nups	Nucleoporins
P1	Parental line
RISC	RNAInduced Silencing Complex

RNAi	RNA interference
ROI	Region of interest
SAC	Spindle Assembly Checkpoint
SAFs	Spindle Assembly Factors
SEM	Surface-epitope masking
shRNA	Short hairpin RNA
siRNA	Small interfering RNA
Skel	Skeletor
SMC1	Structural Maintenance of Chromosome protein 1
SPB	Spindle Pole Body
TFR	Total Fertility Rate
Tpr	Translocated Promoter Region
UAS	Upstream activation sequence
UV	ultraviolet
VDRC	Vienna *Drosophila* Resource Center
WHO	World Health Organization
1n	haploid cell
2n	diploid cell
+	plus ends microtubules
-	minus ends microtubules

Chapter 1

Introduction

1.1 The impact of infertility

Industrial revolutions, medical and agricultural progress have always contributed to the world's population growth. However, in the past few decades the rise of infertility across the globe has changed the scenario (Roser, 2014).

Fertility is defined as the ability to initiate a clinical pregnancy, while infertility is the couple's incapability to do so for more than 12 months (Zegers-Hochschild et al., 2017). In mammals, a pregnancy is established after fusion of male and female gametes: sperm and egg cells, respectively. The merging of these haploid cells (fertilisation) results in the formation of a cell with the full diploid complement (2n) of chromosome, characteristics of humans, most mammals and many animals.

Fertility is measured by the Total Fertility Rate (TFR), which counts the number of children per woman. A low TFR has an impact on the economy, as the reduction in childbirths creates countries demographically older and less economically competitive (International Strategic Analysis, 2019). The World Health Organisation (WHO) has included infertility in the list of the diseases that cause disability (Burns, 2007). Furthermore, it has also established a minimal 2.1 TFR to guarantee a successful replacement, which is defined as the population's ability to replace itself from an existing generation to the next one, without migration. A recent study estimated that in the

next 80 years there will be a lower TFR than the replacement rate for 183 countries (Vollset et al., 2020). Some of these, such as Japan, have already experienced a low TFR for decades (World Bank Data, 2019), while other countries are facing the issue for the first time after years of demographic expansion. New Zealand, for example, has recently reached its lowest TFR to date, 1.6 (StatsNz, 2021).

Based on TFR data, it was calculated that infertility affects almost 48.5 million couples (Ombelet et al., 2008; Mascarenhas et al., 2012; Agarwal et al., 2015). Aging, especially for women, combined with delays in choosing to have children is one of the reasons for couple infertility (Battaglia et al., 1996; Kidd et al., 2001). However, infertility can be linked to factors which negatively impact male and female gametogenesis (Vander Borght and Wyns, 2018). Therefore, both men and women can contribute to infertility (Turner et al., 2020). Agarwal et al. (2015) have indeed determined that males are responsible for $20 - 30\%$ infertility cases worldwide.

Male fertility and formation of genetically stable sperm (spermatogenesis) requires two specialised and sequential cell divisions, termed meiosis I (MI) and meiosis II (MII), followed by a complex postmeiotic development pathway (Holstein et al., 2003). When errors occur during meiotic chromosome segregation, the daughter cells can receive an improper number of chromosomes (aneuploidy), which can cause various degrees of infertility or results in genetically abnormal progeny post fertilisation (Boveri, 1902; Bond, 1987; Nagaoka et al., 2012).

Due to the great socio-economic burden caused by male infertility, a deeper understanding of the molecular events responsible for male meiosis is needed. These data will provide insights for the development of target therapies or prognosticative assays that will help tackle the problem of low global fertility rate.

1.2 *Drosophila* spermatogenesis: a model system for studying male fertility

Humans and flies share most of the key developmental stages occurring during sperm formation, or spermatogenesis (Preston et al., 2019) (Figures 1.1 A and B). Therefore, the fruit fly *Drosophila melanogaster* is one of the most used model systems (Bonilla and Xu, 2008). These insects are easily genetically manipulated and their short reproductive cycles create a high number of offspring within a few weeks. Additionally, the *Drosophila* has only four chromosomes: chromosome I as sex chromosome, two autosomes (chromosomes II and III) and a small chromosome IV which contains few genes. This limited *Drosophila* karyotype provides easier analyses of chromosome behaviour during cell division.

Drosophila spermatogenesis occurs in the testis, a 2 mm long tube with a diameter of approximately 100 microns (Bairati 1967 Figure 1.1 D). Each male *Drosophila* fly contains two coiled testes which are connected to the seminal vesicles and the ejaculatory duct (Figure 1.1 C). During *Drosophila* spermatogenesis, the involved cells progressively differentiate and migrate from the apical tip to the end of the testis, which facilitates their identification (Fuller, 1993) (Figures 1.1 D and F).

The *Drosophila* testis contains two different classes of stem cells: the germline stem cells (GSCs) and the cyst somatic cells (CySCs) (Bairati, 1967). The GSCs are surrounded by two CySCs and both these types of stem cells are maintained and anchored to the testis's apical tip by the hub cells, a cluster of non-dividing cells (Hardy et al., 1979). The spermatogenesis begins when GSCs start to divide.

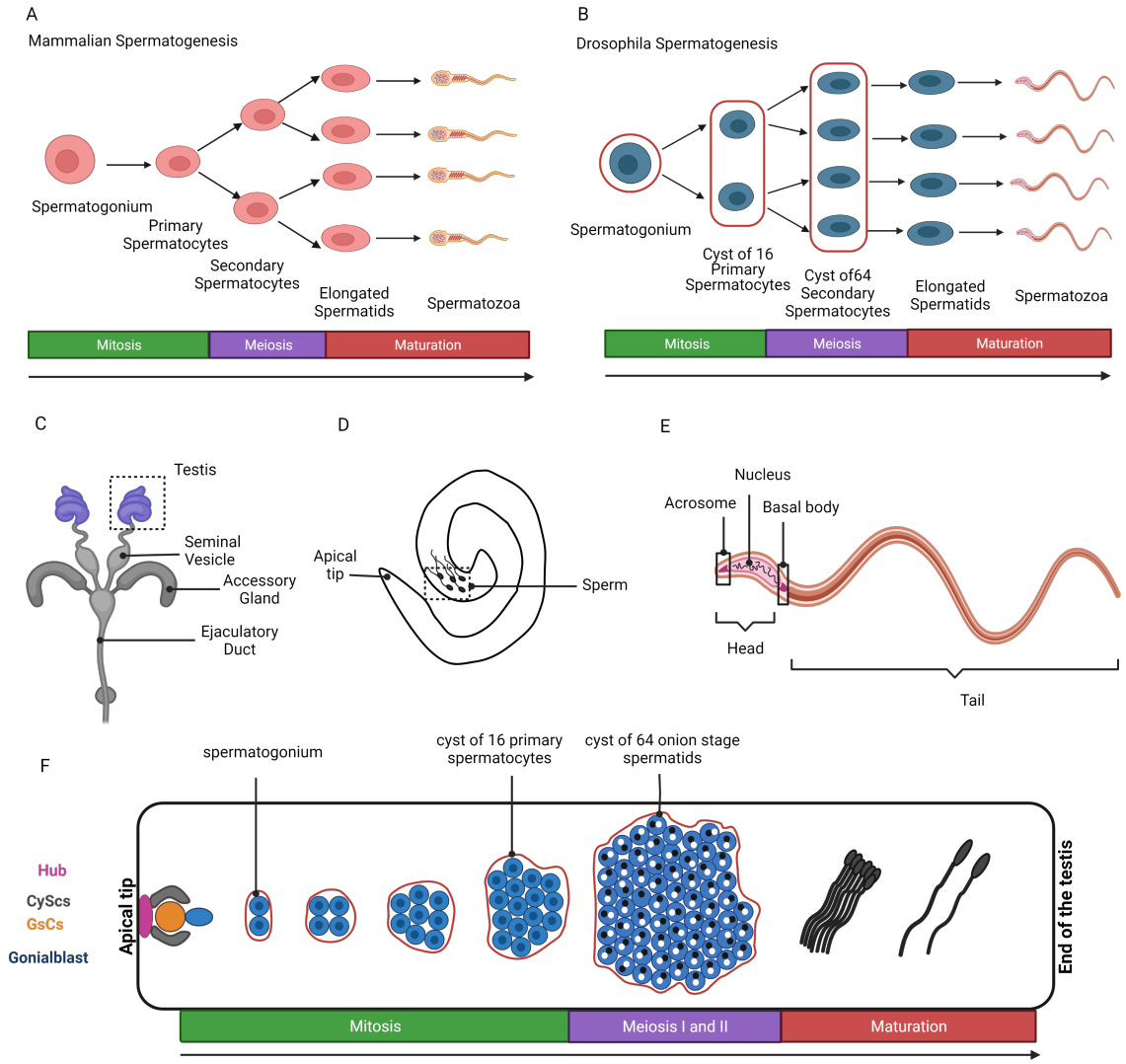

Figure 1.1: Overview of spermatogenesis. Similarities between mammalian (A) and *Drosophila* (B) spermatogenesis (original drawings, generated with reference to Preston et al. (2019)). Schematic representation of male *Drosophila* reproductive system (C), *Drosophila* testis (D) and mature *Drosophila* sperm (E). Detailed diagram of *Drosophila melanogaster* spermatogenesis (F). GsCs is the germline stem cells and CySCs is cyst somatic stem cells.

This process will generate two different types of cells. The first one will remain attached to the hub and will keep the stem cells feature (such as self-renewal Cuevas and Matunis 2011), the other sister cell – called a gonialblast - will start to differentiate asymmetrically through four cycles of mitosis to create cyst of 2, 4, 8 and then 16 interconnected spermatogonial cells, or primary spermatocytes. At the end of mitosis,

the primary spermatocytes undergo a single round of DNA replication and enter the first of the two meiotic divisions (Cenci et al., 1994).

After two cycles of meiosis (MI and MII), these now haploid (1n) spermatocytes differentiate into 64 individual 'onion-stage' spermatids interconnected by ring canals. Onion stage spermatids are characterised by a nucleus and equally sized round mitochondrial derivatives, called a nebenkern (Tates, 1971). The ratio nebenkern to nuclei is 1:1 and variations in the ratio can be used as read outs of meiotic errors (González et al., 1989). Following extensive morphological changes, such as nuclear elongation and tail formation, the 64 spermatids mature into spermatozoa (Tokuyasu et al., 1974).

During sperm individualisation, the last step of spermatogenesis, each spermatozoon become fully independent and migrates to the seminal vesicle, where it will be stored until fertilisation (Fuller, 1993; Tokuyasu et al., 1972a,b). If properly formed, a mature sperm is constituted by an elongated head, a flagellum or sperm tail, and a basal body connecting the two (Fabian and Brill, 2012), (Figure. 1.1 E). The head restrains the nucleus and the acrosome. While the latter is important for the fusion with the female gamete during fertilisation, the nucleus carries the genetic information or DNA. The sperm tail is essential for sperm movement and contains an axoneme core that extends from the basal body (Alberts et al., 2002; Mohri et al., 2012).

1.3 The GAL4/UAS system in *Drosophila melanogaster*

Drosophila melanogaster is a powerful model system to study gene expression and function due to its ability of being easily genetically manipulated through a large range of techniques. These have allowed the production of engineered mutants and transgenic fly lines, many of which are available from stock centres such as Vienna *Drosophila* Resource Center (VDRC), Kyoto *Drosophila* Genetic Resource Center and Bloomington *Drosophila* Center (BDC).

The GAL4/UAS system allows the expression or "driving" of an engineered target gene in a specific tissue or cell-type (Brand and Perrimon, 1993). This system is based on

the GAL4 yeast transcriptional activator under the control of an upstream activation sequence (UAS) and a target gene with a promoter containing a GAL4 binding site (Fischer et al., 1988). Depending on the absence or presence of its activator, the gene of interest will remain silent or get activated. The use of this system requires the creation of two lines of transgenic flies. One of these lines carries the GAL4 gene fused to a tissue specific enhancer, also called a GAL4 driver, the other line contains the UAS fused to the transgene of interest. The crossing of these two transgenic parental lines (P1) yield progeny (F1) that will express the GAL4 gene. This will bind to the UAS regulatory region, inducing the expression of the gene of interest (Figure 1.2 A).

The GAL4/UAS system is a versatile technique capable not only of driving the expression of a specific transgene, but also its tissue specific mediated knockdown. Indeed, it is an extremely valuable tool for the functional analysis of any unknown gene involved in a particular process in which its mutants are lethal (Qi et al., 2004). For this purpose, it is sufficient to combine the GAL4/UAS system's properties to the endogenic gene silencing pathway present in many eukaryotic cells and termed RNA interference (RNAi) (Fire et al., 1998; Paddison et al., 2002). This pathway is normally triggered by the production of double stranded RNA (dsRNA) after either bidirectional transcription or transcription of an inverted repeated sequence. The dsRNA formed is cut into small interfering RNAs (siRNAs) which are ultimately degraded by the enzyme Dicer and by the RNA-induced silencing complex (RISC) (Hannon, 2002; Wilson and Doudna, 2013). Therefore, in the GAL4/UAS mediated knockdown, the expression of a transgene specific inverted repeated sequence will create short hairpin RNAs (shRNAs) that will be cleaved by the Dicer machinery, inducing the transgene silencing (Figure 1.2 B).

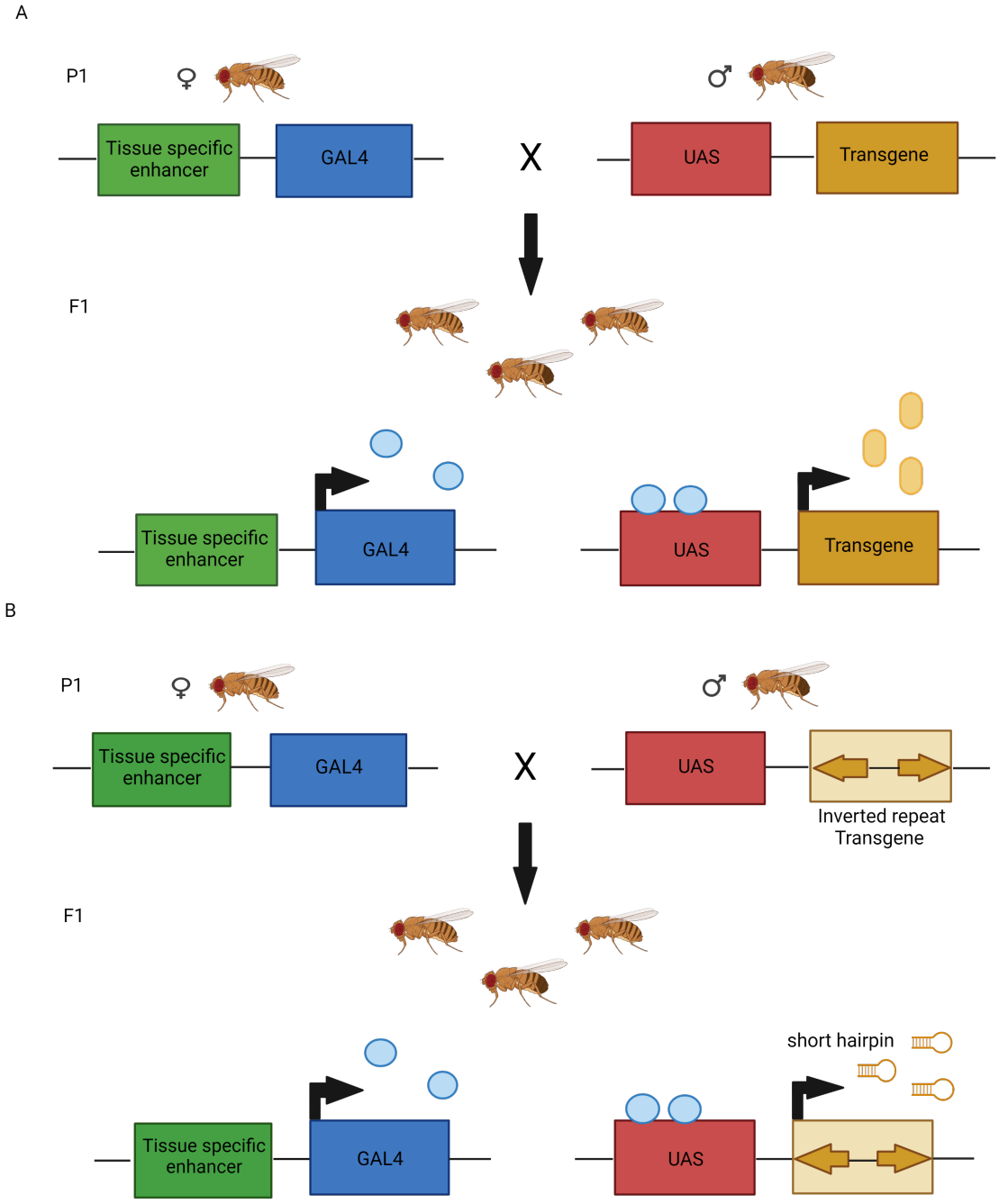

Figure 1.2: The GAL4/UAS system and in vivo gene knockdown in *Drosophila melanogaster*. The GAL4/UAS system allows the expression (A) and the silencing (B) of a desiderable transgene in a tissue-specific manner. In the parental lines (P1) *Drosophila* virgin female flies carrying the GAL4 gene fused downstream to a tissue specific enhancer (GAL4 driver) are crossed to male flies carrying an Upstream activation sequence (UAS) fused to the sequence of a target gene (A) or an inverted repeat sequence of the transgene (B). In progeny flies (F1), the product of GAL4 will bind to UAS, allowing the tissue specific expression of the transgene (A) or the formation of short hairpin RNAs for gene silencing (B). Original drawings generated with reference to Brand and Perrimon (1993) and Perrimon et al. (2010).

1.4 Overview of meiotic stages

Mitosis and meiosis are two types of division responsible for cell replication. While mitosis occurs in the somatic cells and ensures the production of two genetically identical daughter cells, meiosis occurs in the germline and ultimately halves the number of chromosomes in the gametes. This meiotic reduction is achieved by two consequent rounds of chromosome segregation, termed meiosis I (MI) and meiosis II (MII), without an intervening DNA replication event (Figure 1.3). While MII is similar to mitosis, MI is distinctive to the germ cells. All divisions are composed by different stages and their onset or phase-transition are mediated by fluctuation in the levels of cyclin and their Cdk1 complexes (Fisher et al., 2012; Webster et al., 2019).

Meiosis I starts with prophase I, which is characterised by extensive changes in the cells. Striking among these is the reorganisation of the microtubule (MTs) cytoskeleton. Unlike interphase, during early stages of division, these polymers of α- and β-tubulin are found exclusively radiating from the two centrosomes, the dominant sites of nucleation within the cell. The two centrosomes migrate around the still intact nuclear envelope to opposite sides through the actions of motor proteins (Whitehead et al., 1996; Gönczy et al., 1999; Robinson et al., 1999; Sharp et al., 1999, 2000; Mitchison et al., 2005).

During prophase I the DNA condenses into homologous chromosomes that become paired. Each condensed chromosome consists of four chromatids, two sisters from the replicated maternal chromosome and two from the father. Like mitosis, cohesion is responsible for adhesion between sister chromatids (Watanabe and Nurse, 1999; Buonomo et al., 2000; Watanabe, 2005; Nasmyth and Haering, 2009; Ishiguro et al., 2011), while in many systems DNA recombination is responsible for pairing between the homologoues (Von Wettstein, 1971; Webber et al., 2004). In addition to compacting, each homologous chromosome begins to assemble a pair of kinetochores, protein super-complexes positioned at the two opposingly positioned centromeres. Due to their diverse composition, kinetochores perform the key events of division and are responsible

for chromosome movement as well as for cell cycle exit (described in section 1.5.3).

As cells transit into prometaphase I, microtubules radiating from the two centrosomes penetrate into the nuclear space in the vicinity of the chromosomes. At prometaphase I, as MTs contact the kinetochores, they are "captured" leading to attachment of the kinetochore/chromosome and spindle formation (Kirschner and Mitchison, 1986; Hayden et al., 1990; Rieder and Alexander, 1990). The opposing placement of the two MTs-nucleating centrosomes along with that of each bivalents' centromere-bound kinetochores drives the formation of a bipolar spindle, capped at each end by a centrosome. Each kinetochore progressively acquires more MTs from its closest centrosome, leading to a robust bundle of kinetochore fibre that exclusively attaches each kinetochore in the bivalent to one pole (Holy and Leibler, 1994; Khodjakov et al., 2003; Maiato et al., 2004). This leads to a "tug-of-war" of forces towards each spindle pole as chromosomes "congress" to the spindle equator (Kapoor et al., 2006; Cai et al., 2009).

Alignment of all of the chromosomes at the equator marks metaphase I. If all of the kinetochores have become properly attached to the spindle, cells satisfy the spindle assembly checkpoint (SAC), a regulatory system which halts the cell cycle in case of improper attachment, and advances into anaphase I (described in section 1.5.2). At onset of anaphase I, the cohesin complexes are removed only from the chromosome arms (Waizenegger et al., 2000; Watanabe, 2005). Therefore, the chromosomes are pulled away from each other (anaphase A) and then polewards, allowing spindle elongation (anaphase B).

The last two stages of meiosis I are telophase I and cytokinesis I. During telophase I chromosomes decondense and nuclei reform. At cytokinesis I the cytoplasm is also partitioned through the formation and constriction of the cytoplasm by an acto-myosin contractile ring that assembles at the spindle equator (Matsumura, 2005). Thus, at the end of MI, the two daughter cells carrying half of the original genetic content are ready to enter the second meiotic division.

Meiosis II repeats the same events as meiosis I. During prophase II the chromatin

condenses into distinct chromosomes each of which now consists of two sister chromatids. At prometaphase II, spindle formation occurs allowing the chromosomes to move as kinetochores interact with microtubules. Their congression to the equator identifies the beginning of metaphase II. During anaphase II, the remaining cohesin complexes are removed allowing for chromatid separation and segregation (Watanabe and Nurse, 1999). This is followed by chromosome decondensation in telophase II and the formation of daughter nuclei with the subsequent cleaving of the cytoplasm during cytokinesis II.

The net result of MI and MII is the formation of four haploid daughter cells which will ultimately be transformed into eggs or sperm, depending on the tissue.

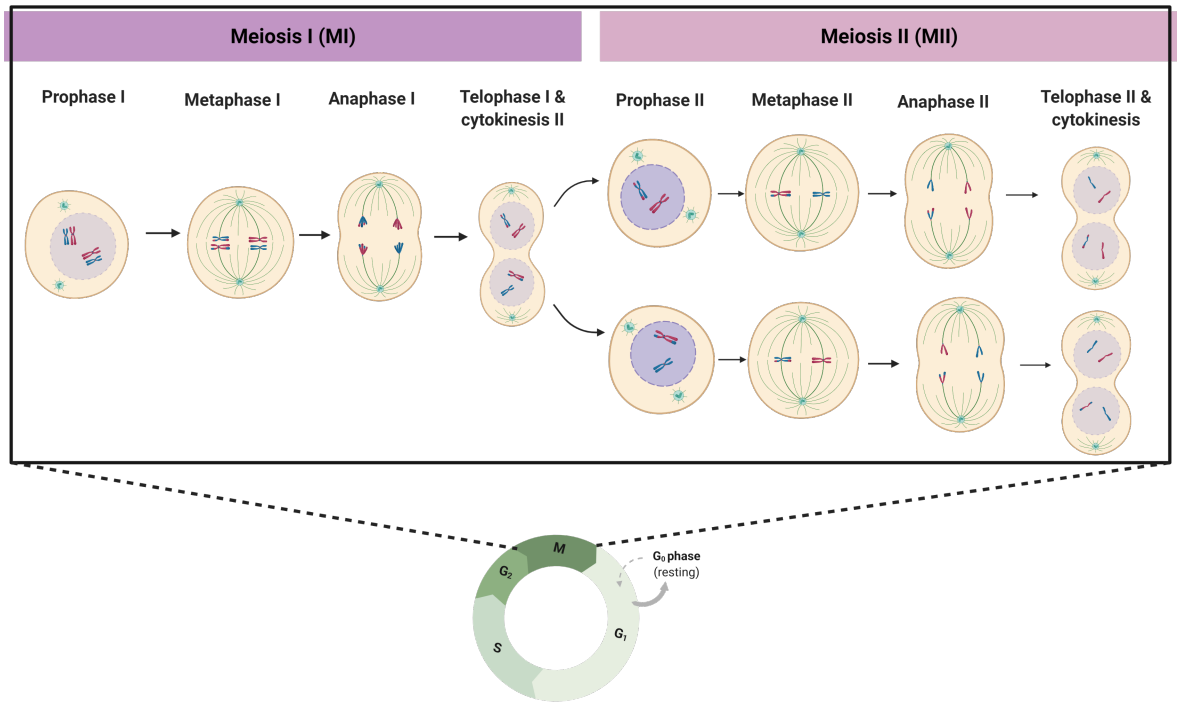

Figure 1.3: Schematic representation of meiotic stages. Homologous chromosomes are separated during meiosis I (MI) and chromatids are separated in meiosis II (MII). See text for more info. G1 is for Gap1 or cellular growth phase. S represents the synthesis phase where the genome is replicated. G2 or Gap2 is the second cellular growth phase, needed before meiosis (M).This cartoon represents stages of generic (not male *Drosophila* flies) meiosis.

1.4.1 Exceptional meiotic features in male *Drosophila melanogaster*

As described in section 1.2, meiosis in male *Drosophila* flies begins after the production of cyst of 16 interconnected primary spermatocytes. After the last cycle of mitosis, DNA replication occurs for 3 hours, followed by an extensive growth period (G2) of almost 80 hours, during which the cells increase their volume and produce the cellular content needed for the progression into spermatogenesis (Cenci et al., 1994).

For almost the entirety of prophase I, the DNA is decondensed and chromatin masses occupy the nuclear lumen. Homologous chromosomes are believed to be paired in some way during early prophase I, but the mechanisms responsible for pairing remain subject to debate (Vazquez et al., 2002). By contrast, it is well established that recombination and, by extension, crossing over events or chiasma do not occur in male *Drosophila* flies (Morgan, 1914; Hawley, 2002). Furthermore, the "conjunction" of the homologoues may be genetically controlled (Thomas et al., 2005).

The cohesin complexes in *Drosophila*, which are vital for chromosomes (during MI) and chromatids (in MII) segregation, do not contain the specific and conserved meiotic core subunit Rec8. Instead, *Drosophila* appears to rely on two unique cohesion proteins (McKee et al., 2012; Yan and McKee, 2013). In addition, male meiosis in *Drosophila*, like most insects, is characterised by having a semi-open division. Probing by centrosome-derived microtubules (for kinetochore interaction at prometaphase) occurs through large holes in the envelope that occur near the centrosomes. This differs from many other animals, including mammals, where the nuclear envelope completely disintegrates during spindle formation. In *Drosophila* the residual envelope membranes surround the spindle as a "spindle envelope" that may serve to concentrate molecules within the spindle region (Yao et al., 2012).

1.5 Mechanism and components of chromosome movements during cell division

Successful chromosome segregation in cell division occurs through the regulated interplay of a spindle and chromosome-bound kinetochores (Rieder and Salmon, 1998) (Figures 1.4 A and B).

Microtubules are inherently dynamic structures that can grow when subunits of tubulin are added (polymerisation) or shrink when removed (depolymerisation) (Gorbsky et al., 1988; Mitchison, 1989; Zhai et al., 1995). Microtubules within the spindle have two ends: the ones which protrude away from their nucleation site are called plus ends (+), and the others are the minus ends (-). In cells, MTs are nucleated from the microtubule organising centres (MTOCs), commonly the centrosomes, organelles consisting of centrioles and an amorphous cloud of nucleating material (Bornens and Azimzadeh, 2007; Blachon et al., 2008; Kim et al., 2013; Arquint and Nigg, 2016).

Three classes of microtubules are present in the spindle: astral microtubules which extend from the centrosomes to the cell cortex, interpolar microtubules that radiate towards the opposite pole, sustain the spindle structure and, through interaction, push the spindle poles apart during anaphase B. The last class of spindle microtubules are called kinetochore microtubules (kMTs) and are organised into bundles or fibres (k-fiber) which are bound by kinetochores, (Figure 1.4 A).

Kinetochores are key determinants of cell division. They perform three major functions: (i) attachment to the spindle, (ii) generating or transducing the forces for chromosome movement and (iii) serving as a catalytic platform for the spindle assembly checkpoint (SAC). These functions are possible due to its diverse composition and structure (De Wulf et al., 2003; Przewloka and Glover, 2009; Akiyoshi and Gull, 2014) (Figure 1.4 C and D).

Traditionally kinetochore has been defined as having an inner and outer plate enriched in over 100 proteins of different classes (Musacchio and Desai, 2017) (Figure 1.4 B).

The inner plate - composed of the centromere-associated network (CCAN) - binds centromeric chromatin proteins, or nucleosomes, which are characterised by unconventional histones (Earnshaw and Rothfield, 1985; Mellone et al., 2011). The kinetochore's outer plate - generally called the KMN network (Knl1/Mis12complex/Ndc80) - binds the plus ends kMTs and recruit the SAC proteins (Cheeseman et al., 2006).

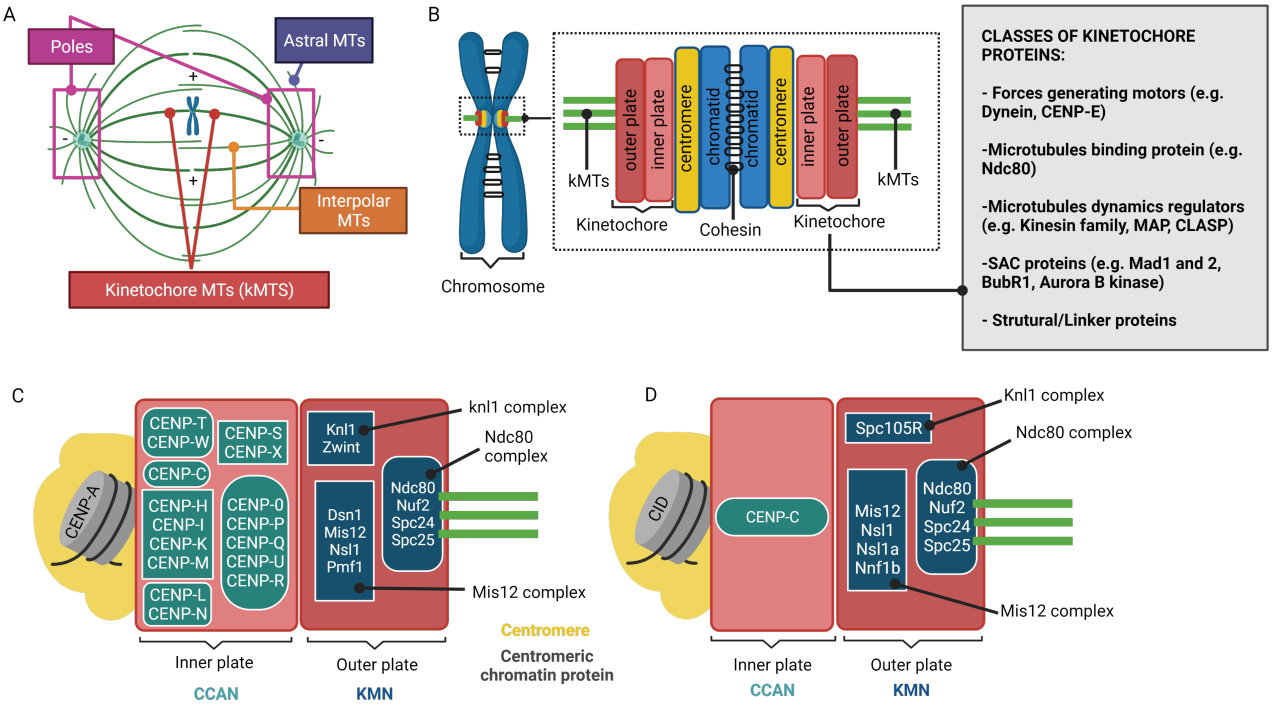

Figure 1.4: Spindle and kinetochore architecture during cell division. Three classes of microtubules (MTs) radiate from the centrosome to assemble the bipolar spindle (A). The kinetochore microtubules (kMTs) bind the centromere region of the chromosomes through the kinetochore, a complex structure of inner and outer plate of different classes of proteins (B). Examples of kinetochore compositions: humans (C) and *Drosophila* (D). Original drawings created with reference to Singleton (2016) and Musacchio and Desai (2017).

1.5.1 Kinetochore functions: spindle attachment

In centrosome-containing cells such as those of the male germline and soma, spindle formation initiates at prometaphase.

Dynamic astral MTs probe the cell until contacting a kinetochore (Kirschner and Mitchison, 1986). Light and electron microscopy studies have shown that the first

contacts occur laterally with a single MT contracting and extending beyond kinetochore (Hayden et al., 1990; Merdes and De Mey, 1990; Rieder and Alexander, 1990; Tanaka et al., 2005). The presence of the minus end directed motor dynein on the kinetochore causes rapid gliding of the chromosome towards the centrosome (Rieder and Khodjakov, 2003).

Attachment to both centrosomes and biorientation requires that the chromosome move away from the bound centrosome or spindle pole, towards the unattached centrosome. This is accomplished by a variety of mechanisms all of which utilise MT plus end directed kinesin (Desai et al., 1999; Mimori-Kiyosue et al., 2005; Manning et al., 2007; Brouhard et al., 2008; Al-Bassam et al., 2010; Walczak et al., 2013). This facilitates MT capture by the unattached kinetochore and a proper attachment of each kinetochore to an opposing centrosome or spindle pole. Attachment of each kinetochore in a bivalent (MI) or sister chromatid (MII, mitosis) is necessary for equal DNA distribution (Goldstein, 1981; Lee et al., 2000; Petronczki et al., 2003; Corbett et al., 2010).

Although the layout of the kinetochores and bipolar nature of the spindle help to ensure the exclusive attachment of each kinetochore to a single and opposing spindle pole (amphitelic attachment, Figure 1.5 A) errors can still occur.

These aberrant attachments are called syntelic, monotelic and merotelic. Syntelic attachments occur when both kinetochores are bound to the same pole (Figure 1.5 B). In monotelic attachments, just one kinetochore is linked to one pole (Figure 1.5 C), while in merotelic attachment a single kinetochore is attached to both poles (Figure 1.5 D). Anaphase onset in the presence of such errors would lead to genetic instability. Accordingly, a highly conserved surveillance system dubbed "the spindle assembly checkpoint" (SAC) has evolved to inhibit anaphase onset.

The mechanisms that perceive and correct the improper kinetochore-microtubules attachment have been the subject of much investigation. Studies in mantids (Li and Nicklas, 1995, 1997) and *Drosophila* spermatocytes (Chaurasia and Lehner, 2018) revealed that at the most fundamental level, it is driven by mechanical tension sensing:

a lack of tension on kinetochores, as it occurs during most malorientations, prevents anaphase onset until it is correct. However, merotelic malorientations, which introduce tension, are invisible to the SAC and a prominent cause of aneuploidy (Cimini et al., 2001, 2002). More recent studies have identified the molecular players and events which this pathway operates (Tanaka et al., 2002; Gruneberg et al., 2004; Kapoor et al., 2006; Liu et al., 2009).

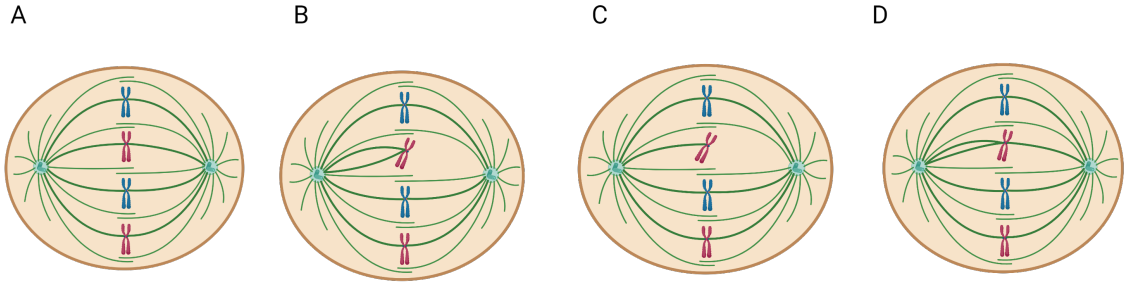

Figure 1.5: Schematic representation of kinetochore-microtubules attachment during cell division. During amphitelic attachment each kinetochore is bound to kinetochore microtubules nucleated from each pole (A). In syntelic attachment both kinetochores are bound to the same pole (B). During monotelic attachments a single kinetochore is bound to one pole (C). In merotelic attachments a kinetochore is bound to both poles (D).

1.5.2 Kinetochore functions: Spindle Assembly Checkpoint activity

The spindle assembly checkpoint (SAC) is a surveillance system that ensures genomic stability in the daughter cells during cell division (Musacchio and Salmon, 2007; Foley and Kapoor, 2013; Sacristan and Kops, 2015). First discovered in yeast, it is highly conserved across eukaryotes (Musacchio and Hardwick, 2002; Musacchio and Salmon, 2007; Kops et al., 2020). It eludes the premature disjoining of the chromosomes, thus aneuploidy, by preventing the activation of the Anaphase Promoting Complex/Cyclosome (APC/C), a multi-subunit ligase that leads to the degradation of multiple targets such as Securin for cohesion removal and the cyclins thereby leading to chromosomes segregation and cell division exit (Musacchio and Salmon, 2007).

Under normal conditions, the presence of a single unattached kinetochore is sufficient to trigger a robust response of the SAC which induces the so-called "wait anaphase" signal, until correction of the improper kinetochore attachments (Rieder et al., 1995). In agreement with this, disruption of the spindle leads to prolonged arrest (Hoyt et al., 1991; Rieder and Maiato, 2004), while loss of SAC protein function leads to exit and aneuploidy (Hardwick et al., 1999; Shonn et al., 2003).

The precise mechanism by which the SAC operates remains to be elucidated. Tanaka et al. (2002) and Liu et al. (2009) have shown that these mechanical tensions involve Aurora B, a serine-threonine kinase found at the centromeres from prophase to metaphase (Gruneberg et al., 2004). Unattached or improperly attached centromeres lack tension, which places Aurora B proximal to the kinetochore. This position triggers the Aurora B kinase dependent phosphorylation of KMN network proteins with a consequent loss of microtubules binding. By contrast, bipolar amphitelic attachment generates tension that makes Aurora B kinase distal to the kinetochore and unable to phosphorylate key sites needed for MTs release. In addition, this tensionless placement of Aurora B makes it available to phosphorylate other substrates.

Unattached kinetochores or attachments that fail to generate tension triggers the recruitment of specific SAC proteins to form the APC inhibiting MCC (mitotic checkpoint complex). This complex is constituted by the Cdc20 (Cell division cycle 20), Mad2 (mitotic-arrest deficient 2) and the Bub proteins (budding uninhibited by benzimidazole) Bub3 and BubR1 (Sudakin et al., 2001). Its formation is catalysed by Mad1, another SAC protein, that recruits Mad2 at the kinetochore for SAC signal amplification (Mapelli and Musacchio, 2007). The amplification is also triggered by the Aurora B kinase through mechanical kMts tension signaling (Tanaka et al., 2002; Liu et al., 2009) and depends on the recruitment of the SAC protein Mps1 (Monopolar Spindle 1), which phosphorylates the KNL1 proteins present at the outer plate of the kinetochore (Saurin et al., 2011).

After the MCC assembly, the complex inhibits the APC/C making it inactive and unable to add polyubiquitin chains to both Securin and Cyclin B for their degradation by the proteasome (Fang et al., 1998; Wassmann and Benezra, 1998; Morrow et al., 2005). This results in the Securin being linked to the protease Separase which is unable to remove the cohesin complex that held the chromatids, thus preventing their disjunction (Thornton and Toczyski, 2004) (Figure 1.6 B). By contrast, when the chromosome biorientation and kMTs tension are established, the MCC is shed. Therefore, Cdc20 is able to bind the APC/C, triggering its activation. Securin and Cyclin are then degraded which promote the chromatid disjunction and anaphase transition (Figure 1.6 A).

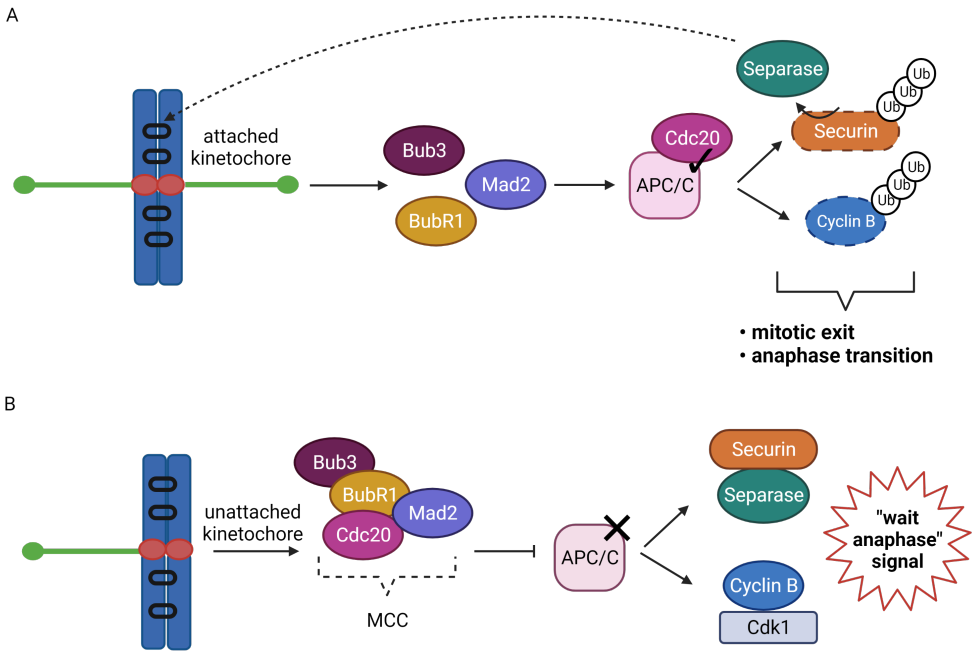

Figure 1.6: Schematic representation of the spindle assembly checkpoint. When sister kinetochores become bioriented, the mitotic checkpoint complex (MCC) is removed (A). Cdc20 binds and activates the Anaphase Promoting complex/Cyclosome (APC/C) with consequent Securin and Cyclin B ubiquitination. These events promote chromatid disjunction upon removal of the cohesin (black circle), and anaphase transition. Unattached kinetochore (B) triggers the recruitment of SAC proteins to form the MCC. MCC inhibits the APC/C and prevents consequent degradation of Separase and CyclinB. In this state, the cell cycle is halted until errors in attachments are corrected. Original drawing generated with reference to Musacchio and Hardwick (2002)

.

Most of the SAC proteins discovered in mitosis are conserved in many eukaryotes and their localisation/functions have been studied for decades (Musacchio and Hardwick, 2002; Vleugel et al., 2012). By contrast, SAC proteins in meiosis have been studied just recently. In budding yeast, the loss or disruption of Mad1 and Mad2 during meiosis leads to high rates of chromosome segregation defects, when compared to mitosis (Hardwick et al., 1999; Shonn et al., 2003). Furthermore, time-lapse microscopy analysis and MTs depolymerisation experiments by Savoian et al. (2000) and Rebollo and González (2000) revealed complete segregation failure, proving for the first time the activity of a meiotic spindle checkpoint in *Drosophila*. Furthermore, the meiotic spindle checkpoints are generally believed to be feeble (Malmanche et al., 2006; Buffin et al., 2007; Gorbsky, 2015). Therefore, in *Drosophila* spermatocytes the meiotic SAC activity operates with less efficiency or be regulated by different mechanisms than mitosis (Church and Lin, 1988).

1.5.3 Kinetochore functions: generating or transducing the forces for chromosome segregation

The molecular details that dictate chromosome segregation are not fully understood. Through studies in mitosis, what is known is that the chromosome movements are the results of forces generated by different elements. Due to the binding and insertion of the kMT plus ends into the kinetochore's outer plate (Goldstein, 1981; Church and Lin, 1988), poleward movement requires MT depolymerisation.

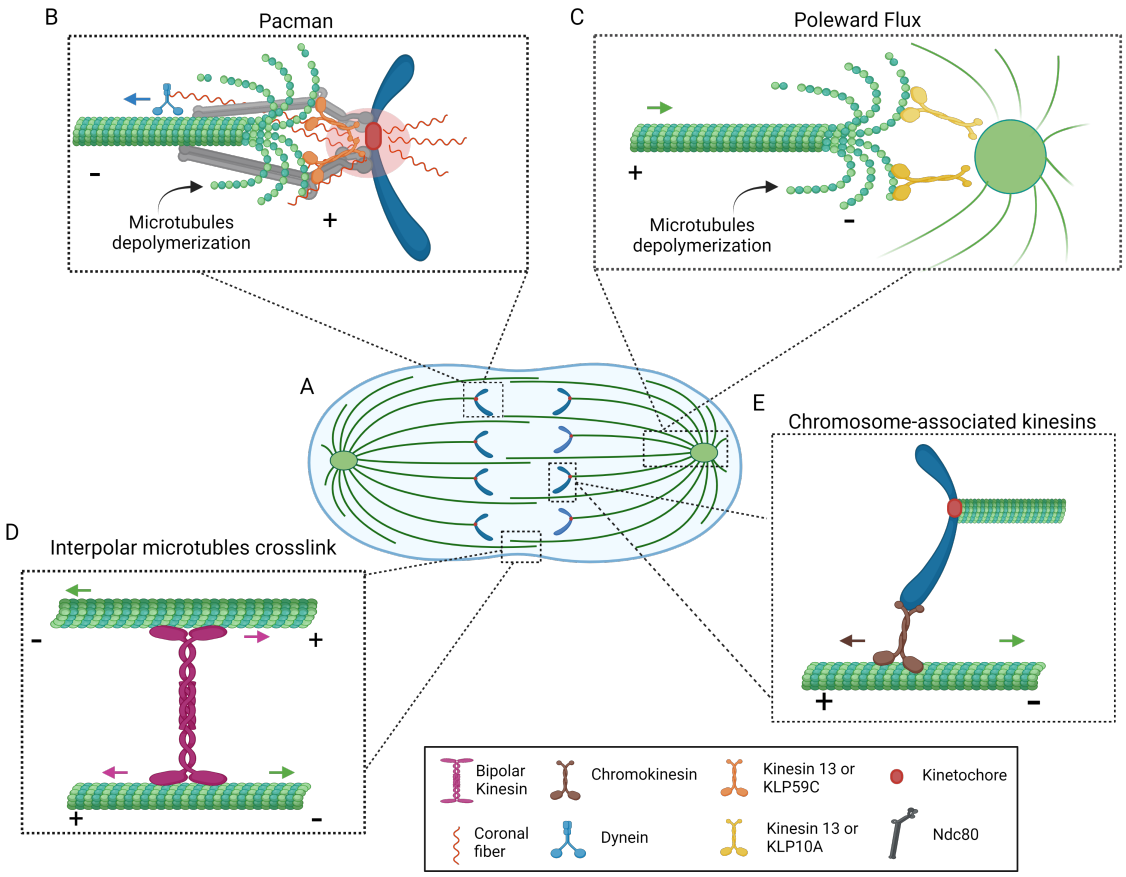

Figure 1.7: The poleward forces generated during anaphase. Anaphase is characterised by the disjunction of the chromatids and their movement polewards through the kinetochore-bound microtubules (A). In the Pacman model, the kinesins 13 (or KLP59C in *Drosophila*) trigger the depolymerisation of the kMTs plus-ends, while the motor protein dynein generates the pulling forces on chromosomes by walking towards the kMTs minus ends (B). In the Poleward flux model: the kMTs' minus ends at the spindle poles are depolymerised by the kinesin 13, or by the kinesin like KLP10A in *Drosophila* (C). Interpolar microtubules sliding through bipolar kinesins (D) and the action of chromokinesins (E) favor the chromatids movement poleward and spindle elongation during anaphase B. Original drawings generated with reference to Rogers et al. (2004).

At the onset of anaphase, the plus ends polymerisation activity decreases (Rogers et al., 2004) and while the kinesin 13 (KLP59C in *Drosophila*) trigger the kMts depolymerisation, the minus end directed motor protein dynein "walks" on kinetochore microtubules, generating pulling forces on the chromosomes, (Pfarr et al., 1990; Steuer et al., 1990; Antonio et al., 2000; Li et al., 2007). This process is called the Pacman model (Cassimeris et al., 1987) (Figure 1.7 B). Perturbation of dynein in vertebrates

(Vorozhko et al., 2008) and *Drosophila* embryos (Sharp et al., 2000) has displayed attenuation in the rate of chromosome poleward segregation during mitosis. This attenuation has been also indirectly observed in meiosis, using dynein binding mutant *Drosophila* spermatocytes (Savoian et al., 2000).

During anaphase, microtubules also start to be shortened at their minus ends, through removal of tubulin subunits by kinesin 13 (KLP10A in *Drosophila*) present at the poles, in a process called Poleward flux (Figure 1.7 C). Photobleaching studies in *Drosophila* spermatocytes have shown that Flux-Pacman model is conserved in meiosis (Gorbsky et al., 1988; Sharp et al., 2000; LaFountain Jr et al., 2004; Savoian, 2015). Other forces that assist chromosome movement are generated by the crosslink and consequent sliding of the interpolar microtubules through bipolar kinesins (Figure 1.7 D) and the binding of the interpolar microtubules with chromosome-associated kinesins (Figure 1.7 E). These events mark the beginning of spindle elongation or anaphase B.

1.6 The Spindle matrix

Several pieces of data have suggested that the spindle does not act as an independent or isolated cell division structure. Electron microscopic analysis of isolated sea-urchin mitotic spindles showed the presence of additional components that are different to spindle microtubules, and which appear to remain in their absence and help maintain spindle structure (Goldman and Rebhun, 1969; Leslie et al., 1987). In diatoms, additional components were able to aid chromosome segregation even after microtubules depolymerisation by colchicine (Pickett-Heaps et al., 1980). Such observations point toward the existence of a spindle matrix, a structure surrounding the spindle that could interact with microtubules and, if disrupted, compromise the spindle function (Pickett-Heaps et al., 1984, 1996).

Microsurgery studies using ultraviolet microbeams in mitotic newt fibroblasts (Spurck et al., 1997), *Drosophila* S2 cells (Maiato et al., 2004) as well as meiotic crane fly spermatocytes (Sillers and Forer, 1983; Forer et al., 1997, 2003) led to the hypothesis that

the matrix could have elastic properties that affect chromosome segregation. In these latter studies, ultraviolet microbeams were used to sever a k-fiber immediately before anaphase onset (Figure 1.8 A). Despite cutting their spindle attachments in half, the chromosome still segregated as the kinetochore associated microtubules "stubs" translocated polewards (Figure 1.8 B). Moreover, the velocity of the chromosome attached to the kinetochore stubs increased compared to the chromosomes with uncut k-fibers (Forer et al., 2015).

An alternative explanation proposes that following kMTs severing, the motor protein dynein is recruited to the minus end of the kinetochore stubs where it interacts with adjacent non-kMTs to drag the kMTs stub poleward (Figure 1.8 C). Consistent with this, inhibition of dynein prevents kMTs stub movement (Sikirzhytski et al., 2014). However, these findings have been recently challenged (Forer et al., 2018). Thus, the role of the matrix in chromosome movement remains unclear.

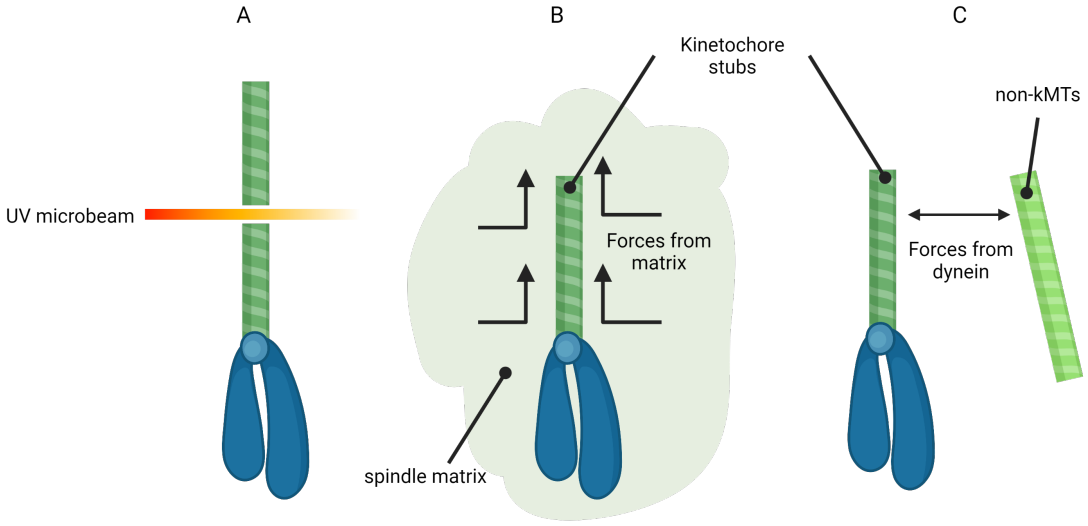

Figure 1.8: Chromosome movement after microtubules severing. Kinetochore microtubules (kMTs) are severed by ultraviolet microbeam (UV) creating kinetochore stubs that are no longer attached to the spindle poles (A). In the spindle matrix model, the poleward movement of kinetochore stubs (and chromosomes), is promoted by forces generated by the spindle matrix, rather than microtubules (B). In the dynein model, this motor protein gathers to the minus end of the kinetochore stubs, interacts with near microtubules to propel the poleward chromosome movement (C). Original drawing generated with reference to Forer et al. (2018).

The composition of the matrix is still elusive. Studies in different systems and cell types have revealed a host of molecules that collect around the spindle. Some spindle matrix proteins includes Lamin B (Hayes, 2006; Tsai et al., 2006), cell cycle regulators like Cyclin B and Polo kinase (Yao et al., 2018), actin and Titin (Janmey et al., 1995; Chang et al., 2005; Fabian et al., 2007a,b; Pickett-Heaps and Forer, 2009). Others are nucleoporins (Nups), proteins of the Nuclear Pore Complex (NPC) (Joseph and Dasso, 2008; Katsani et al., 2008; De Souza et al., 2009; Hashizume et al., 2010).

In *Drosophila*, co-immunoprecipitation experiments have identified multiple interacting proteins subsequently shown be part of the spindle matrix: Megator (Lince-Faria et al., 2009), Chromator (Rath et al., 2004), Skeletor (Walker et al., 2000), EAST (Qi et al., 2005) and Asator (Qi et al., 2009). These proteins form a spindle-like structure during prophase which persists at metaphase, even after microtubules are removed by drug treatment. Moreover, their perturbations through RNAi mediated proteins depletions lead to malformed microtubules and chromosome missegregation (Walker et al., 2000; Rath et al., 2004; Qi et al., 2005; Ding et al., 2009; Lince-Faria et al., 2009). However, only one has been identified so far as a spindle matrix component across several specices: the nucleoporin Tpr/Mlp1/Mlp2/Megator (Cordes et al., 1997; Zimowska et al., 1997; Qi et al., 2004; De Souza et al., 2009).

1.6.1 The conserved spindle matrix protein Tpr/Mlp1/Mlp2/Megator

Nucleoporins (Nups) are a highly conserved family of 30 different proteins that assemble into the well-characterised nuclear pore complex (Grossman et al., 2012) (Figure 1.9 A and B). In this complex they act as a selectively permeable barrier for the cargoes trafficking between nucleus and cytoplasm (Anderson and Hetzer, 2007; Wente and Rout, 2010; Zhang et al., 2010; Grossman et al., 2012). However, recent research has highlighted that nucleoporins have multiple functions such as gene regulation (Ishii et al., 2002; Brickner and Walter, 2004; Taddei et al., 2006), DNA repair (Galy et al.,

2004; Zhao et al., 2004) and cell division (Hashizume et al., 2010; Lussi et al., 2010; Mishra et al., 2010; Nakano et al., 2010; Wozniak et al., 2010; Salsi et al., 2014).

Tpr (Translocated promoter region) is a highly conserved nucleoporin which has homologues in trypanosomes (Holden et al., 2014), budding yeast: Mlp1 and Mlp2 (Myosin like protein) (Kölling et al., 1993; Strambio-de Castillia et al., 1999), fission yeast: Nup211 and Alm1 (Jiménez et al., 2000; Bae et al., 2009; DeGrasse et al., 2009) , Arabidopsis: NUA (Nuclear pore anchor, Xu et al. (2007)), Aspergillus: An-Mlp1 (De Souza et al., 2009; De Souza and Osmani, 2009) and in *Drosophila melanogaster*: Megator (Zimowska et al., 1997; Qi et al., 2004; Lince-Faria et al., 2009).

Tpr was first identified as an activator of the protooncogenes met, raf and trk (Park et al., 1986; Soman et al., 1991; Greco et al., 1992), but subsequent studies have shown that is a 265 kDa mammalian protein, found during interphase in the nuclear basket of the nucleopore complex (Cordes et al., 1997; Zimowska et al., 1997; Frosst et al., 2002; Krull et al., 2004; Hüve et al., 2008) and at the mitotic spindle during metaphase (Sauer et al., 2005; Lince-Faria et al., 2009).

Tpr is composed of an α-helical coiled-coil NH2-terminal domain with almost 1,600-residues, and a non-coiled COOH-terminal domain enriched of acidic residues (Mitchell and Cooper, 1992; Hase et al., 2001). Its anchoring to the NPC is mediated by the Nup153 (Hase and Cordes, 2003) through the amino acids 436–606, while its nuclear localisation is mediated by the 1812-1867 residues in the Carboxyl-terminal domain (Cordes et al., 1998) (Figure 1.9 C).

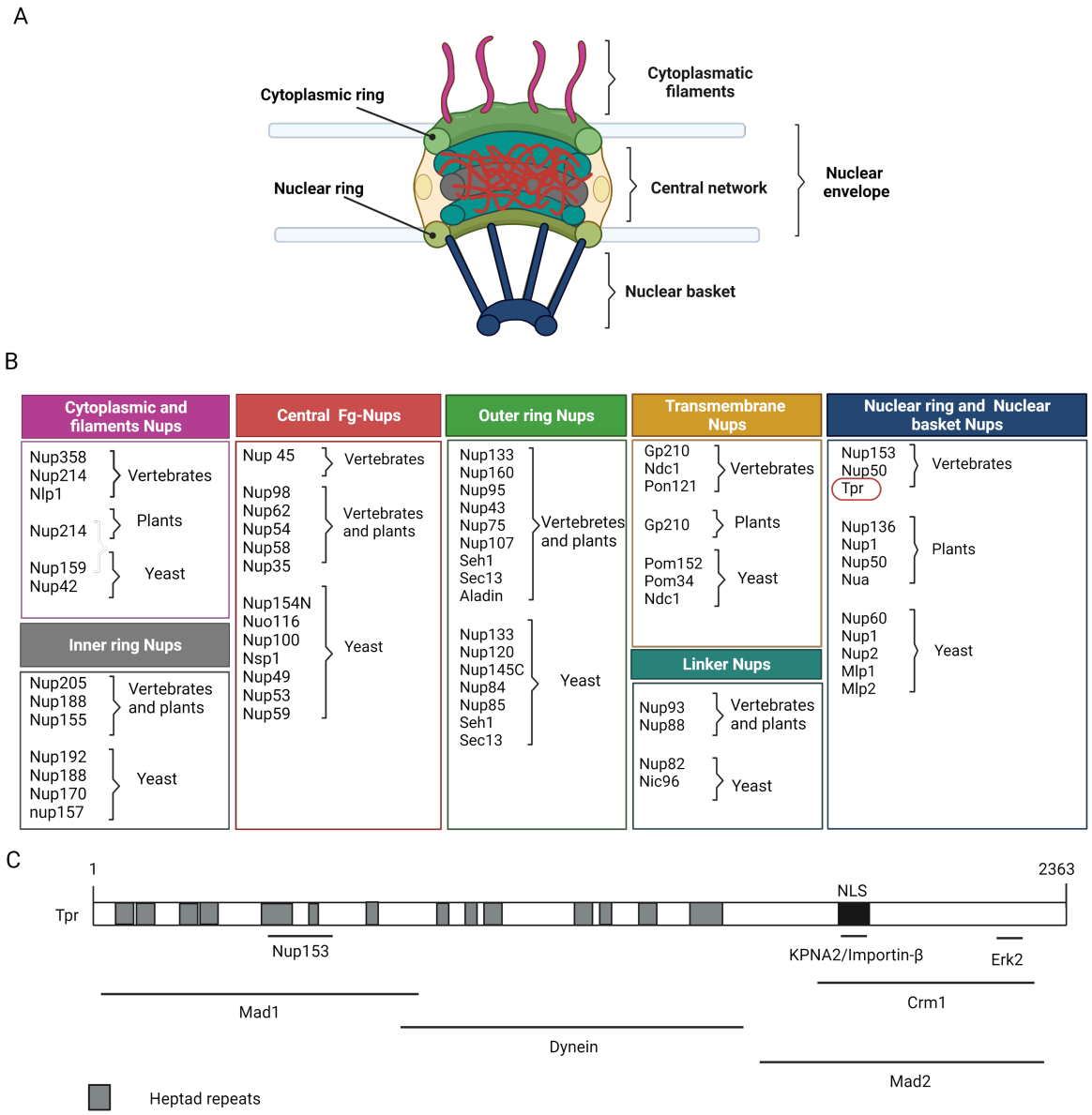

Figure 1.9: The nucleopore complex and Tpr architecture. The nuclear pore complex (NPC) comprises a central channel surrounded by multiple parts, commonly classified in three ring-like structures: the cytoplasmic ring, a central ring and nucleoplasmic ring, plus two additional structures: the cytoplasmic filaments and the nuclear basket (A). Color coded tables indicate the nucleoporins (Nups) that localise in these regions (B). Most of the Nups are followed by a number that states their molecular mass and the FG-Nups are Nups enriched in phenylalanine-glycine. The structure and protein interactions of the nucleoporin Tpr (Translocated promoter region) are shown in (C). NLS is the nuclear localisation signal, Crm1 is Chromosomal Maintenance 1 and KPNA2/Importin-β is Karyopherin subunit alpha 2/Importin-β. Original drawings generated with reference to Grossman et al. (2012) (A and B), Krull et al. (2004) and Snow and Paschal (2014) (C).

Tpr is implicated in several functions. Consistent with being a nucleopore protein, it mediates protein import/export (Frosst et al., 2002; Shibata et al., 2002; Vomastek et al., 2008; Ben-Efraim et al., 2009; Snow et al., 2013). Tpr perturbation by specific knockdown or antibody injections leads to disruption in its ability to bind the Crm1 (Chromosomal Maintenance 1), a mammalian cargo export protein (Frosst et al., 2002). Furthermore, analysis of fibroblasts from patients affected by Hutchinson-Gilford Progeria Syndrome (HGPS) shows defects in Tpr-mediated cargo import and implicate Tpr in premature aging (Kelley et al., 2011; Snow et al., 2013).

Similarly, Tpr has been demonstrated to be essential for mRNA export (Bangs et al., 1998; Xu et al., 2007; Rajanala and Nandicoori, 2012; Lee et al., 2020) and overexpression or knockdown triggers the nuclear accumulation of unspliced RNA (Shibata et al., 2002; Coyle et al., 2011; Rajanala and Nandicoori, 2012). Similar observations have been made in yeast (Green et al., 2003; Galy et al., 2004; Vinciguerra et al., 2005).

Several data also implicate Tpr in gene regulation. Under stress conditions, it associates with the HSP70 promoter (Heat Shock Protein 70 kilodaltons) and the HSF1 (Heat Shock Transcription Factor 1), suggesting an involvement in the regulation of inducible genes (Skaggs et al., 2007). This idea was strengthened by observations of the x-linked genes' expression decreasing after knockdown in *Drosophila* of both Tpr and Nup153 (Mendjan et al., 2006). Consistent with this finding, Tpr was also hypothesised to play roles in chromatin organisation by keeping heterochromatin exclusion zones near the NPC. Indeed, knockdown of Tpr in transfected HeLa cells shows heterochromatin presence in proximity to the NPC (Krull et al., 2010).

Tpr has also been implicated in cell signalling through phosphorylation of the MAPK/ERK (mitogen-activated protein kinase/extracellular signal-regulated kinase) and McCloskey et al. (2018) found that the Tpr-ERK complex negatively controls the number of NPC per cell nucleus.

1.6.2 The spindle matrix protein Tpr during cell division

Studies in different systems have underlined the role of Tpr and its homologues during mitosis (Qi et al., 2004; Niepel et al., 2005; Lee et al., 2008; De Souza et al., 2009; Lince-Faria et al., 2009; Nakano et al., 2010; Schweizer et al., 2013). In budding yeast, Mlp2 regulates the Spindle pole body (SPB), a microtubule nucleating structure functionally similar to the centrosome. When Mlp2 is depleted, smaller SPBs are formed with consequent SPBs components erroneously positioned in the nucleus (Niepel et al., 2005). In fission yeast, Jiménez et al. (2000) reported that functional disruption of the Alm1 gene is linked to elongated cells and impairment in the germination process.

Tpr and its homologues have a highly conserved SAC function during mitosis (De Souza et al., 2009; Lince-Faria et al., 2009; Qi et al., 2009; Nakano et al., 2010). As described in 1.5.3, Mad1 and Mad2, essential proteins for SAC function, are recruited to unattached kinetochores by Mps1 where they bring about the formation of the MCC complex and subsequent APC/C inhibition.

The SAC activity starts after the releasing of Mad1 and Mad2 from the Tpr (Lee et al., 2008) by the coordinated action of the Cyclin B-CDK1 and MPS1 (Morin et al., 2012; Cunha-Silva et al., 2020; Jackman et al., 2020). Lee et al. (2008) found that human Tpr binds to Mad1 and Mad2, through residues 1–774 of the N-terminal region and 1700–2350 in the C-terminus, respectively. Phosphorylation on Tpr residue S2059 is needed for its Mad1-Mad2 interactions (Rajanala et al., 2014). Once Mad1-Mad2 are released, they are recruited to the unattached kinetochore by BUB1 to start the assembly of the MCC and SAC response amplification (Saurin et al., 2011; Faesen et al., 2017; Ji et al., 2017; Allan et al., 2020; Jackman et al., 2020).

Knockdown of Tpr by siRNA prevents the correct recruitment of Mad1-Mad2 at kinetochore, causing inactivation of SAC and chromosome segregation defects. This suggests that Tpr could act as a scaffold for Mad1/Mad2 localisation (Lee et al., 2008).

Consistent with this, Schweizer et al. (2013) show that depletion of Tpr leads to impairment in SAC proteins levels at kinetochore, in particular Mad1 and Mad2. Furthermore, Nakano et al. (2010) reported that Tpr association with the motor protein dynein spatiotemporally regulates the recruitment of Mad1 and Mad2 during metaphase/anaphase transition. Accordingly, knockdown of either Tpr or dynein leads to lagging chromosomes (Nakano et al., 2010).

Although Tpr has been demonstrated to promote Mad1/2 loading on mitotic kinetochores, they colocalise to interphase nuclear pore complexes as well. Two independent studies found that Mad1 construct lacking Tpr binding domain is still able to interact with Mad2 in interphase, which challenged the idea of Tpr being needed for the Mad1-Mad2 interaction (Rodriguez-Bravo et al., 2014; Lara-Gonzalez et al., 2019). However, Rodriguez-Bravo et al. (2014) show that Tpr is important for MCC formation even prior to the beginning of mitosis. Displacing Mad1-Mad2 from the NPC during interphase, prevents MCC formation with subsequent accelerated anaphase, leading to malorientations and lagging chromosomes. Furthermore, a recent study in *Drosophila* shows that the Mps1 kinase is crucial for Tpr phosphorylation and consequent releasing of Mad1 and Mad2 from the NPC to the nucleoplasm (Cunha-Silva et al., 2020).

1.6.3 The *Drosophila* spindle matrix protein Megator

The *Drosophila* spindle matrix protein Megator (Mtor), first identified as Bx34, is a protein of 2346 amino acids with a total mass of 260 kDa (Mitchell and Cooper, 1992; Byrd et al., 1994; Bangs et al., 1998). 70% of Megator's amino-terminus is a predicted coiled-coil region, while the remaining 30% carboxy-terminus is enriched in negatively charged amino-acid residues. Although sequence comparisons reveal 28% identity, the domain structures and functions are highly conserved (Zimowska et al., 1997; Lince-Faria et al., 2009).

Studies in mitosis show that Megator localises to the nuclear rim at interphase and in the spindle at metaphase (Zimowska et al., 1997; Qi et al., 2004; Lince-Faria et al.,

2009). This dynamic distribution is not affected by the depolymerisation of microtubules, therefore Megator is considered a spindle matrix protein (Qi et al., 2004; Lince-Faria et al., 2009). Megator's localisation to the NPC and spindle matrix is mediated by its amino-terminus coiled-coil domain, while the carboxy-terminus domain is responsible for Megator's localisation during interphase (Yao et al., 2012). Early mutational studies by Qi et al. (2004) demonstrated that Megator is an essential gene and homozygous Megator mutants are lethal.

Similar to Tpr, depletion of Megator in *Drosophila* S2 tissue cells showed significant reduction of both Mad2 and Mps1 recruitment at kinetochores, resulting in a premature entry into anaphase (Qi et al., 2004; Lince-Faria et al., 2009). Lince-Faria et al. (2009) also reported that Mad2 depleted S2 cells have the same premature exit and lagging chromosome phenotype as Megator depleted cells, underlying Megator's role for the SAC function. This raises the possibility that loss of Megator function in the germline may affect fertility, similarly to *Drosophila* Mad2-null mutants, which experience a 50% reduction in fertility and viable progeny (Buffin et al., 2007).

As mentioned in 1.6, Megator interacts with other *Drosophila* spindle matrix proteins: Skeletor and Chromator. Skeletor is an 81 kDa protein that lacks structural motifs (Walker et al., 2000). The 101 kDa Chromator protein is composed of an amino-terminus chromodomain with a site for Skeletor interaction present in the carboxy-terminus at residues 601-926 (Rath et al., 2004; Wasser et al., 2007). During interphase, Megator is present at the nuclear rim in polytene containing chromosomes and occupies the intranuclear space around the chromosomes. In contrast, Chromator and Skeletor localise to the chromosome's interband regions (Walker et al., 2000; Qi et al., 2004).

Despite these different localisation, all three proteins surround the spindle to form the spindle matrix during mitosis, and retain their organisation after spindle removal through MTs depolymerising drugs (Walker et al., 2000; Qi et al., 2004; Rath et al., 2004; Lince-Faria et al., 2009). Furthermore, protein depletion studies yield phenotypes with mitotic defects, such as chromosome misalignment and missegregation being

prevalent (Rath et al., 2004; Ding et al., 2009; Lince-Faria et al., 2009).

1.7 Megator's role during meiosis

Haploid sperm formation and male fertility require two specialised male meiotic divisions to reduce the number of chromosomes in each daughter cell. To do so, each chromosome interacts and segregates at anaphase via the spindle and kinetochores. Errors in chromosome segregation cause genetic instability and can generate various pathologies, from cancer to male sterility or developmental abnormalities in the progeny. Much of the understanding of meiosis comes from studies of somatic cell mitosis. However, despite common molecular components, the two processes are not entirely interchangeable.

Recent works in somatic cells mitosis have shown that proteins of the nuclear pore complex also perform extra-nuclear functions during cell division. Megator, the *Drosophila* homologue of vertebrate Tpr, is a conserved nucleoporin present in the nuclear basket. Along with two additional proteins, Skeletor and Chromator - Megator redistributes around the spindle during cell division forming a spindle matrix, a hydrogel-like structure proposed to supply mechanical support to microtubules for chromosomes segregation.

Megator/Tpr is also involved in the spindle assembly checkpoint (SAC) during somatic cell mitosis. Indeed, RNAi-mediated depletions of Megator/Tpr in *Drosophila* and vertebrate tissue culture cells lead to chromosome segregation defects due to its role in recruitment of the essential SAC protein Mad2 to kinetochores.

In *Drosophila* testes, Megator is also involved in the regulation and maintenance of the asymmetric division of the stem cells (Liu et al., 2016). The asymmetric division of GSCs required Apc2 and E-cadherin, two proteins that work together to anchor the spindle (Yamashita et al., 2003). Liu et al. (2016) show that the depletion of Megator alters the localisation/expression of Apc2 and produces a significant reduction of E-cadherin, resulting in increased frequency of lagging chromosomes and spindles with

half-formed or not clear spindle poles. Furthermore, Megator depletion in the CySCs triggers defects in GSCs differentiation, suggesting that Megator is essential for the maintenance of GSCc in the testes. Also, CySCs-Megator mutants started to move away from the niche and differentiate in cyst cells, indicating that the Megator's role in CySCs is to regulate their attachment to the niche.

Despite its importance in mitosis, no information is available on Megator's function during male meiosis or on the existence of a spindle matrix. Therefore, this project aims to:

1. Characterise Megator distribution during meiosis I and II.
2. Determine if Megator is required for correct chromosome segregation in meiosis I and II.
3. Identify if Megator regulates correct chromosome segregation by performing a conserved role in the SAC.

Chapter 2

Materials and Methods

2.1 *Drosophila melanogaster* strains

The *Drosophila* fly strains used in this thesis are listed and desribed in the Appendix, Table A.1. Shorthand names are used, following the nomenclature approved by FlyBase[1]. Italics is only used for gene names and genotypes, not for proteins and phenotypes.

Relative crossing between the original fly lines to produce progeny with the desire genotype, are illustrated in section 2.3.

2.2 Fly strains maintenance

Flies were raised at 25°C. Standard fly media was prepared from 10 g agar, 40 g yeast, and 110 g polenta dissolved in 1 L of distilled water. The mixture was brought to boil and then let to simmer for two minutes while stirring. The resulting product was removed from the heat to add 130 g granulated white sugar, 20 mL molasses and 3.3 g of Moldex (methyl 4-hydroxybenzoate) diluted in 37 mL 95% ethanol. Approximately 8 mL of the final mixture was poured into 30 mL vials (for fly crossing). Volumes of 40 mL were poured into 100 mL bottles (for stock maintenance). Once cooled, the media

[1]https://wiki.flybase.org/wiki/FlyBase:Nomenclature

was supplemented with yeast sprinkled on food and each vial or bottle was sealed with a foam plug or sponge plug.

2.3 Genetic crosses

In order to carry out genetic crossing for functional studies, virgin female flies were collected from stocks in the morning. Virgin females *β-tubulinEGFP//;bam-GAL4//* and males carrying genotypes in accordance to experiments were mated together maintaining a 3:1 ratio of females to males. The mating process took place in the vials prepared with the fly media as stated above. Adult flies were removed after five days, while the progeny was due to eclose after ten days at 25°C. A schematic representation and descriptions of the crosses utilised in this study are shown (Figure 2.1).

Control flies were generated by crossing *β-tubulinEGFP//;bam-GAL4//* virgin female flies to w(CS10) fly. The functional analysis of Megator was performed by using tissue-specific RNAi-based protein depletion under the GAL4/UAS system as homozygous Megator mutants are lethal (Qi et al., 2004). Virgin female flies carried the tissue specific bam-GAL4 driver which drives Megator knockdown only in *Drosophila* late spermatogonia and early spermatocytes (Bunt et al., 2012). For further studies on Megator function, virgin *βtubulinEGFP//;bam-GAL4//* female flies were crossed with either of two different lines expressing the fluorescent protein tagged Megator-mCherry (Yao et al., 2018).

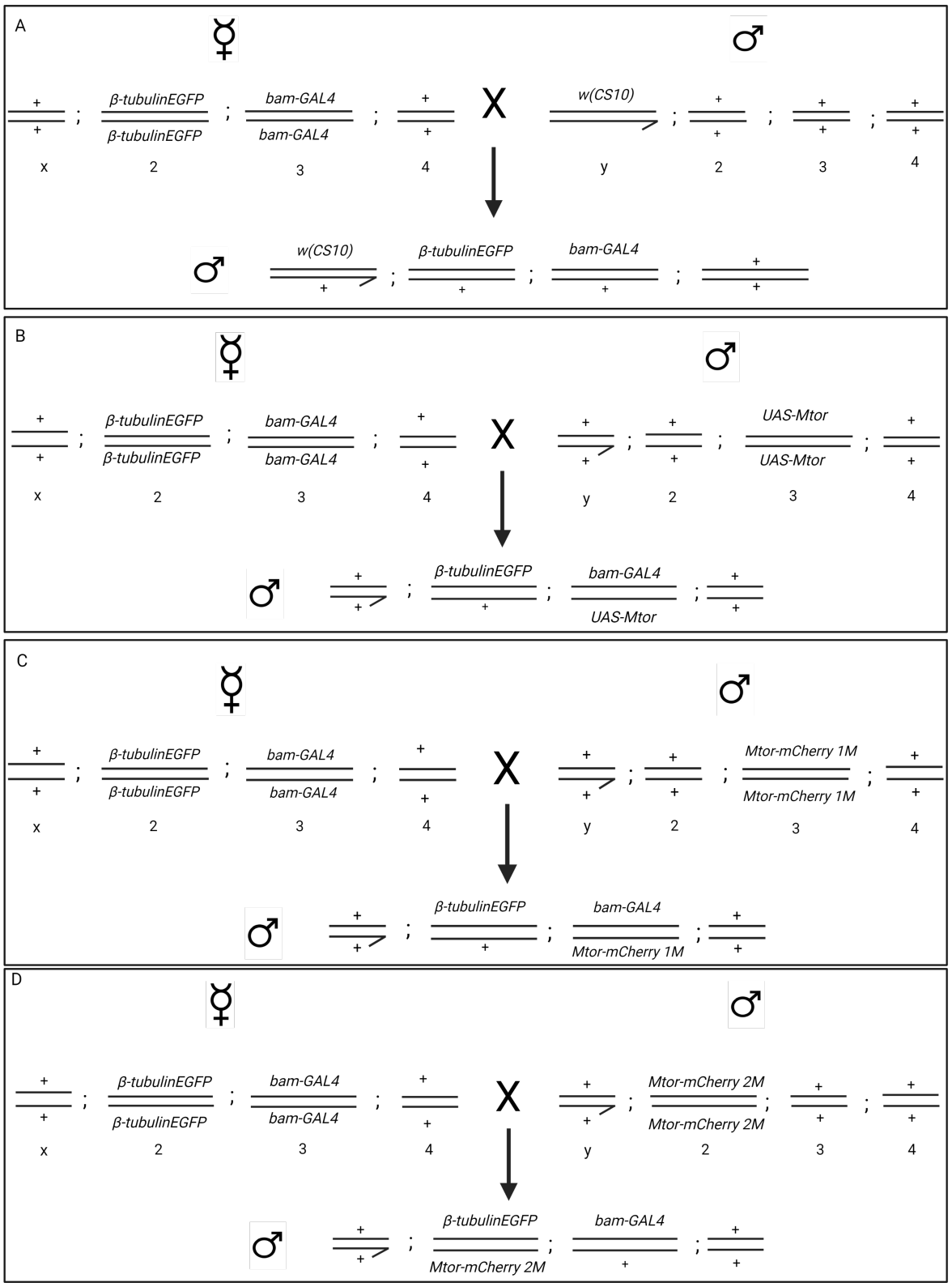

Figure 2.1: Schematic representation of *Drosophila* crossing performed in the study. Typical crosses generated to produce: control flies (A), flies with Megator (Mtor) tissue-specific knockdown (B) and flies expressing two different lines of the fluorescent protein Mtor-mCherry (C and D). Female and male sex chromosomes are indicated with x and y, respectively. + indicates a wild-type chromosome.

2.4 *Drosophila* testes isolation and fixation

Drosophila testes were dissected in a drop of phosphate-buffered saline (PBS, pH 7.4) with dissecting needles under a dissecting microscope. After the removal of unwanted material, six testes were transferred to frosted slides in 3 μL of PBS supplemented with 5% glycerol. Testes were punctured a few times and covered with coverslip (22x22 mm, thickness No.1) to allow meiotic cells to be released. Slides were plunged into liquid nitrogen until frozen. Slides were then removed and the coverslips were rapidly discarded before placement in dry ice cooled methanol for thirty minutes for fixation. After several rinses in PBS, testes were extracted for ten minutes with a solution of 0.5% Triton X-100 in PBS (Pisano et al., 1993; Cenci et al., 1994). Slides were then washed in PBS for three times (five minutes each) and left in PBS for one hour at room temperature for subsequent staining.

2.5 Immunostaining of *Drosophila* testes

Primary antibodies (Table 2.1) were diluted in a solution of 0.05% Triton X-100 in PBS supplemented with 1% bovine serum albumin (w/v) BSA. Slides were pat dry around the sample and a square was drawn with a hydrophobic barrier pen. Then, 50 μL of the solution containing the primary antibodies was loaded onto the testes and the slides were incubated overnight at 4°C in a moist chamber. The following day samples were washed three times (five minutes each) with PBS. Subsequently, secondary antibodies were applied (Table 2.2) and the slides incubated at room temperature for three hours.

After this period, testes were washed again three times in PBS (five minutes each) and two times with distilled water. Vectashield mounting media containing DAPI was applied on the samples. A coverslip (22x22mm, thickness No. 1) was placed on top of the slide in alignment with the square previously drawn. Excess liquids were pat dry around the edges before sealing with nail polish. Samples were kept in the freezer at −20°C until analysis with Zeiss LSM900 Airyscan 2 super-resolution scanning confocal

microscope (Zeiss).

Name	Target	Class	Host	Source	Code	Dilution
12F10-5F11	Megator	Monoclonal	mouse	DSHB	AB_2721935	1:100
12H9-4A2	Chromator	Monoclonal	mouse	DSHB	AB_2721936	1:25
1A1-3C2	Skeletor	Monoclonal	mouse	DSHB	AB_2721937	1:25
ADL101	Lamin Dm0	Monoclonal	mouse	DSHB	AB_528332	1:50
Chicken anti-CID	CID	Monoclonal	chicken	Przewloka and Glover (2009)		1:500

Table 2.1: List of primary antibodies and corresponding dilutions. DSHB stands for Developmental Studies Hybridoma Bank.

Name	Target	Class	Origin Species	Source	Code	Dilution
Goat anti-chicken IgY Alexa Fluor 647	Chicken	Polyclonal	Goat	ThermoFisher	A-21449	1:500
Goat anti-chicken IgY Alexa Fluor 633	Chicken	Polyclonal	Goat	ThermoFisher	A-21103	1:500
Goat anti-mouse IgG CF568	Mouse	Polyclonal	Goat	Merck	SAB4600312	1:500

Table 2.2: List of secondary antibodies and corresponding dilutions.

2.6 Microscopy.

All images were acquired using a Zeiss 980 Airyscan 2 super-resolution scanning confocal microscope (Zeiss) using a 63x (N.A. 1.4) lens.

Images in scanning confocal (without super-resolution mode) were acquired with the following settings: DAPI excitation wavelength: 405 nm, signal collected from 405 nm to 605 nm, detector gain 699V, 0.8% laser power. EGFP excitation laser wavelength: 488 nm, signal collected between 488-575 nm, detector gain 232V, 0.7% laser power. Megator-mCherry (Mtor-mCherry) and Megator antibody signals excitation wavelength: 561 nm, signal collected from 561 nm to 650 nm, detector gain 670V, 2.6% laser power. For all z-series step size was 0.21 μm and a zoom of 1.3 was used.

Images in super-resolution scanning confocal mode were acquired with the following settings: DAPI excitation wavelength: 405 nm, signal collected from 405 nm to 517 nm,

detector gain 748V, 2.7% laser power. EGFP excitation wavelength: 488 nm, signal collected between 488-575 nm, detector gain 738V, 1.8% laser power. Megator/Skeletor/Chromator antibody signals excitation wavelength: 561 nm, signal collected from 561 nm to 650 nm, detector gain 784V, 1.4% laser power. Cid (Far-red) excitation wavelength: 640 nm, signal collected between 640-700 nm, detector gain 715V, 3.7% laser power. Step size was 0.14 μm and a zoom of 1.3 was used.

Images were assembled in Fiji-Imagej (Schneider et al., 2012) and texts on the panels were added with GNU Image Manipulation Program (Team, 2021). All the images acquired in super-resolution scanning confocal mode, assembled in panels and presented in the study are z-projections of variable number of steps ranging between 76 to 125. All the assembled panels of images in scanning confocal only are single sections.

2.7 Quantification of Megator depletion.

Megator function was assayed using tissue-specific RNAi-based protein depletion under the bam-GAL4/UAS system. Because Megator is not depleted testes-wide using this strategy (Insco et al., 2009; Bunt et al., 2012), protein levels in meiotic cells were determined with quantitative microscopy (in scanning confocal mode only) by measuring the fluorescence intensity of a specific region of interest (ROI) in both the spindle and cytoplasm regions. Single optical sections only were selected from control (n=28) and Megator depleted cells (n=24) during prometaphase I. Within these single sections, a circle with an area of $7.62\mu m^2$ was positioned in the largest region of the spindle that did not contain chromosomes or microtubules, abstractions which would affect the accuracy of the measurements.

An identical circle was also placed in a spindle free region. Mean intensity values of these areas were tabled (Appendix, A.2) and consequently presented in a bar plot. To evaluate the statistical significance of the difference in intensity counts between cytoplasm and spindle in both control and Megator depleted cells, a T-test for difference of means was used. Confidence intervals at 95% and p-value are provided with the

calculation. Because the assumptions of the T-test are not fully met, due to the small sample size, the Wilcoxon sign rank test was employed. Both bar plot and test were produced using R (R Core Team, 2017).

2.8 Counting of onion stage spermatids.

Testes from each homozygous parental fly line and the heterozygous progenies (Figure 2.1 A and B) were dissected in a drop of PBS with dissecting needles, under a dissecting microscope. Four testes for each genotype were then transferred to a slide in a drop of PBS and covered with a 22x22 mm coverslip. Filter paper was used to blot liquid from the coverslip edges to allow the rupture of the testes, with consequent outflow of the content by pressure of the coverslip on the specimens. Slides were visualised using a 40x lens (0.75 NA) on a Leica DMRBE Microscope, Phase contrast optics (Leica microsystems). The ratio nebenkern to nuclei was determined and tabulated (Appendix, Table A.3). A ratio of 1:1 indicates correct chromosome segregation and cytokinesis, while 1:0, 0:1, 2:0, 0:2, 2:1, 1:2 and any combinations of these (termed "others") were considered indicative of failed division.

Chapter 3

Results

3.1 Characterisation of Megator distribution during meiosis I and meiosis II

As a first step in the evaluation of the role played in meiosis by the conserved nucleoporin Tpr/Megator, its distribution during both meiosis I and meiosis II was determined. Control male flies (flies with endogenous levels of Megator) were generated by crossing virgin female flies expressing both the *β-tubulinEGFP* which labelled microtubules (Inoue et al., 2004) and the testes-specific driver *bam-GAL4* (Bunt et al., 2012), to w(CS10) male flies (crossing scheme: Figure 2.1 A). This cross was performed to ensure that the progeny were heterozygous for both transgenes.

Male progeny were then collected three days after eclosion and their testes were dissected and fixed according to the methanol fixation procedure (described in section 2.4). Subsequently, immunofluorescence staining was performed using previously established antibodies raised against Megator and CID (the centromeric histone H3-like protein identifier), a marker for kinetochore position. Additionally, DNA was counterstained with DAPI. Their signals were visualised by super-resolution scanning confocal microscopy (parameters described in section 2.6).

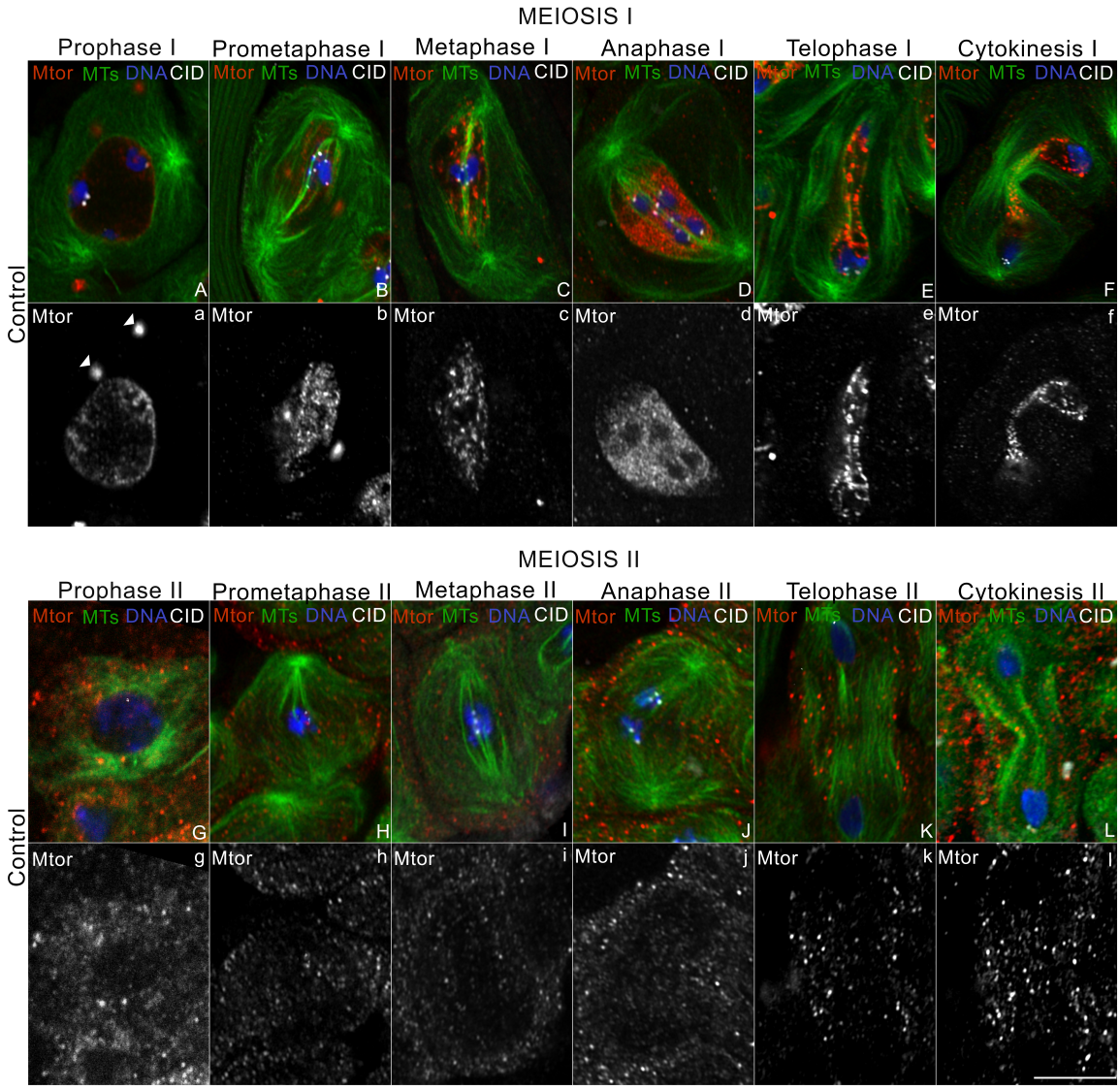

Figure 3.1: Megator shows distinct distribution throughout meiosis I and II. Super-resolution scanning confocal microscope images of Megator (red; Mtor) distribution in meiosis I (A-F) and II (G-L) in control cells, compared with DNA in blue, microtubules (MTs) in green and the centromere marker CID in white. Corresponding images of Megator only, during meiosis I (a-f) and meiosis II (g-l). White arrowheads indicate Megator aggregates in the cytoplasm not corresponding to spindle microtubules or centrosomes. All images are z-projections. Scale bars 10μm.

At prophase I, during chromosome condensation, Megator was present in aggregates of variable size throughout the nuclear volume and at the nuclear rim (Figure 3.1 A and a). This speckled nuclear rim appearance is consistent with Megator being part

of the nucleopore complex (Zimowska et al., 1997). Additionally, a few Megator spots were observed in the cytoplasm (Figure 3.1 a, white arrowheads). However, this signal did not correspond to microtubules or centrosomes, as revealed by the β-tubulinEGFP signal (Figure 3.1 A).

After microtubule invasion into the nuclear space and consequent spindle formation, Megator moves into the space of the spindle (Figure 3.1 b), similar to previous findings of Megator being a component of the spindle matrix during mitotic cell division (Qi et al., 2004, 2005; Lince-Faria et al., 2009; Yao et al., 2018). During metaphase I, Megator robustly concentrates in the spindle region as revealed by the bright red signal in the merged figure (Figure 3.1 C). Furthermore, Megator forms aggregates which are excluded from the space occupied by the chromosomes, as shown by the regions without staining in the Megator channel only (Figure 3.1 c). Consistently, when chromosomes separate during anaphase I, Megator is still visible in the spindle region as agglomerates excluded from the space occupied by the DNA (Figure 3.1 d).

Following spindle elongation, in accordance to previous findings in mitosis (Qi et al., 2004, 2005), Megator aggregates redistribute in the central spindle during telophase I and, close to cytokinesis I onset, it redistributes back near the daughter nuclei. Throughout meiosis I, minimal Megator signal is detected in the cytoplasm (Figure 3.1 a-f).

At the beginning of meiosis II, Megator does not occupy the nuclear volume and is not present at the nuclear rim (Figure 3.1 g). This may suggest that nucleopores are either not present or are different at this stage. More surprisingly, in contrast to meiosis I, the Megator signal remains at background levels in the form of small, scattered granules. This is also consistent throughout all of meiosis II. Following spindle formation, the cytoplasm region displayed Megator aggregates that appeared to be excluded from the spindle microtubules as shown in the merged figures by the absence of red speckles in the spindle (Figure 3.1 H-J), as well as by the regions without staining in Megator channel only (Figure 3.1 h-j). Likewise, during telophase II and cytokinesis

II, numerous Megator particles were still detected in the cytoplasm (Figure 3.1 k and l).

Together, these data reveal a different distribution of Megator between meiosis I and meiosis II. This suggests that Megator may be a spindle matrix protein in meiosis I but not in meiosis II or have other different functions.

3.1.1 Validation of Megator's localisation during meiosis: Chromator and Skeletor distributions

The unexpected dissimilarities in Megator distributions between meiosis I and II raised the possibility that the spindle matrix composition may substantially differ between the two division types. Therefore, the distributions of two additional mitotic spindle matrix proteins, Chromator and Skeletor (Walker et al., 2000; Rath et al., 2004; Ding et al., 2009),were investigated. Both these proteins interact with Megator (Qi et al., 2004; Yao et al., 2012).

To compare Chromator and Skeletor localisation, testes from control male flies (crossing scheme visible in Figure 2.1 A) were dissected and fixed. Subsequently, testes were counterstained with DAPI and immunostained against CID, Chromator or Skeletor and analysed through super-resolution scanning confocal microscopy (Figure 3.2).

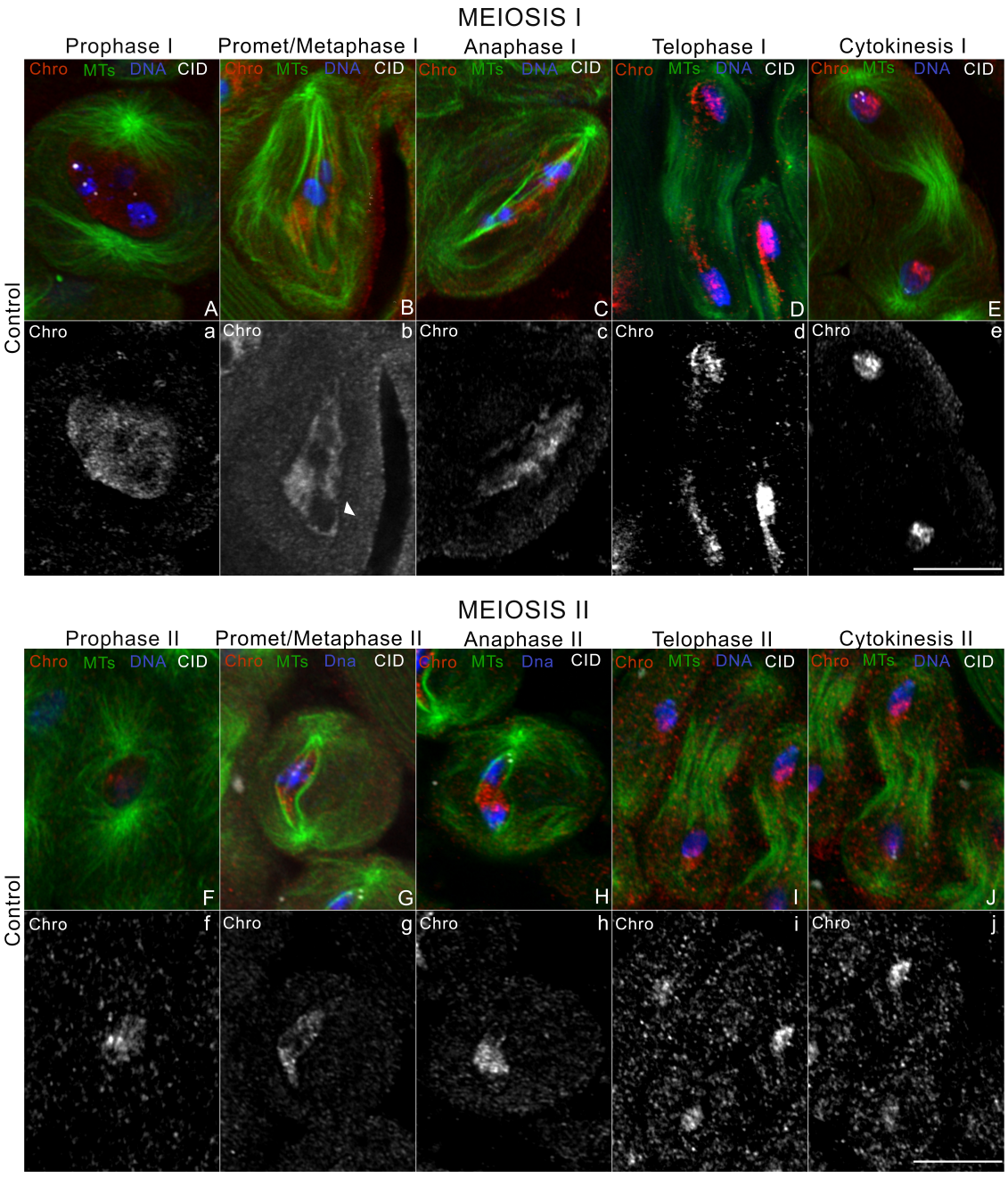
MEIOSIS I
Prophase I
Promet/Metaphase I
Anaphase I
Telophase I
Cytokinesis I
Chro MTs DNA CID
Control
A
B
C
D
E
Chro
a
b
c
d
e
MEIOSIS II
Prophase II
Promet/Metaphase II
Anaphase II
Telophase II
Cytokinesis II
Chro MTs Dna CID
F
G
H
I
J
f
g
h
i
j

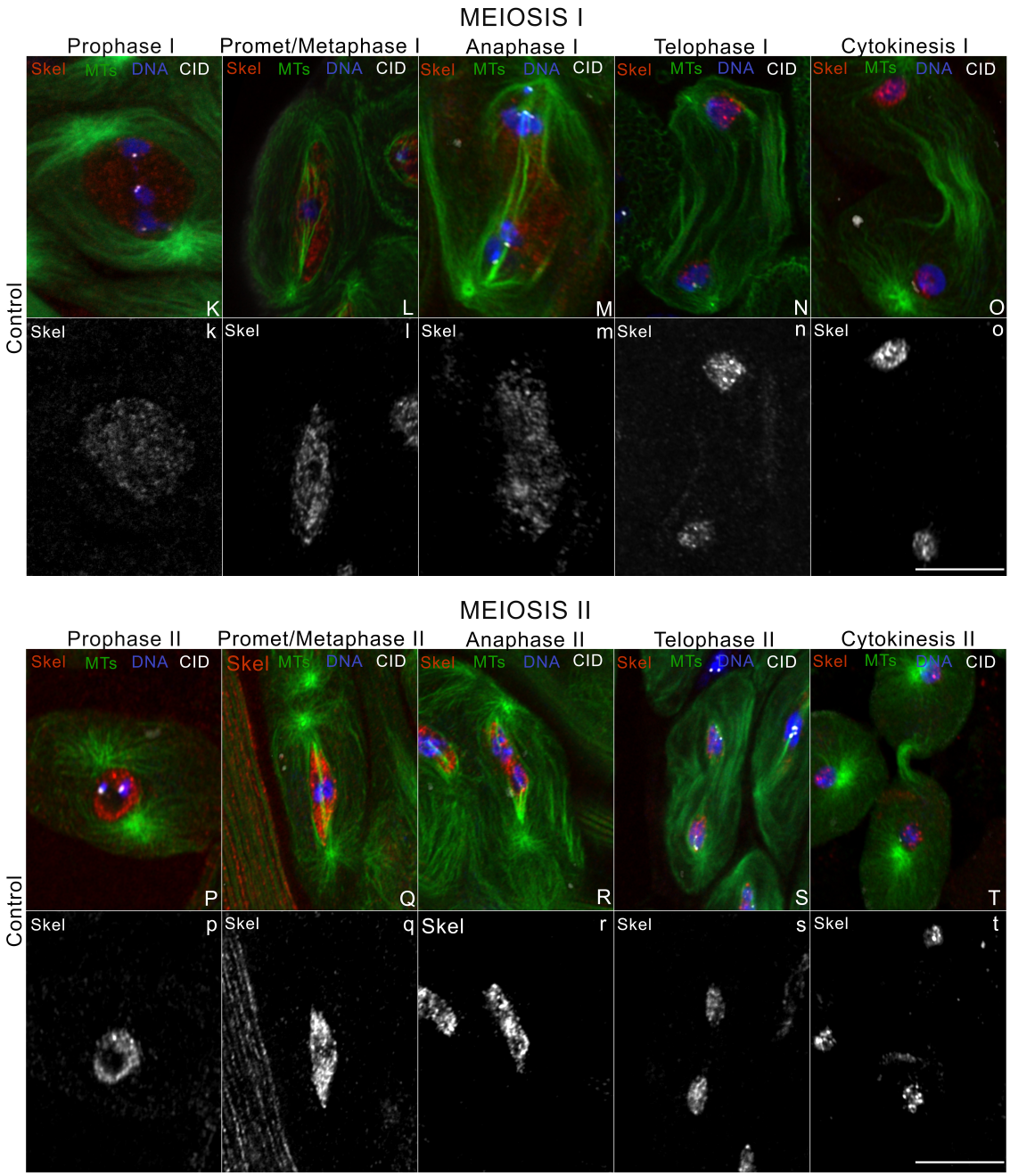

Figure 3.2: Chromator and Skeletor are spindle matrix proteins during meiosis I and meiosis II. Comparative super-resolution scanning confocal microscope images of control cells stained for Chromator and Skeletor (both in red) during meiosis I (A-E and K-O) and meiosis II (F-J and P-T), relative to DNA in blue, microtubules (MTs) in green and CID in white. Corresponding images of Chromator and Skeletor only, during meiosis I (a-e and k-o) and II (f-j and p-t). Arrowhead indicates an unstained region non corresponding to DNA. All images are Z-projection. Scale bars 10μm.

During prophase I, both Chromator and Skeletor concentrate in the nuclear region (Figure 3.2 a and k), similar to what was observed with Megator (Figure 3.1 a). However, in contrast to Megator, they do not localise to the nuclear rim which is consistent with Chromator and Skeletor not being nuclear envelope proteins. Following spindle formation, in accordance to previous studies in mitosis (Walker et al., 2000; Rath et al., 2004), Chromator and Skeletor redistribute into the spindle during prometaphase/metaphase I and anaphase I (Figure 3.2 b and c, l and m). Their signals are excluded from the regions occupied by the chromosomes. In particular, during Chromator's metaphase I, areas without staining (also non corresponding to the DNA) are observed (Figure 3.2 b, arrowhead).

These Chromator and Skeletor localisation in the spindle matrix are consistent with studies of Megator in mitosis (Qi et al., 2004, 2005) as well as Megator distribution during meiosis I (Figure 3.1 b and c). However, Megator's appearance in the spindle is heavily speckled, while both Chromator's and Skeletor's signals show much finer granules. The background signal of Chromator in the cytoplasm is low in comparison to its spindle's localisation, during metaphase I and anaphase I (Figure 3.2 b and c). However, these signals appear considerably stronger in comparison with those of Skeletor and Megator at the same stages (Figure 3.2 l and m, Figure 3.1 c and d).

As reported for mitosis (Walker et al., 2000; Qi et al., 2004), during telophase I both Chromator and Skeletor colocalised with the DNA, as shown by the merged figures (Figure 3.2 D and N). However, in contrast to Chromator and Megator, Skeletor's signal does not trail in the spindle's, but is close to the DNA (Figure 3.2 n). At cytokinesis I onset, both Chromator and Skeletor colocalise with the DNA, as shown by the merged figures (Figures 3.2 E and O).

At the beginning of the second meiotic division, consistent with meiosis I distribution, both Chromator and Skeletor displayed nuclear localisation during prophase II with low signal intensity in the cytoplasmic areas (Figure 3.2 f and p). During metaphase II as well as anaphase II, Chromator's and Skeletor's distributions mirror meiosis I:

both proteins mainly accumulate in the spindle with their signal excluded from the areas occupied by the chromosomes (Figure 3.2 g and h, q and r). Furthermore, Chromator exhibits a background signal much more pronounced than Skeletor (Figure 3.2 g and h, q and r). During telophase II and cytokinesis II, as seen in meiosis I and studies in mitosis (Walker et al., 2000; Qi et al., 2004), both Chromator and Skeletor colocalise with the DNA (Figure 3.2 I and J, S and T). Consistently, Chromator forms cytoplasmic aggregates, something not seen when staining for Skeletor. It is unclear if this represents lack of specificity due to the antibody.

The super-resolution scanning confocal analysis of Chromator and Skeletor revealed that their distriburions during meiosis I and meiosis II are largely similar. Chromator and Skeletor localise in the nuclear space at the beginning of meiosis I and meiosis II and near the nuclei during cytokinesis I and II. More importantly, they redistribute at the spindle at metaphase and anaphase, during both meiosis. These findings are consistent with Chromator and Skeletor being spindle matrix proteins during mitosis. However, they are also in striking contrast with Megator which localise in the spindle region only during meiosis I. Together, these data suggest that only Chromator and Skeletor are spindle matrix proteins during both meiosis I and meiosis II.

3.1.2 Confirmation of Megator's distribution during Meiosis II: Megator-mCherry distribution

Megator placements suggest the existence of a spindle matrix in meiosis I but not in meiosis II (Figure 3.1). To exclude the possibility that the absence of a Megator spindle signal in meiosis II was due to surface-epitope masking effects blocking the Megator antibody or other technical artefacts, the fluorescent protein tagged Megator was studied. Two different previously described fly lines expressing Megator fused to mCherry (Mtor-mCherry) (Yao et al., 2018) were crossed, as with the antibody-based studies, with *β-tubulinEGFP//;bam-GAL4//* flies to allow imaging of microtubules (crossing scheme: Figure 2.1 C and D). Testes from the progeny were dissected, fixed,

counterstained with DAPI and analysed by scanning confocal microscopy (parameters described in section 2.4).

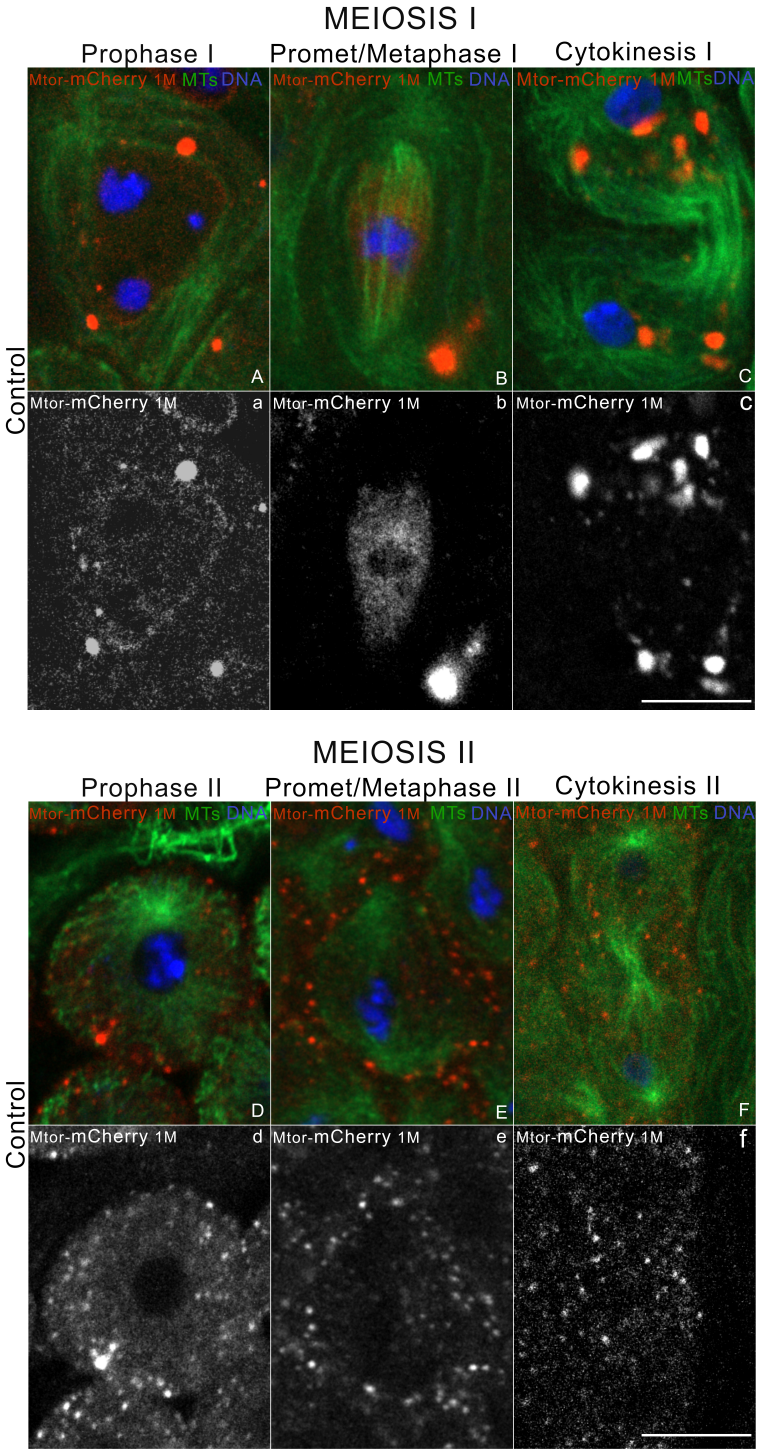

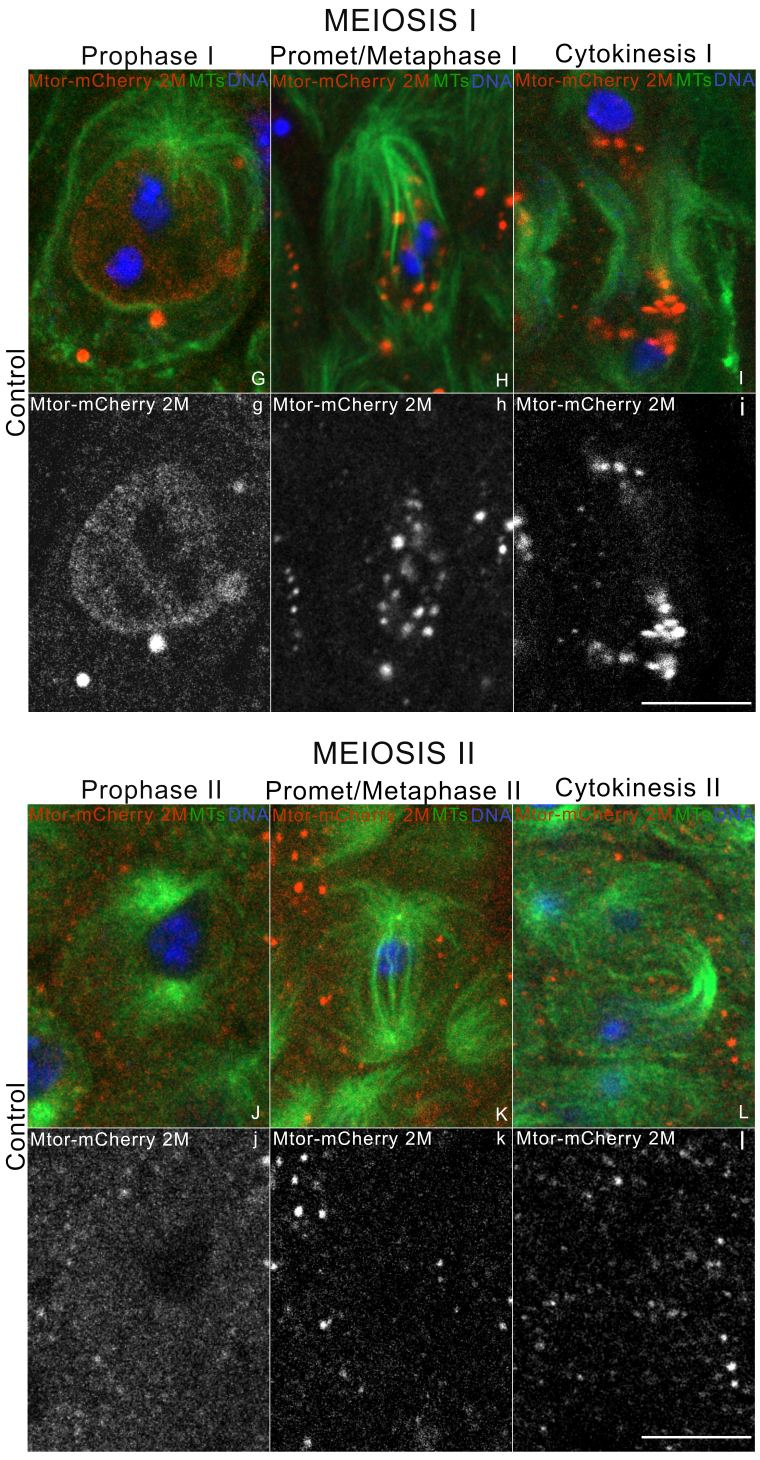

Figure 3.3: Megator-mCherry localisation during MI and MII confirm Megator antibody distributions. Comparative single sections of scanning confocal images of cells isolated from flies expressing the fluorescent protein Megator mCherry (Mtor-mCherry 1M or 2M) with microtubules (MTs) in green and DNA in blue, throughout MI (A-C and G-I) and MII (D-F and J-L). The corresponding Mtor-mCherry 1M and 2M single channel distributions in meiosis I (a-c and g-i) and MII (d-f and j-l).. Scale bars 10μm.

In both Mtor-mCherry lines, Megator accumulates in aggregates first around the nuclear rim during prophase I and then in the nuclear spindle region throughout the rest of meiosis I (Figure 3.3 a-c and g-i). These distributions are identical with that observed using Megator antibody (Figure 3.1 a-f). Interestingly, Megator spots were again observed in the cytoplasm with both of the Mtor-mCherry expressing lines. These speckles did not correspond to the spindle microtubules or chromosomes (Figure 3.3 B and H). This indicates that during MI, there is no significant Megator antibody surface-epitope masking (SEM).

An examination of Mtor-mCherry distribution in meiosis II confirmed the results of the fixed cell antibody-stained experiments (Figure 3.1 g-l). At no time during MII did either Mtor-mCherry expressing line have a signal at the nuclear rim during prophase II or concentrate in the spindle matrix during prometaphase/metaphase II (Figure 3.3 d and e, j and k). Rather, as seen with the antibody staining, it remains at, or possibly less than, background levels throughout all meiosis II (Figure 3.3 d-f and j-l). Together these data suggest that the absence of Megator signal in meiosis II is not due to a Megator antibody SEM. This contrasts with the mitotic cells examined to date, which display Megator homologues in a matrix-like localisation. It raises questions of Megator and spindle matrix function in the testes.

3.2 Identifying Megator meiotic functions

As described in section 1.6.2, Megator roles have been studied only in mitosis, and its functions in meiosis, if any, are unknown. Because Megator is an essential gene (Qi et al., 2004) which also plays roles in the earliest stages of *Drosophila* spermatogenesis prior to meiosis (Liu et al. (2009), Figure 1.1 F), traditional mutants and gene knockouts cannot be used to test protein functions. Therefore, the GAL4/UAS system was employed to drive tissue specific Megator depletion in the late spermatogonia and early spermatocytes through the bam-GAL4 driver (Insco et al., 2009; Bunt et al., 2012). *β-tubulinEGFP//;bam-GAL4//* virgin female flies were crossed with

males carrying *UAS-Megator* for Megator's tissue specific knockdown (crossing scheme: Figure 2.1 B. Validation of Megator's depletion efficiency is described below). The *β-tubulinEGFP//;bam-GAL4//* virgin female flies were also crossed to *w(CS10)* flies, as a control, to ensure that any phenotypes observed did not result from unequal copy numbers of the *β-tubulinEGFP* transgene (crossing scheme: Figure 2.1 A). Male progeny from both crosses were collected and their testes dissected, fixed and immunostained. The effects of Megator depletion were then analysed by super-resolution scanning confocal microscopy.

3.2.1 Quantifying Megator's depletion by quantitative microscopy

The use of bam-GAL4 to drive protein depletion in a subset of cells in the testis makes Western blot-based assays non-representative of the actual protein levels in the cells being studied. Therefore, Megator depletion efficiency was carried out by quantitative microscopy and the endogenous Megator fluorescence accumulation was analysed in both the spindle and cytoplasm regions of control and Megator shRNA expressing cells using antibody staining (Figure 3.4).

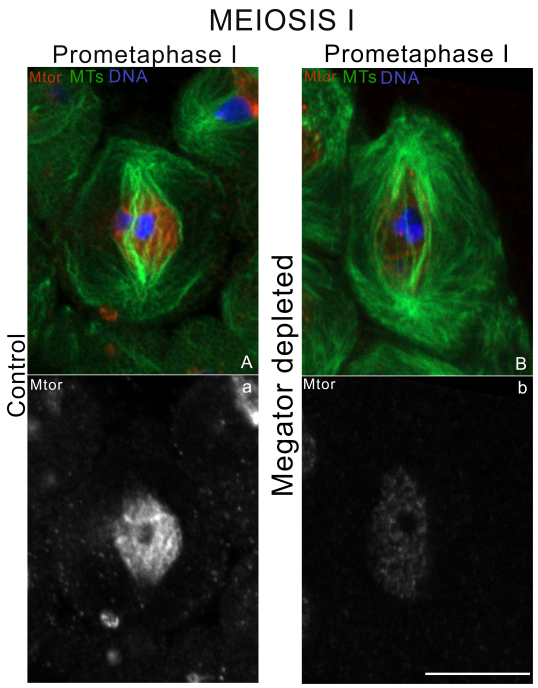

Figure 3.4: Megator shRNA expressing cells have significantly reduced Megator protein fluorescence's depletion efficiency. An example of single section scanning confocal images used to determine Megator intracellular levels in controls (A) and Megator depleted cells (B) during prometaphase I. Scale bar 10μm.

A qualitative examination of single section scanning confocal images acquired under identical conditions revealed a striking difference in the brightness of the Megator signal between treatments. In control cells Megator appeared as a robust prometaphase I spindle matrix signal with the presence of large aggregates (Figure 3.4 A). By contrast, in the Megator shRNA cells the Megator signal was consistently dimmer, sometimes difficult to see above background, and characterised by small speckles (Figure 3.4 B). Thus, the depletion strategy is able to reduce protein levels in meiotic cells. In order to quantify the depletion efficiency, the fluorescence intensity of both the spindle and cytoplasm was measured and compared between control and knockdown cells according to the methodology described in section 2.7. The resulting fluorescence counts (Appendix, Table A.2) were then plotted (Figure 3.5).

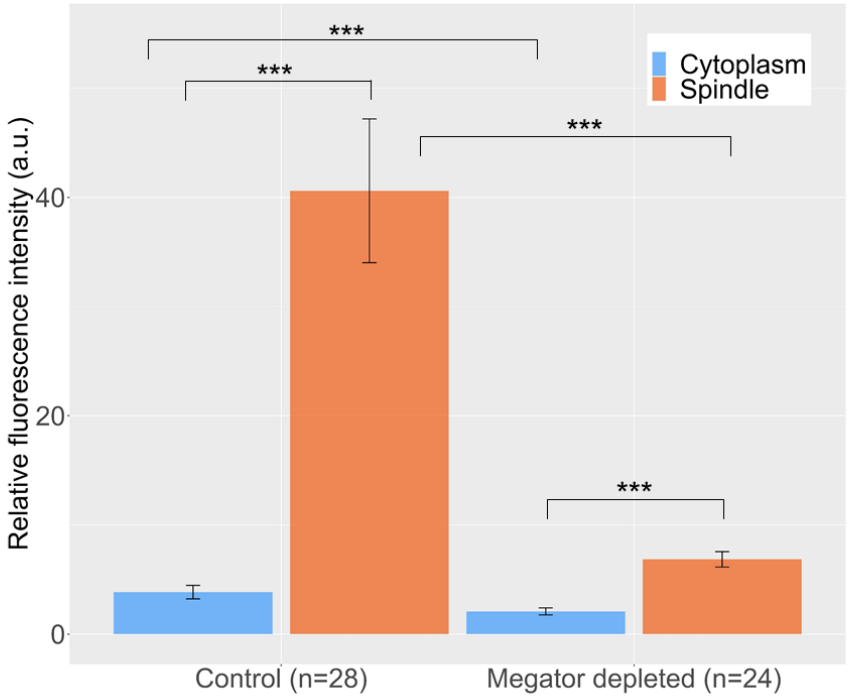

Figure 3.5: Megator shRNA efficiently depletes Megator in MI cells. Differences in Megator's spindle and cytoplasmic accumulations in fixed prometaphase I control (A) and Megator depleted cells (B). The bar plot describes the relative fluorescence intensity of a circle of $7.62\mu m^2$ positioned in the maximum chromosome-free spindle or microtubules-free cytoplasmic area in control (n=28) and Megator depleted cells (n=24) during prometaphase I. Stars indicate the level of significant difference between group averages, calculated with Wilcoxon sign rank test.

The bar plot confirms the fluorescence accumulation in the spindle of Megator depleted cells is considerably reduced compared to control cells. As expected from a visual examination of the images, the difference in fluorescence levels between spindle and cytoplasm in control cells is very large, with the average relative fluorescence intensity in the spindle of control cells being tenfold the average fluorescence in the cytoplasm. Quantification of fluorescence intensity between control and Megator shRNA expressing cells reveals an 85% drop in signal intensity at the spindle matrix. Indeed, matrix and cytoplasm intensities are significantly different following depletion ($p < 0.0001$, Wilcoxon sign rank test), with the fluorescence intensity in the spindle matrix being threefold the one in the cytoplasm.

Notably, the large confidence intervals in the spindle regions of the control cells reflect

the much larger variability of fluorescence that can occur due to the variation in Megator aggregates numbers and sizes (standard error: 3.29, Table 3.1). By contrast, the presence of less aggregates in the Megator depleted cells reflect the reduced variability in the spindle (standard error: 0.35, Table 3.1). The variability in the spindle of Megator depleted cells is a tenth of the variability of fluorescence in the spindle of control cells. The difference in variability is also reduced between cytoplasm and spindle in the depleted cells, as the spindle region has only twofold the fluorescence of the cytoplasm.

	Location	Mean	Standard deviation	Standard error
Control	Cytoplasm	3.85	1.63	0.31
	Spindle	40.60	17.40	3.29
Megator depleted	Cytoplasm	2.08	0.79	0.16
	Spindle	6.85	1.73	0.35

Table 3.1: Fluorescence intensity is significantly reduced in the spindles of Megator depleted cells.

Because of the small size of the sample analysed, the statistical significance of the results was further confirmed with the Wilcoxon sign rank test. This is a non-parametric test used to evaluate the significance of an hypothesis when the standard t-test cannot be performed due to non-satisfied assumptions (e.g., normality, as in this case). Each test produced a p-value: if small ($p < 0.05$), it confirms the significant difference between groups. The test confirmed the existence of a difference between spindle and cytoplasm in the control cells, while there was no significant difference between these pools in the case of Megator shRNA, at a 95% confidence level. Together, these data show that the Megator shRNA can efficiently deplete Megator protein.

3.2.2 Megator promotes matrix localisation of Chromator and Skeletor throughout meiosis

The interaction between Chromator, Skeletor and Megator during mitosis has been documented (Walker et al., 2000; Qi et al., 2004; Rath et al., 2004), but no information is available in meiosis. Therefore, Megator depleted cells (crossing scheme Figure 2.1

B) were stained for Chromator and Skeletor and the distribution of each was analysed by super-resolution scanning confocal microscopy (Figure 3.6).

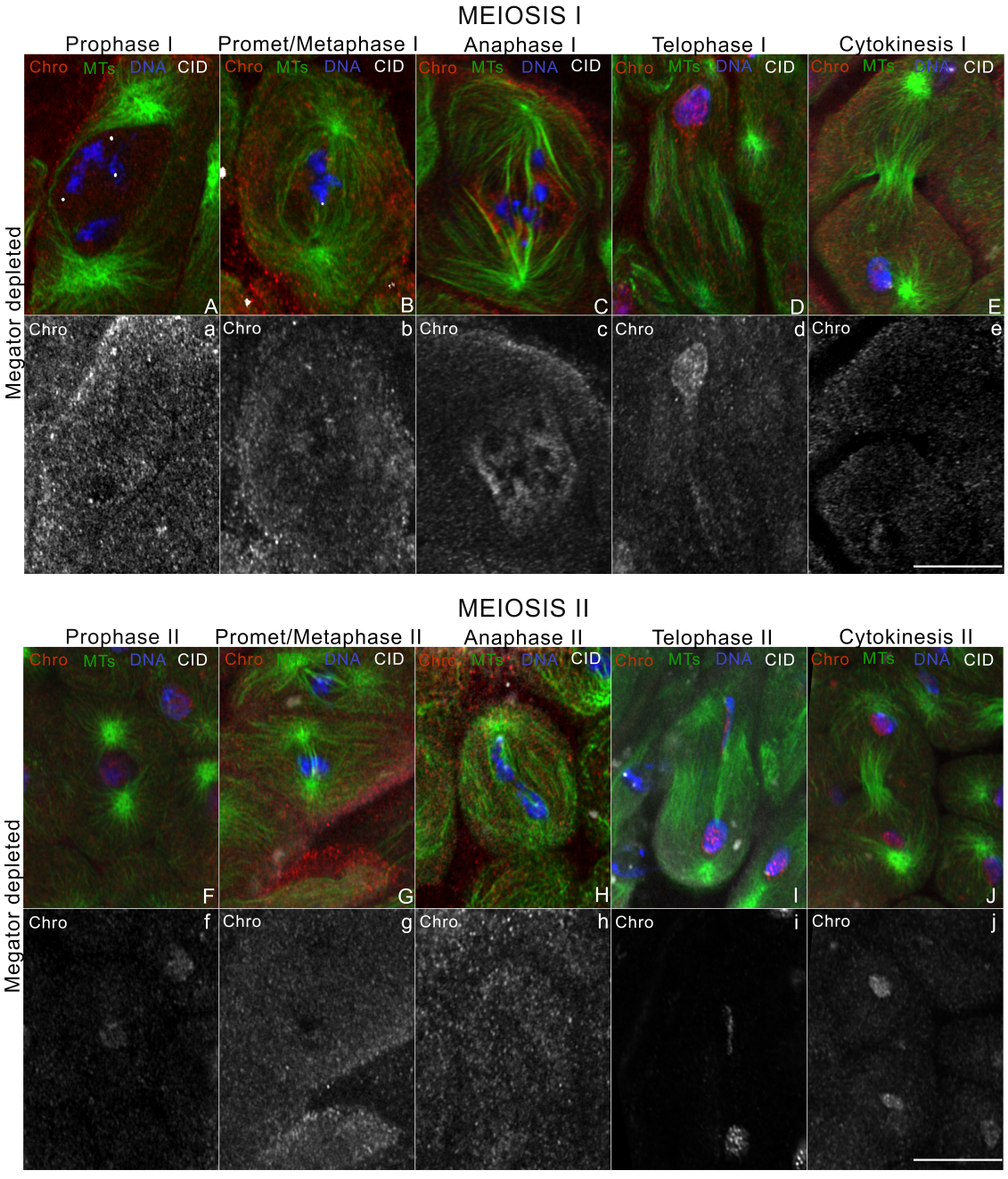

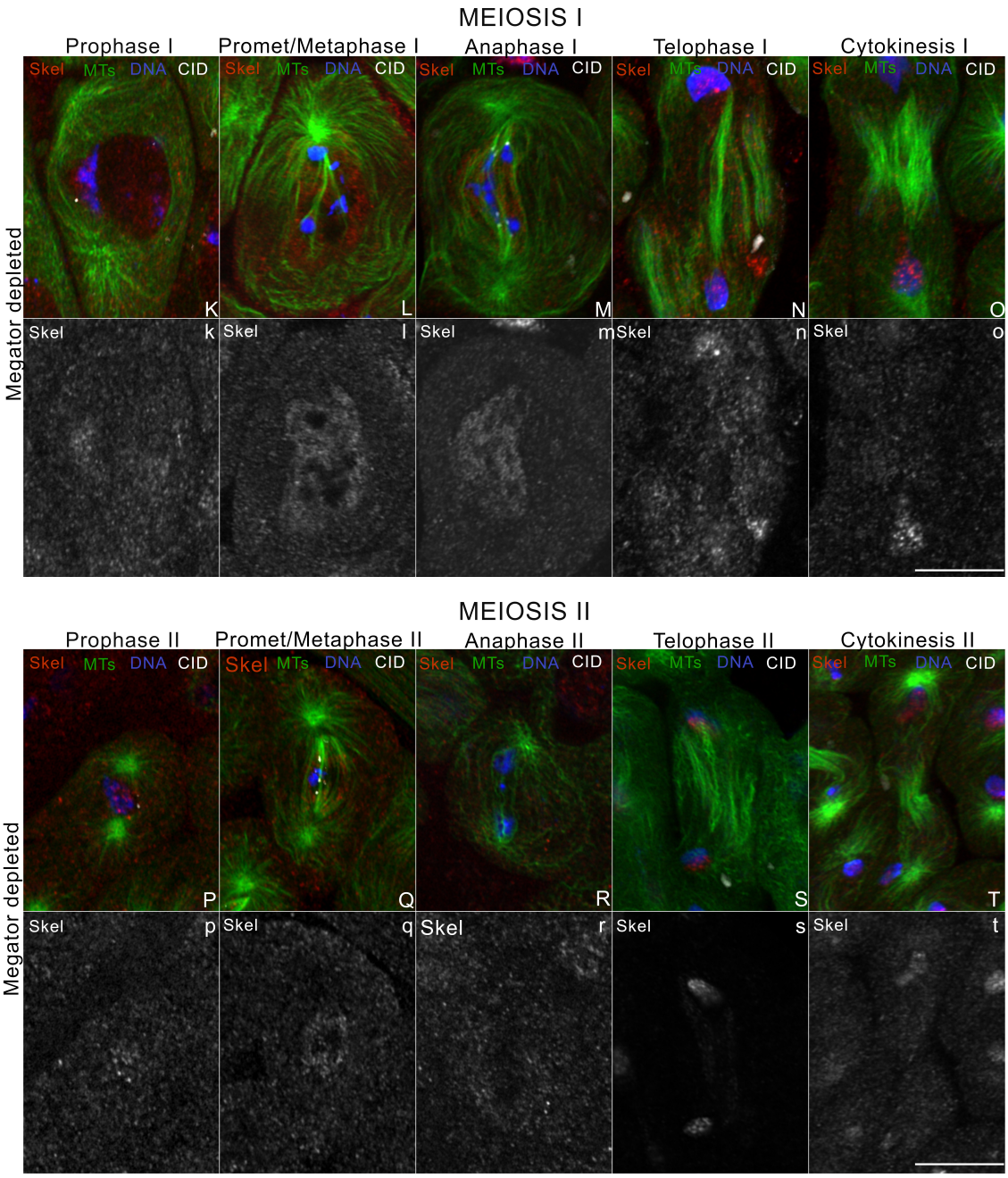

Figure 3.6: Megator depletion decreases the recruitment of the spindle matrix proteins Chromator and Skeletor. Comparative super-resolution scanning confocal microscope images of Megator depleted cells stained for Chromator and Skeletor (both red) during meiosis I (A-E and K-O) and meiosis II (F-J and P-T), relative to DNA (blue), microtubules (MTs, green) and CID (white). Images of Chromator and Skeletor only, during meiosis I (a-e and k-o) and meiosis II (f-j and p-t). All images are Z-projection. Scale bars 10μm.

In Megator depleted cells both Chromator and Skeletor appear reduced during meiosis I (Figure 3.6 a-e and k-o). During prophase I, unlike in control cells (Figure 3.2 a and k), Chromator and Skeletor fail to robustly distribute in the nuclear volume (Figure 3.6 a and k). Instead, their signals are not distinguishable from the background levels. Similarly, during prometaphase/metaphase I and anaphase I, there is less obvious contrast between their spindle regions occupancy and background (Figure 3.6 b and c, l and m). Furthermore, during Skeletor's metaphase I and Chromator's anaphase I, while chromosomes show missegregation, large non-stained regions non corresponding to the area occupied by the chromosomes are present (Figure 3.6 c and l).

During telophase I and cytokinesis I, both Chromator and Skeletor colocalise with the DNA (Figure 3.6 D and E, N and O). However, unlike Chromator, Skeletor does not trail in the spindle's midbody during telophase. These findings during the last stages of meiosis are consistent with what was observed in control cells (Figure 3.2 d and e, n and o), suggesting that the diminished spindle signal of both Chromator and Skeletor are not linked to artifacts or failures of the staining process.

Similarly to meiosis I, Chromator and Skeletor localisation after Megator depletion are reduced during meiosis II. Their signals at the nuclear volume during prophase II, as well as at spindle during metaphase II and anaphase II, appear dim and less in contrast with the background (Figure 3.6 f-h and p-r), especially when compared to Chromator and Skeletor localisation in control cells (Figure 3.2 f-h and p-r). During telophase II and cytokinesis II, Chromator and Skeletor colocalise with the DNA (Figure 3.6 i and j, s and t), suggesting once again that their reduced signals in the previous stages of meiosis are not the results of failures of the staining process.

Together, these data indicate that Megator depletion impairs the Chromator and Skeletor recruitment at the spindle matrix during both meiosis I and meiosis II, suggesting that Megator might play a role in their recruitment in the spindle region during meiosis. Furthermore, the Chromator and Skeletor colocalise with the DNA during both telophase I-II and cytokinesis I-II may suggest that Megator is not involved in the

process.

3.2.3 An examination of Megator's relationship with the *Drosophila*'s Lamin B/Dm0

Lamin B is a highly conserved component of the nuclear lamina which underlines the nuclear envelope in many eukaryotes (Gerace and Burke, 1988; Goldman and Rebhun, 1969). It has also been proposed to be part of the spindle matrix in Xenopus and Hela cells (Tsai et al., 2006; Ma et al., 2009) as well as *Drosophila* embryos (Shi et al., 2014). Lamin B interacts with Tpr in vertebrate cells (Fišerová et al., 2019). Therefore, Lamin B distribution was analysed in *Drosophila* meiosis by super-resolution scanning confocal microscopy using an antibody against *Drosophila*'s Lamin B homologue, Lamin Dm0. (Figure 3.7).

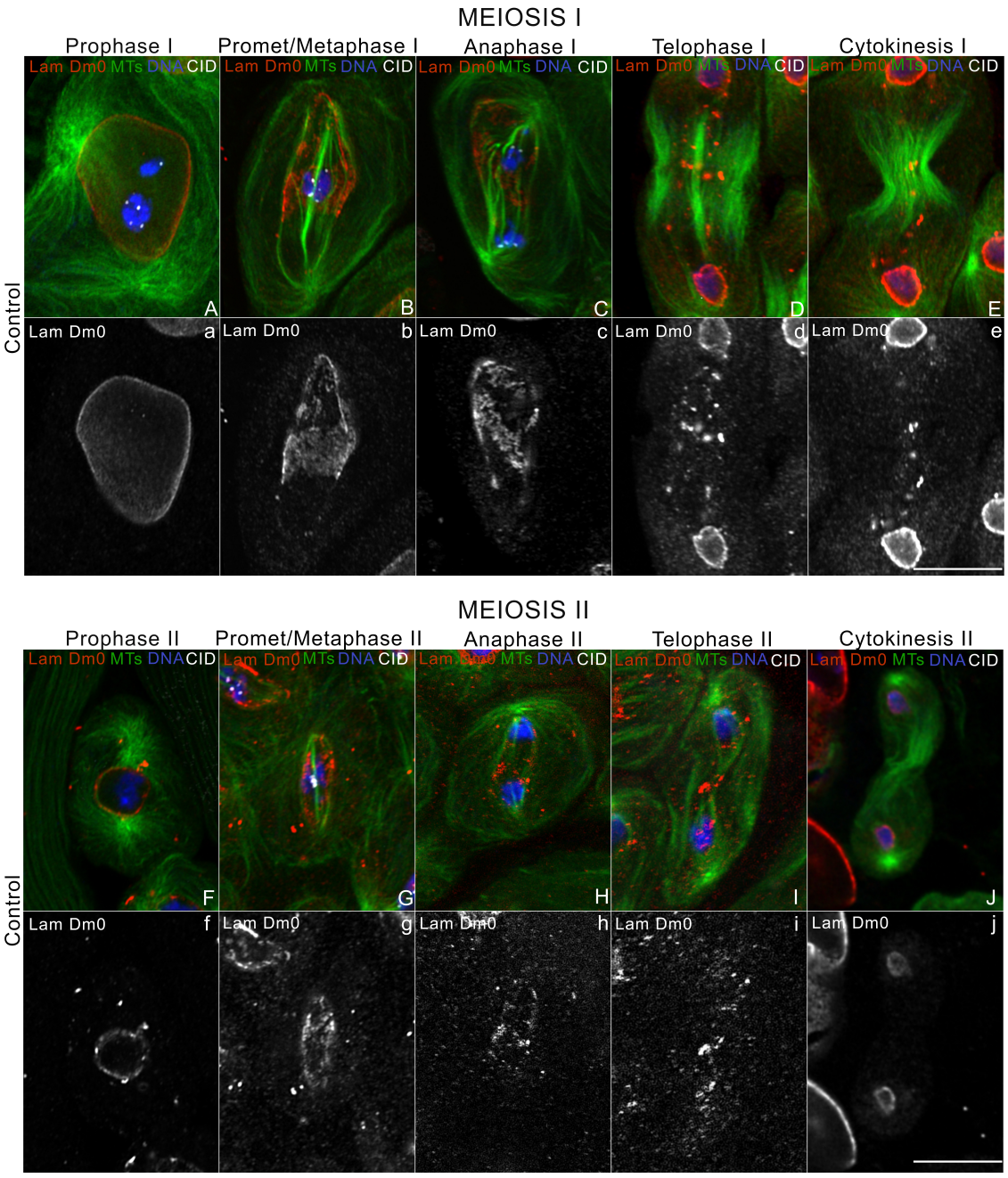
MEIOSIS I
Prophase I
Promet/Metaphase I
Anaphase I
Telophase I
Cytokinesis I
Lam Dm0 MTs DNA CID
Control
A
B
C
D
E
Lam Dm0
a
b
c
d
e
MEIOSIS II
Prophase II
Promet/Metaphase II
Anaphase II
Telophase II
Cytokinesis II
F
G
H
I
J
f
g
h
i
j

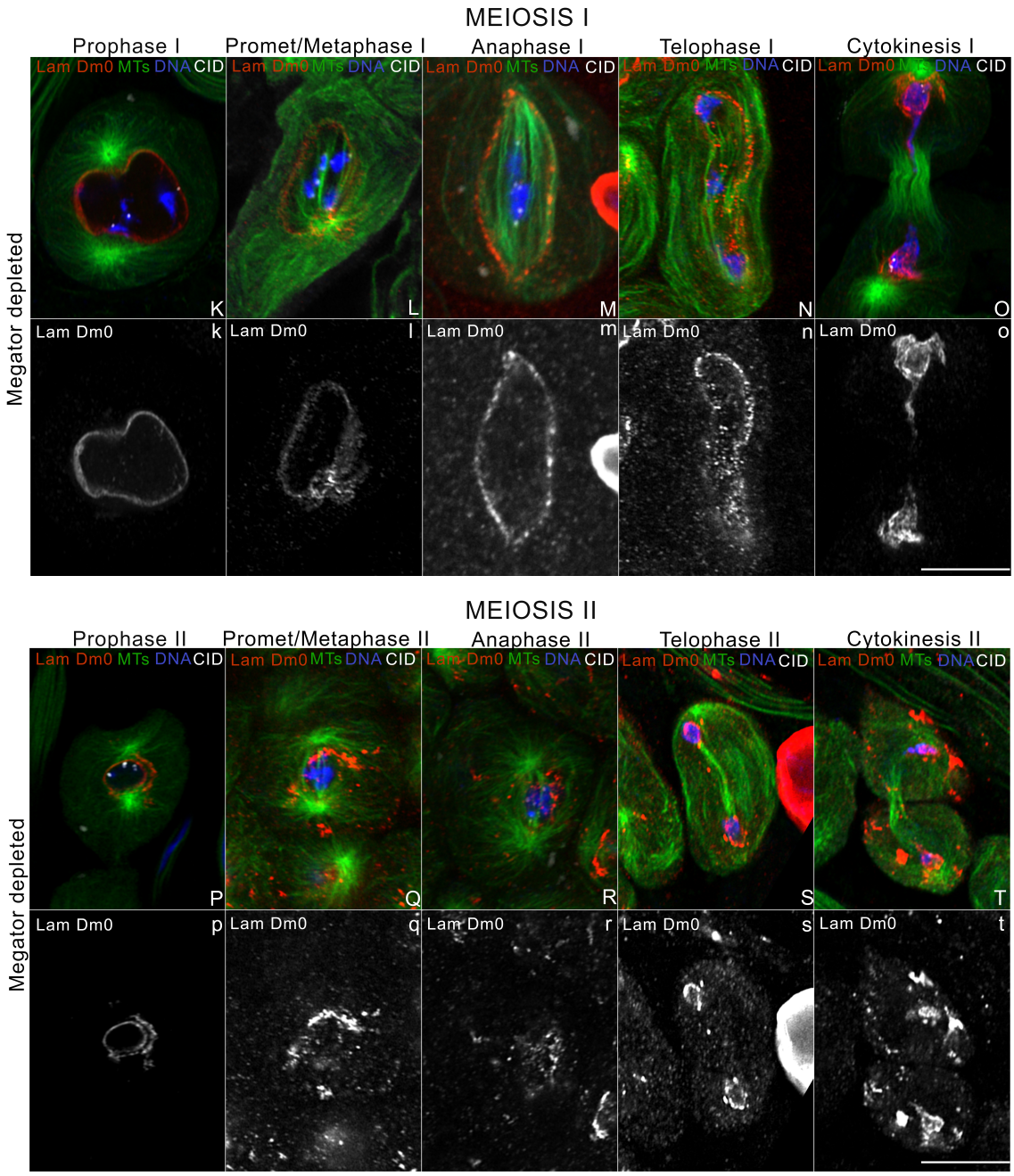

Figure 3.7: Megator depletion induces Lamin Dm0 mislocalisation during meiosis. Super-resolution scanning confocal microscope images of Lamin Dm0 (red) in control and Megator depleted cells during meiosis I (A-E and K-O) and meiosis II (F-J and P-T) relative to the DNA (blue), microtubules (MTs, green) and CID (white). Lamin Dm0 distribution only during meiosis I (a-e and k-o) and meiosis II (f-j and p-t). All images are Z-projection. Scale bars 10 μm.

In control cells, at prophase I, Lamin Dm0 surrounds the nucleus and appears as a sharp ring, indicating the presence of the nuclear lamina (Fig. 3.7 a). During metaphase I, Lamin Dm0 still surrounds the spindle near the spindle envelope (Hayashi et al., 2016). However, its signal concentrates in the centre of the spindle and becomes less visible at the poles, suggesting a breakdown of the nuclear lamin around that area (Hayashi et al. (2016), Figure 3.7 b). This phenomenon becomes more visible during anaphase I, where both poles show less Lamin Dm0 signal (Figure 3.7 c). During telophase I and cytokinesis I, the Lamin Dm0 surrounds the nuclei with few spots present along the axis of the elongated spindle (Figure 3.7 D and E).

In control cells, the Lamin Dm0 distributions during meiosis II are similar to the one in meiosis I: at prophase II, Lamin Dm0 surrounds the nucleus (Figure 3.7 f), while at both metaphase II and anaphase II the Lamin Dm0 signal is absent near the spindle poles (Figure 3.7 g and h). During late anaphase-early telophase II the signal of Lamin Dm0 was hardly detectable near the DNA (Figure 3.7 i). However, Lamin Dm0 is yet again clearly visible during cytokinesis II, where its signal collects around the daughter nuclei, as seen in meiosis I (Figure 3.7 j).

In Megator depleted cells, during prophase I Lamin Dm0 collects around the nucleus, as seen in control cells (Figure 3.7 k), while at prometaphase/metaphase I and anaphase I, it still surrounds the spindle envelope (Figure 3.7 l-m). However, in contrast to control cells during the same stages, Lamin Dm0 does not accumulate in the central areas of the spindle in the region of the matrix. Additionally, rather than being removed at the poles, it appears to surround the spindle and be punctuated or made of small particles (Figure 3.7 l and m).

Similarly, during telophase I, Lamin Dm0 does not concentrate around the nuclei, in contrast to what is seen in control cells. Although, fragments of the nuclear lamina are still visible, with traces in the spindle length (Figure 3.7 n). At cytokinesis I onset, Lamin Dm0 mirrors its localisation in control cells. However, as the nuclei appear misshaped, the Lamin Dm0 signal is less defined (Figure 3.7 o).

During prophase II, following Megator depletion, Lamin Dm0 redistributes around the nucleus indicating the reforming of the nuclear lamina at the beginning of meiosis II (Figure 3.7 p). Throughout prometaphase/metaphase II and anaphase II, Lamin Dm0 is scattered in fragments or in bands near the spindle envelope, suggesting a fragmentation of the nuclear lamina (Figure 3.7 q and r). During telophase II and cytokinesis II, despite the Lamin Dm0 signal relocating to the nuclei, the fragments are still visible (Figure 3.7 s and t).

Together these data show that, in the presence of endogenous levels of Megator, Lamin Dm0 distributions are similar during meiosis I and II. Indeed, Lamin Dm0 is present at the nuclear envelope from the onset of prophase to anaphase, and later associates with the DNA during telophase and cytokinesis. However, upon Megator depletion, Lamin Dm0 fails to be efficiently redistributed in the spindle. Therefore these data indicate that Megator may not be essential for its recruitment, but rather regulates Lamin Dm0's organisation.

3.2.4 Megator is required for accurate chromosome segregation in meiosis

Previous studies on the impact of Tpr/Megator depletion in somatic cells reported lagging chromosomes (Qi et al., 2004; Lince-Faria et al., 2009; Nakano et al., 2010). In the fixed cells analysis carried so far, glimpses of these abnormalities have been observed (Figures 3.6). Furthermore, misshapen nuclei at telophase during both meiosis I and meiosis II as a consequence of Megator depletion (Figure 3.7), suggests the presence of karyokinesis errors. Therefore, analysis of onion stage spermatids followed by super-resolution scanning confocal microscopy to quantify defects and characterise phenotypes, was carried out.

Onion stage spermatids are the post-meiotic cells that differentiate into sperm (Figure 1.1, F). Viewed under phase contrast microscopy, each spermatid has one nucleus and one nebenkern, a large mitochondrial derivative. Their ratio, in the absence of both

chromosome segregation and cytokinesis errors, is therefore 1:1. Examining this ratio is a well-established read-out of meiotic fidelity (González et al., 1989): the presence of multiple nuclei, as well as the total absence of it, indicates defects at cytokinesis, while neberken defects are related to errors in the chromosome segregation. Thus, the nebenkern to nuclei ratios (phase dense structures and phase light structures, respectively. Figure 3.8 A-E) were determined (as described in section 2.8) in all homozygous parental lines and their progeny (Table 3.2 and in the Appendix, Table A.3).

In each of the homozygous parental lines, as well as in the control cells progeny, the total percentage of defects was always less than 2%. In contrast, the total percentage of defects for Megator depleted progeny was almost 30%, with 0.1% of cells having a 1:2 nebenkern to nuclei ratio, 1.2% with 2:1, 1.3% cells exhibiting 0:1 and 3.3% with 2:0. The most commonly observed ratio was 19% for cells with 1:0. These data suggest the presence of several defects in the Megator depleted cells.

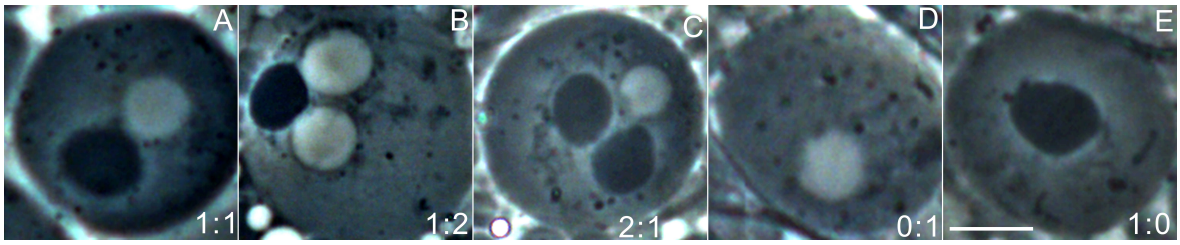

Figure 3.8: Onion Stage spermatids reveal multiple defects in Megator depleted cells. Phase contrast images of normal nebenkern (phase dense structure) to nuclei (phase light structure) ratio in the onion stage spermatids (A). Examples of abberrations in the nubenkern to nuclei ratios observed in the Megator depleted cells (B-E). Scale bar is 10μm.

Shortened genotype name	Nebenkern to Nuclei Ratio %								n	Defect (%)
	1:1	1:2	2:1	0:1	1:0	2:0	0:2	Other		
$+;\beta\text{-}tubulinEGFP//;bam\text{-}GAL4//;+$	99.2	0.2	0.4	0.0	0.2	0.0	0.0	0.0	1203	0.83
$+;+;UAS\text{-}Mtor//;+$	98.3	0.3	0.1	0.2	0.5	0.3	0.0	0.4	1109	1.71
$w(CS10)//;+;+;+$	99.1	0.1	0.2	0.0	0.1	0.3	0.0	0.2	1471	0.88
$+;\frac{\beta\text{-}tubulinEGFP}{+};\frac{bam\text{-}GAL4}{UAS\text{-}Mtor};+$	70.4	0.1	2.1	1.3	19.4	3.3	0.6	2.9	1384	29.62
$\frac{w(CS10)}{+};\frac{\beta\text{-}tubulinEGFP}{+};\frac{bam\text{-}GAL4}{+};+$	99.1	0.1	0.1	0.0	0.4	0.1	0.0	0.3	1126	0.89

Table 3.2: Megator depletion leads to high rates of meiotic defects. The table shows the percentage of defects in all the homozygous parental lines (first three strains in the table) and in the progeny (two bottom strains in the table), based on the nebenkern to nuclei ratios counted in their onion stage spermatids.

The onion stage spermatid counts revealed failure in accurate chromosome segregation during meiosis. To determine the nature of the segregation defects and whether they occur in meiosis I or meiosis II, super-resolution microscopy was employed to directly examine dividing cells. Therefore, control and Megator depleted cells were analysed by scanning super-resolution microscopy to investigate (i) chromosome placement and (ii) the interactions between the spindle and kinetochores (Figure 3.9).

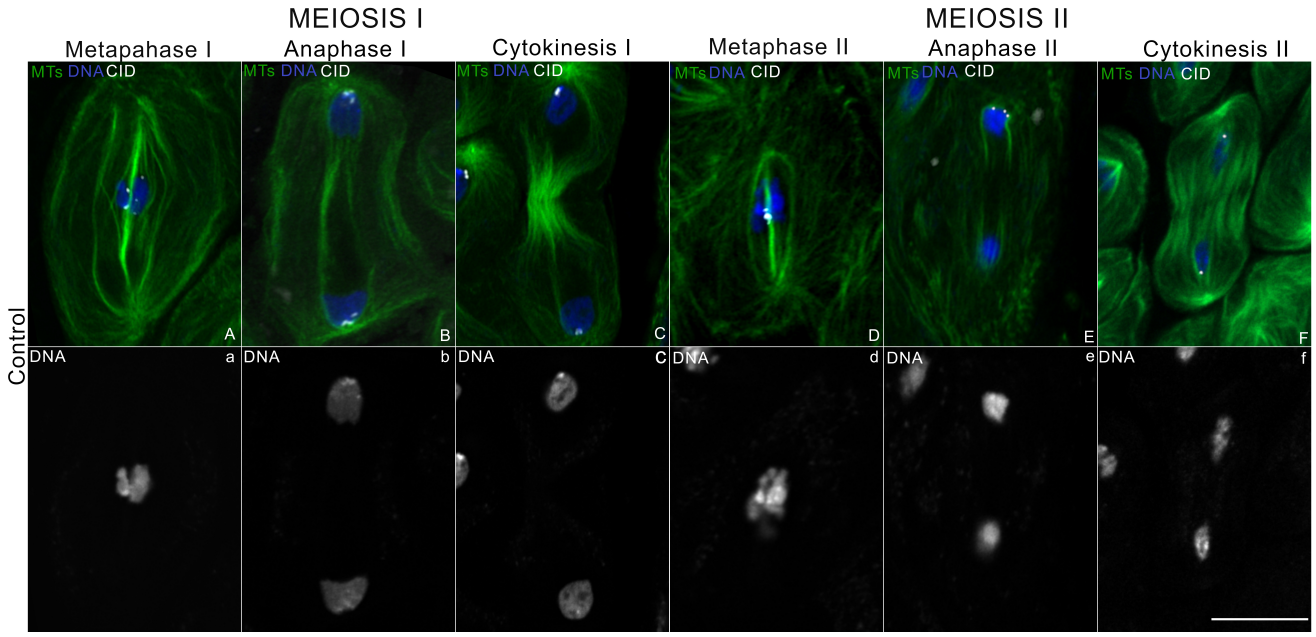
MEIOSIS I
MEIOSIS II
Metapahase I
Anaphase I
Cytokinesis I
Metaphase II
Anaphase II
Cytokinesis II
Control
MTs DNA CID
DNA
A
B
C
D
E
F
a
b
c
d
e
f

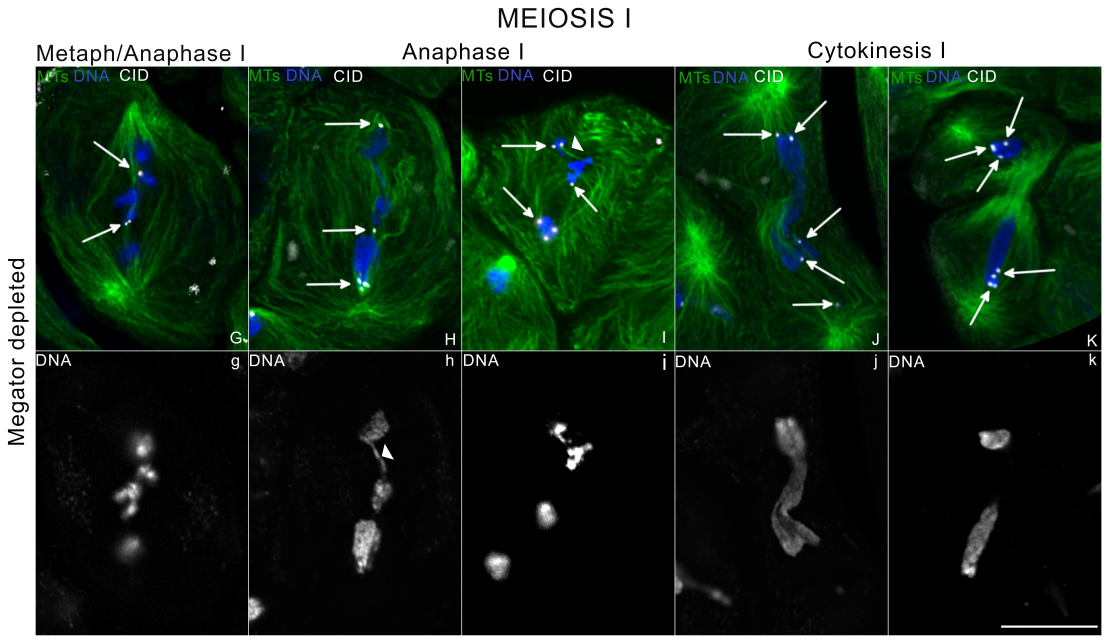
MEIOSIS I
Metaph/Anaphase I
Anaphase I
Cytokinesis I
Megator depleted
MTs DNA CID
DNA
G
H
I
J
K
g
h
i
j
k

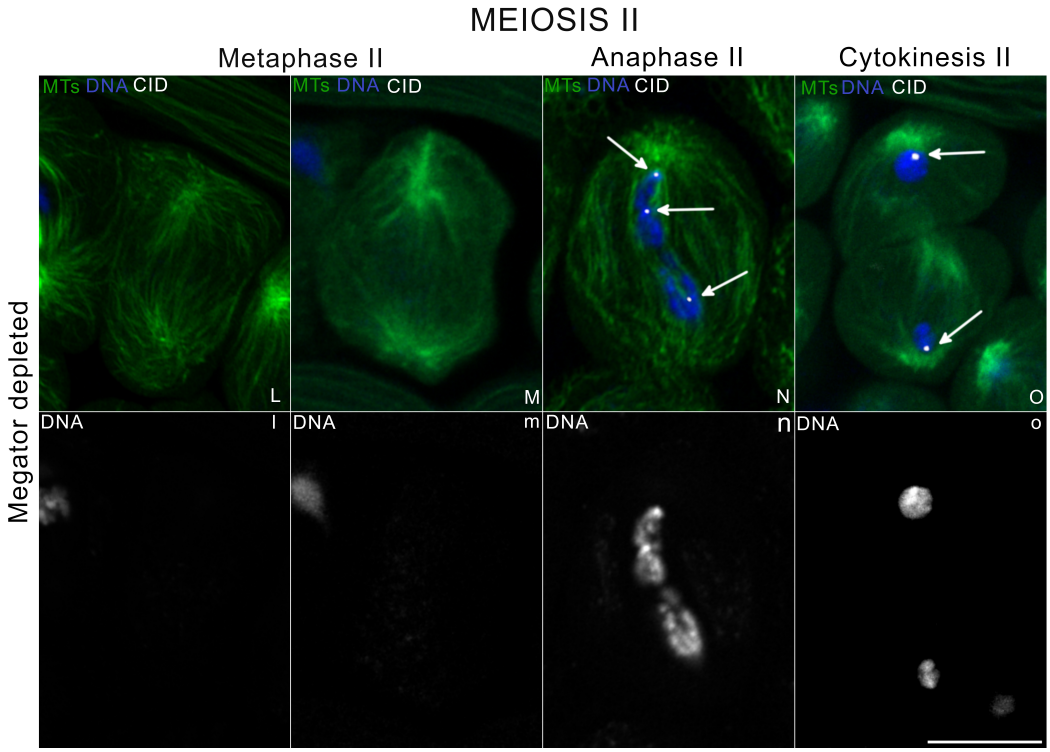

Figure 3.9: Megator is crucial for correct chromosome segregation in both meiosis I and meiosis II. Super-resolution scanning confocal images of control cells during meiosis I (A-C) and meiosis II (D-F). Gallery of some defects observed following Megator depletion during meiosis I (G-K) and meiosis II (L-O). DNA is blue, microtubules (MTs) are green and CID is white. Arrows highlight centromeres. Arrowheads indicate chromosomes linked together by a single microtubule (I) and chromatin bridges (h). All images are Z-projection. Scale bars 10 μm.

In control cells at metaphase I and II, the spindles have a well-defined fusiform shape with well-organised microtubules. The k-fibres bind chromosomes to the spindle through their kinetochores (indicated by CID) (Figure 3.9 A and D). During late anaphase I and II, the spindle is elongated with the chromosomes evenly distributed in the opposite region of the spindle (Figure 3.9 B and E). During cytokinesis I and early cytokinesis II, the bipolar spindle remodeled into the central spindle (Figure 3.9 C and F). The DNA is symmetrically distributed in these two forming daughter cells, as shown by the equally sized chromatin masses (Figure 3.9 c and f).

In contrast, Megator depleted cells display a wide range of defects in both meiosis I and II. During meiosis I, spindles could be disorganised to varying extents. The astral

microtubules could be wavy (Figure 3.9 G-I) and the k-fibers appear not straight and thick as in control, but rather thin and bent (Figure 3.9 G). Likewise, although the CID label was sometimes difficult to detect in these cells, the centromeres did not appear to bind the regular, short and linear k-fibres seen in controls. Instead, they were attached to long often wavy or bent microtubules. Frequently, bundles of microtubules invade the spindle volume, making the cells almost devoid of any defined spindle shape (Figure 3.9 H and I). Furthermore, the increased number of microtubules produces bridges between multiple dispersed chromosomes (Figure 3.9 I, arrowhead).

In some cases microtubules appear to emanate from opposing or multiple regions of the spindle and contact the single chromosome in anaphase, suggesting that some of these chromosomes are merotelically oriented (Savoian M. S., unpublished observations). Once again, during cytokinesis I microtubules are wavy and poorly organised. In some cases cells also display a not well-formed central spindle (Figure 3.9 J). The DNA during meiosis I is equally undefined. During late metaphase I, chromosomes associated with the k-fibre are lagging in the spindles (Figure 3.9 g), instead of being equally segregated as in control. Chromatin bridges are present between highly decondensed DNA of different sizes (Figure 3.9 h, arrowhead).

Cells in cytokinesis are unable to cleave the original cells in two, and the DNA appears as a long undefined mass occupying the central volume of the original cells (Figure 3.9 j). Some cells show the formation of two daughter cells, but the highly decondensed DNA is unequally distributed, as shown by the different sizes of the chromatin masses (Figure 3.9 k). These findings suggest that Megator is crucial for correct chromosome segregation as well as may play a role in spindle morphology in meiosis I.

During meiosis II, multiple defects were visible, some of which were more severe than the one observed during meiosis I. Following Megator depletion, the spindle microtubules appear disorganised. During metaphase II, some cells show abnormally shaped astral microtubules and a lack of bipolar spindle (Figure 3.9 L and M). Remarkably, some cells are completely devoid of DNA, as confirmed by examining the DNA channel

(Figure 3.9 l and m). This could be the direct effect of the defects occurring during cytokinesis I. During anaphase II, some cells show spindles with wavy or bent astral microtubules (Figure 3.9 N). Consistent to defects observed in meiosis I, the chromosomes in these spindles are highly decondensed. Instead of being collected at the two ends of the spindle, as in control cells, the chromatin masses fill much of the space of the spindle volume including its equator (Figure 3.9 n). During cytokinesis II, the chromosomes are again unevenly distributed between the two daughter cells (Figure 3.9 o).

Together these results show that Megator depletion leads to a large range of defects in both meiosis I and II. Similar to mitosis (Qi et al., 2004; Lince-Faria et al., 2009; Nakano et al., 2010), after Megator depletion chromosomes are lagging throughout the spindle volume and, during cytokinesis, unequally distributed. This suggests that Megator is crucial for chromosome segregation. Unlike studies in mitosis, where no major defects in spindle morphology have been found, Megator depletion in meiosis may also affects spindle organisation.

Chapter 4

Discussion and future directions

The experiments proposed here provide the first data on Megator distributions during meiosis I and II. The data reveal that this protein displays a different localisation between meiosis I and II, suggesting that Megator may be a spindle matrix protein in meiosis I, but not in meiosis II or have other functions.

Analysis of the functional effects of its RNAi mediated depletion provide the first evidence on Megator crucial roles during meiosis. Immunostaining of Megator depleted cells for other spindle matrix proteins - Chromator, Skeletor and Lamin B - showed that Megator depletion attenuates Chromator and Skeletor recruitment to the spindle region and triggers the fragmentation of structures composed of Lamin Dm0, the *Drosophila*'s Lamin B homologue. Importantly, Megator knockdown also led to high rates of karyokinetic and cytokinetic errors, as revealed by the counting of neberken to nuclei ratios in the onion stage spermatids.

Furthermore, the cytological analysis of each division using super-resolution scanning confocal microscopy showed a large range of aberrations that include wavy and bent microtubules, lagging chromosomes and, in some cases, cells lacking DNA or any trace of a spindle. This indicates that Megator plays a crucial role in chromosome segregation during meiosis and may be involved in the process of spindle formation or maintenance.

4.1 The spindle matrix is a highly conserved feature of dividing cells

The spindle matrix is a cell division structure that has been suggested in order to account for non microtubules structures or behaviours displayed by the spindle (Forer and Goldman, 1969; Pickett-Heaps et al., 1982; Spurck et al., 1997; Forer et al., 2003; Maiato et al., 2004; Sauer et al., 2005; Johansen and Johansen, 2009).

One proposed spindle matrix function is to serve as a barrier that restricts and confines the spindle assembly factors (SAFs) after nuclear envelope breakdown in mitotic cells (Katsani et al., 2008). These factors would supply mechanical support for microtubules during chromosome segregation (Walker et al., 2000; Qi et al., 2004; Rath et al., 2004; Pickett-Heaps and Forer, 2009; Lince-Faria et al., 2009; Ding et al., 2009) or be a catalytic platform for the recruitment of the spindle assembly checkpoint (SAC) proteins (Lee et al., 2008; Lince-Faria et al., 2009; De Souza et al., 2009; Rodriguez-Bravo et al., 2014).

The spindle matrix in mitosis has an heterogeneous collection of components (Janmey et al., 1995; Rath et al., 2004; Qi et al., 2004; Chang et al., 2005; Tsai et al., 2006; Hayes, 2006; De Souza and Osmani, 2009; Lince-Faria et al., 2009; Qi et al., 2009; Yao et al., 2018). Some of these components - Megator, Chromator, Skeletor, EAST and Asator (Walker et al., 2000; Rath et al., 2004; Qi et al., 2004, 2005, 2009) - have been all found in *Drosophila*. However, only the nucleopore protein Megator (Tpr in mammalian) is consider to be a mitotic spindle matrix protein highly conserved across species (Cordes et al., 1997; Zimowska et al., 1997; Strambio-de Castillia et al., 1999; Qi et al., 2004; Xu et al., 2007; Bae et al., 2009; De Souza et al., 2009; Lince-Faria et al., 2009; Holden et al., 2014).

The conservation of Megator-like proteins as well as their distribution and function in mitotic systems, suggests that the spindle serves a conserved purpose. However, no information is available on Megator function during meiosis or the existence of a

meiotic spindle matrix.

In this study, immunofluorescence imaging of *Drosophila* primary spermatocytes revealed that at the onset of the first meiotic division, Megator is present in the nuclear volume and at the nuclear rim, consistent with Megator being a nucleopore protein (Zimowska et al., 1997). From prometaphase I to anaphase I, the protein surrounds the microtubules of the spindle in the position of the predicted spindle matrix. Along with a general distribution, it formed aggregates of variable size.

Following exit from anaphase I and telophase I, the Megator signal can be seen near the nuclei. The distribution is similar to the one seen in mitotic cells, indicating that Megator forms a matrix in meiosis I (Zimowska et al., 1997; Qi et al., 2004, 2005; Lince-Faria et al., 2009; Yao et al., 2012). Hence, a Megator-based spindle matrix is a conserved feature of mitotic and some meiotic cells.

To further characterise the spindle matrix in meiosis I, the meiotic distributions of Chromator and Skeletor, two other *Drosophila* spindle matrix proteins were studied. Each of these has been characterised in mitotic systems and shown to interact with Megator (Walker et al., 2000; Rath et al., 2004; Qi et al., 2004; Wasser et al., 2007; Ding et al., 2009). Consistent with mitosis (Walker et al., 2000; Rath et al., 2004), both proteins are present in the nucleus during prophase I, robustly redistribute to the spindle during chromosome alignment and segregation and relocate in the daughter cell nuclei during cytokinesis I. Therefore, like Megator, the mitotic spindle matrix proteins Chromator and Skeletor are also conserved during meiosis I.

In mammalian systems Lamin B is a nuclear lamina component (Goldman and Rebhun, 1969) that associates with Tpr as part of the nuclear pore complex (Fišerová et al., 2019). Lamin B localises adjacent to the mitotic spindle in some systems (Xenopus eggs, Hela cells (Tsai et al., 2006; Ma et al., 2009) and *Drosophila* embryos (Shi et al., 2014), making Lamin B a spindle matrix protein. Therefore, the meiotic distribution of Lamin B, Lamin Dm0 in *Drosophila*, was also analysed. Immunofluorescence images

acquired during meiosis I show that Lamin Dm0 occupies the region surrounding the spindle during metaphase I, consistent with a recent report (Hayashi et al., 2016). These data indicate that like Megator and its established partners, Lamin B is also a spindle matrix protein during meiosis I.

Together, these data show that a spindle matrix is conserved between mitosis and meiosis I. They further indicate that four established mitotic spindle matrix proteins represent at least a semi-conserved group of matrix factors.

4.2 The spindle matrix composition is not conserved between mitosis and the two meiotic divisions

In an effort to obtain a more completely characterised matrix conservation in meiosis, the distributions of Megator, Chromator, Skeletor and Lamin Dm0 were also analysed during meiosis II. It was found that all of these show distributions that mirror the ones in meiosis I. Indeed, Chromator and Skeletor localise within the nuclear volume during prophase II, around the spindle during prometaphase and metaphase II and are associated with the DNA at the end of division, during cytokinesis II. Similarly, Lamin Dm0 surrounds the nucleus at prophase II, concentrates around the spindle during chromosome alignment and segregation and again surrounds the daughter nuclei at cytokinesis II.

However, in striking contrast with these findings and the first meiotic division, Megator did not localise to the nuclear volume or at the nuclear rim during prophase II. Nor did it redistribute around the spindle during chromosome movement. Instead, its signal was detected only in the cytoplasm in the form of small scattered granules throughout all of meiosis II.

The absence of Megator signal in meiosis II was also confirmed by the analysis of the fluorescent protein tagged Megator-mCherry. While the possibility of the antibody

epitope masking effect can't be ruled out completely to account the absence of Megator signal in meiosis II, it is unlikely as the Megator distributions observed with the fluorescent protein tagged Megator-mCherry mirror the results obtained with antibody staining.

Together, these data suggest that the spindle matrix is a feature that is highly conserved during meiosis II, as indicated by Chromator, Skeletor and Lamin Dm0 distributions. However, the absence of Megator in the spindle during meiosis II is in contrast with mitotic studies where Megator, along with Chromator, Skeletor and Lamin B, was documented to be spindle matrix proteins (Walker et al., 2000; Rath et al., 2004; Qi et al., 2004; Tsai et al., 2006; Lince-Faria et al., 2009). Also, these findings are in contrast with virtually all mitotic studies in which Tpr has been documented to be the only highly conserved spindle matrix protein (Cordes et al., 1997; Zimowska et al., 1997; Strambio-de Castillia et al., 1999; Qi et al., 2004; Xu et al., 2007; Bae et al., 2009; De Souza et al., 2009; Lince-Faria et al., 2009; Holden et al., 2014). This raises questions about the existence and composition of a minimal or fundamental spindle matrix, not only during meiosis but also between systems.

4.3 Megator may be a master controller of spindle matrix composition

During mitosis, Chromator, Skeletor and Megator interact (Walker et al., 2000; Rath et al., 2004; Qi et al., 2004). Indeed, co-immunoprecipitation experiments show that Skeletor is associated with Chromator (Rath et al., 2004) and Chromator interacts with Megator (Qi et al., 2004). However, no information is available on their relationship in meiosis. Likewise, while the nucleopore protein Tpr is needed for Lamin B organisation in the nuclear lamina in somatic cells (Fišerová et al., 2019), there is no evidence that the same occurs in meiosis. Therefore, to evaluate the role of Megator in recruiting these matrix proteins in meiosis, the protein was depleted using RNAi targeted gene silencing, followed by analysis by super-resolution scanning confocal microscopy.

In meiosis, depletion of Megator impairs Chromator and Skeletor recruitment at the spindle in both meiosis I and meiosis II. Indeed, during both meiosis after Megator depletion, the proteins signals are dimmer in the spindle matrix and increased in the cytoplasm, with the two signals being almost indistinguishable. These findings are in stark contrast with Chromator and Skeletor distributions in presence of endogenous levels of Megator proteins, suggesting that Megator plays an important role in Chromator and Skeletor recruitment efficiency to the spindle matrix. It will be of future interest to determine if the interactions between Megator and Chromator and Skeletor are conserved in meiotic cells, as suggested by these findings.

Examination of the meiotic distributions of the spindle matrix protein Lamin Dm0, following Megator depletion, were equally revealing. Lamin Dm0 signal is excluded from the spindle during both meiosis I and II. How Megator influences Lamin Dm0 recruitment to the matrix is unclear. No direct interactions have been reported in somatic tissues. This may indicate meiotic cell unique interactions. Alternatively, Megator may act as a master scaffold upon which other proteins collect. It will therefore be interesting to study the recruitment hierarchies of the meiotic matrix using RNAi to deplete other matrix proteins such as Chromator, Skeletor and Lamin Dm0 to see how it affects the others.

4.4 The lack of a Megator-defined spindle matrix in meiosis II is in contrast with studies in mitosis

Quite surprisingly, Megator is absent from the nuclear rim at prophase II and its signal is detected only at background level throughout all meiosis II. Yet, in cells with endogenous levels of Megator, Chromator and Skeletor are able to localise in the spindle during metaphase II. Similar events occur with Lamin Dm0 where its signal is detected in the spindle during metaphase II.

At a glance, the Megator absence in meiosis II challenges the idea of Megator being somehow needed for the efficient localisation of Chromator, Skeletor and Lamin Dm0.

However, the possibility cannot be ruled out as (i) in mitosis these spindle matrix proteins interact (Walker et al., 2000; Rath et al., 2004; Qi et al., 2004; Fišerová et al., 2019) and (ii) as shown in this study, following Megator depletion Lamin Dm0 is not present in the spindle while Chromator and Skeletor are not efficiently recruited.

During meiosis, Megator forms aggregates of variable size, not corresponding to the DNA and dispersed in the spindle during meiosis I, and scattered in the cytoplasm during meiosis II. The nature of these aggregates is unknown and difficult to address, as many factors could contribute to the phenomenon (March et al., 2021; De Simone et al., 2012). They appeared smaller and less bright than the particles seen throughout meiosis I. The changes of value intensity from MI to MII may reflect proteolytic degradation of the protein at the end of MI, or a failure to be recruited to the nucleus or spindle matrix and a retention in the cytoplasm. As a consequence, it could be speculated that the Megator concentration accumulated during meiosis I could be enough to trigger the localisation of Chromator, Skeletor and Lamin Dm0 at the spindle during meiosis II. However, it seems unlikely (even without measuring the intensity values) as the granules appear smaller and less bright.

Another possible explanation for the absence of Megator signal during meiosis II is due to the protein being masked by unknown meiosis II proteins that prevent the antibody from binding (Surface Epitope Masking or SEM). To test this hypothesis, two different lines expressing the fluorescent protein tagged Megator-mCherry were used. These strains, originally described in Yao et al. (2018), express the fusion proteins under control of the endogenous *Megator* promoter, making their expression levels and patterns conserved with the endogenous wild type protein. Because this transgene is expressed in the presence of the untagged endogenous protein, it raises the possibility that overexpression effects could occur. This was not reported in the original paper describing the transgenic flies and its investigation was beyond the scope of this work. However, no outstanding abnormalities were noted during the distribution studies reported here.

In both Mtor-mCherry lines aggregates of Megator occupy the nuclear space and the

nuclear rim at prophase I. During prometaphase/metaphase I, Megator redistributes in the spindle and, during cytokinesis I, near the reforming nuclei. By contrast, Megator-mCherry signals were not detected above background level throughout meiosis II. As the Megator-mCherry results duplicate those observed with Megator antibody, it is possible to conclude that there is no significant blocking of Megator recognising epitopes during meiosis. As the Megator-mCherry construct was engineered starting from a genomic region of 949 nucleotides upstream of the start codon, it is presumed to contain all of the endogenous regulatory sequences, including the promoter (Yao et al., 2018). Thus, it is reasonable to predict that the behavior of the protein mirrors the Megator wild type. Consequently, the Megator-mCherry signal observed during meiosis I and II indicates the Megator's actual behavior.

Alternatively, the presence of Megator only at the background level during meiosis II may suggest that Megator may be expendable as a matrix protein in some cell types or conditions. This is in contrast with mitosis where Tpr/Megator, due to its long coiled-coil domain, is considered to be a structural component of the spindle matrix (Qi et al., 2004). However, as suggested by a proteomic analysis, the knowledge on the mitotic spindle is far from being complete (Sauer et al., 2005) and the spindle in MII is largely uncharacterised, thus the matrix composition. It is possible that Megator does not represent a structural component of the spindle matrix in MII and this role is carried out by other components, not characterised in this study.

Therefore, it is clear that Megator is needed for Chromator, Skeletor and Lamin Dm0 efficient recruitment during meiosis I and meiosis II, but further studies - such as the examination of the recruitment hierarchies between proteins and characterisation of the spindle during meiosis II - are needed.

4.5 Megator absence at the nuclear rim at prophase II opens a question about the NPC composition during meiosis II

Notably, Skeletor and Chromator are chromatin binding proteins (Walker et al., 2000; Rath et al., 2004), hence they need to be imported in the nucleus. Similarly, Lamin B, which is part of the nuclear lamina, is imported into the nucleus through the NPC (Newport, 1990; Moir et al., 2001; Jevtić et al., 2019).

The nuclear pore complex (NPC) is a multiprotein complex and selective barrier existing in the nuclear envelope (Sorokin et al., 2007). The primary role of NPC is to control the flow of macromolecules as well as allow the diffusion of smaller ones (Wente and Rout, 2010). Tpr/Megator is implicated in multiple activities and several data show that also mediate protein (Frosst et al., 2002; Shibata et al., 2002; Vomastek et al., 2008; Ben-Efraim et al., 2009; Snow et al., 2013) and mRNA export (Bangs et al., 1998; Xu et al., 2007; Rajanala and Nandicoori, 2012; Lee et al., 2020).

A functional study in mitosis showed that depletion of Tpr by antibody injection leads to disruption in protein export but not import (Frosst et al., 2002). In this study, Megator depletion by RNAi mediated gene silencing resulted in reduced signal intensity in the nucleus and an increased cytoplasmic localisation for Chromator and Skeletor already during prophase I, suggesting an impairment in nuclear import. However, these results were obtained with fixed staining technique, hence they provide a fixed time analysis which makes it impossible to efficiently determine if Megator depletion affects the import, the export or the retention of the other proteins. Furthermore, during meiosis II, the absence of Megator at the nuclear rim may indicate that the NPC is absent in that stage, which may exclude the possibility of Megator being the major regulator of their import. It could be also hypothesised that, during the second meiotic division, cells may already have an atypical nuclear envelope composition as found in *Drosophila*'s mature sperm (Liu et al., 1997; Ashery-Padan et al., 1997; Wolfner and Collas, 2011).

Alternatively, at the end of the first meiotic division, the NPC may also have a peculiar composition that does not include the presence of Megator at the nuclear basket and its absence, maybe just like studies in mitosis, does not affect the NPC distribution within the nuclear envelope (Hase and Cordes, 2003). This will explain the absence of the Megator signal at the nuclear rim with both antibody and Megator-mCherry. However, there is an absence of data on the presence, composition and structure of the NPC during prophase and further research including the use of TEM (transmission electron microscopy) is needed to understand nuclear pore composition and structure during meiosis II. This will not only provide useful information on the NPC structure, but also on the possible roles of Tpr/Megator import during meiosis II.

4.6 Megator may regulate correct chromosome segregation by playing a conserved role in the Spindle Assembly Checkpoint

Lagging chromosomes is the hallmark of aneuploidy, and it is a conserved consequence of Megator depletion (Qi et al., 2004; Lee et al., 2008; Lince-Faria et al., 2009; Nakano et al., 2010; Liu et al., 2016). In this study, loss of Megator function has also been shown to result in aneuploidy as assayed by the counting of the neberken to nuclei ratios in the onion stage spermatids.

Phenotypic analysis of Megator depleted cells by super resolution scanning confocal microscopy reveals a plethora of defects during both meiosis I and meiosis II. Following Megator depletion, chromosomes were seen lagging at non-polar positions including close to the equator, where they often formed chromatin bridges anchoring DNA masses of different sizes. In some cases, single centromeres were seen being contacted by microtubules emanating from different directions or of the spindle, which suggests merotelic orientation (Savoian M. S., unpublished observations). An unequal distribution of chromosomes was also observed at cytokinesis and, during meiosis II, some cells were completely devoid of DNA. It's unclear if the meiosis II defects reflect a

Megator function at this stage or if they are a result of meiosis I problems as no tools or technologies are yet available to discern between the two possibilities.

These findings indicate that Megator depletion is linked to a high rate of defects, suggesting that Megator plays a fundamental role for correct chromosome segregation

Incorrect chromosome segregation is a process mainly prevented by the spindle assembly checkpoint (SAC), molecular machinery that halts the metaphase to anaphase transition when kinetochore attachments fail to generate tension or kinetochores are incorrectly bound to the k-fiber (Musacchio and Salmon, 2007; Foley and Kapoor, 2013). The SAC operates by forming the MCC which inhibits the APC/C and triggers the cell cycle arrest or the so-called "wait anaphase" until kinetochores are correctly attached (Musacchio and Hardwick, 2002).

Studies in mitosis show that Tpr/Megator is involved in the recruitment of Mad2, to the kinetochore (Lee et al., 2008; Lince-Faria et al., 2009; Rajanala et al., 2014; Schweizer et al., 2013). Indeed, the depletion of Tpr/Megator produces significant reduction of Mad2 recruitment at kinetochores, leading to premature entry into anaphase and consequent incorrect chromosome segregation including lagging chromosomes in mitotic systems Qi et al. (2004); Lee et al. (2008); Lince-Faria et al. (2009); Nakano et al. (2010). No information is available on the relationship between Megator and the SAC in meiosis. Also, it is unclear if the SAC behaves as in mitosis (Malmanche et al., 2006; Buffin et al., 2007; Gorbsky, 2015) because it is relatively weak in spermatocytes(Rebollo and González, 2000; Savoian et al., 2000).

To verify whether Megator is also needed for meiotic SAC functioning, a plan involving live cell analysis was outlined. The strategy encompassed the incubation of control and Megator depleted cells for thirty minutes with Demecolcine, a drug that depolymerises microtubules and prevents satisfaction of the SAC, leading to pre-anaphase arrest. Then, cells would be followed by live cell imaging and their timing required for entering anaphase measured. Given that in absence of the checkpoint, wild type cells should

enter anaphase after approximately 70 minutes (Rebollo and González, 2000; Savoian et al., 2000), it was hypothesised that if Megator is required for meiotic SAC function, its depletion should not stop anaphase onset, even in absence of the spindle.

Likewise, if Megator is not involved in spindle assembly checkpoint activity, the metaphase/anaphase transition should be delayed as in control cells. Unpublished data show that treated control cells entered into anaphase I with an average time of 60.79 minutes (standard error 6.09 minutes), while Megator depleted cells entered anaphase I in 28 minutes (standard error 0.81 minutes) (Savoian M. S., unpublished observations).

Lince-Faria et al. (2009) show that Mad2 RNAi mediated depletion in S2 cells display a lower mitotic index compared to cells that were Megator depleted. Unpublished data on time-lapse microscopy of Mad2-RNAi depleted meiosis I spermatocytes, show cells entering into anaphase I with an average of 32.78 minutes (standard error 1.74 minutes), which almost matches the timing of Megator RNAi mediated depleted cells (Savoian M. S., unpublished observations). This suggests that Megator is involved in the SAC at least during meiosis I. It will be important to measure the entry timing of Megator depleted cells during meiosis II. Cells in this stage have been shown to have Mad2 based SAC (Chaurasia and Lehner, 2018).

An important additional experiment will be to directly observe the presence or absence of Mad2 at Megator depleted kinetochores in both MI and II. However, because at least MI cells lack a SAC it will be necessary to arrest them prior to anaphase using proteasome inhibitors following microtubule depolymerisation. Therefore, control and Megator depleted cells treated with both Demecolcine and a proteasome inhibitor, will be stained with Mad2 antibodies. If as in mitosis, Megator is needed for Mad2 recruitment, its levels should be reduced at kinetochores following Megator depletion. This procedure will further confirm Megator's involvement in the recruitment of Mad2, thus Megator's role in the SAC function.

4.7 Megator may control correct chromosome segregation by playing a role in spindle morphology

In addition to chromosome segregation defects, the phenotypic analysis of Megator depleted cells revealed defects in spindle morphology. Some cells showed wavy or bent microtubules with spindles without a well defined structure or filled with bundles of disorganised microtubules. This is in contrast with previous studies in which Tpr/Megator depletion in somatic cells had reported no major defects in the spindle (Qi et al., 2004; Lince-Faria et al., 2009; Nakano et al., 2010).

The spindle matrix is believed to strengthen the spindle during metaphase (Pickett-Heaps et al., 1997; Sharp et al., 2000; Johansen and Johansen, 2002; Mitchison et al., 2005). Experiments applying controlled compression to the spindle result in modification of its shape with the formation of wavy microtubules when the spindle reaches the maximum extensions (Dumont and Mitchison, 2009). However, the mitotic spindle regains its original shape once the compression ends (Dumont and Mitchison, 2009). These experiments pointed towards the idea of existence of an elastic spindle matrix that limits the spindle length. Therefore, the depletion of the spindle matrix protein Megator may alter the spindle matrix elasticity, triggering the formation of wavy and bent microtubules. Alternatively, Megator may regulate spindle morphology directly.

This raises the possibility that presence of lagging chromosomes following Megator depletion, may be the direct result of the absence of proper tension on the chromosomes due to abnormal microtubule dynamics (Savoian et al., 2004).

In addition, loss of Megator may disrupt the structure of composition of the kinetochore. It has been reported that depletion of Tpr reduces levels of motor proteins at the kinetochore including dynein (Nakano et al., 2010). Indeed, perturbation of dynein has been linked to decreases in chromosome poleward movement (Gorbsky et al., 1987; Savoian et al., 2000; Sharp et al., 2000; LaFountain Jr et al., 2004). Therefore, along

with high resolution time lapse live cell experiments to measure chromosome velocities, cells could be stained with a specific dynein antibody to see if the motor protein is present.

4.8 Megator is predicted to affect male fertility

Drosophila spermatogenesis is a process that involves two sequential cycles of meiosis and a postmeiotic development pathway, for the formation of the sperm. After meiosis, a cyst of 64 onion stage spermatids is created (Fuller, 1993). These cells are characterised by a nebenkern to nuclei ratio of 1:1. Variations in this ratio indicate errors and can be used as a way to quantify the fidelity of meiosis (González et al., 1989). In this study, the counting of ratio nebenkern to nuclei in Megator depleted cells indicated multiple aberrations. Megator depletion leads to 30% of post-meiotic cells having defects, with at least 25% of these affecting chromosome segregation (%19.4 in 1:0 ratio nebenkern to nuclei, 3.3% in 2:0 and %2.1 in the 2:1). The subsequent phenotypical analysis of these errors through immunofluorescence staining showed several defects affecting the chromosomes.

The high rate of meiotic defects raises the possibility that fertility is affected. However, although not the subject of this work, unpublished observations (Savoian M. S., unpublished observations) identify subsequent roles for Megator in sperm development. Thus, traditional fertility tests would not directly address the impact of Megator depletion in the meiotic divisions.

4.9 Conclusion

The aims of this study were: (i) characterise Megator distribution during meiosis I and II, (ii) determine if it regulates correct chromosome segregation by (iii) performing a conserved role in the SAC.

Through the analysis of the distributions of three recognised spindle matrix proteins -

Chromator, Skeletor and Lamin Dm0 - it was discovered that the spindle matrix is a cell division feature that is highly conserved in mitosis and meiosis.

The examination of Megator, the only spindle matrix protein believed to be conserved across species, revealed distinct localisation. Thus, the spindle matrix composition differs between mitosis and meiosis. Furthermore, although meiosis I resembles mitosis, it differs from meiosis II.

Functional studies of Megator show that its depletion triggers the mislocalisation of other spindle matrix proteins, Chromator, Skeletor and Lamin Dm0. This raises the possibility of Megator being the master controller of the spindle matrix composition.

Megator deletion also leads to a high rate of defects in the spindle morphology and chromosome segregation. Thus, Megator may be required for correct chromosome segregation by playing a role in the spindle assembly checkpoint or by regulating some aspects of the spindle structure or dynamics.

The highly conserved Megator nucleopore protein is implicated in several functions which make studies solely on its matrix roles during cell division challenging. Despite further research being needed, this thesis provides novel data about the role of Megator during male meiosis and the existence of a spindle matrix during meiosis I and II. The experiments carried out have provided substantive insights into the roles of this protein in cell division for sperm formation despite the research limitations that resulted from the limitations given by the COVID-19 pandemic during the entire period of this master research.

Bibliography

Agarwal, A., Mulgund, A., Hamada, A., and Chyatte, M. A unique view on male infertility around the globe. *Reproductive biology and endocrinology : RB&E*, 13:37, 04 2015. doi: 10.1186/s12958-015-0032-1.

Akiyoshi, B. and Gull, K. Discovery of unconventional kinetochores in kinetoplastids. *Cell*, 156(6):1247–1258, 2014. doi: 10.1016/j.cell.2014.01.049.

Al-Bassam, J., Kim, H., Brouhard, G., van Oijen, A., Harrison, S. C., and Chang, F. CLASP promotes microtubule rescue by recruiting tubulin dimers to the microtubule. *Developmental Cell*, 19(2):245–258, 2010. ISSN 1534-5807. doi: 10.1016/j.devcel.2010.07.016.

Alberts, B., Johnson, A., Lewis, J., Raff, M., Roberts, K., and Walter, P. The cytoskeleton - microtubules. In *Molecular Biology of the Cell. 4th edition*, pages 941–942. Garland Science, 2002. doi: 10.1002/bmb.2003.494031049999.

Allan, L. A., Camacho Reis, M., Ciossani, G., Huis in 't Veld, P. J., Wohlgemuth, S., Kops, G. J. P. L., Musacchio, A., and Saurin, A. T. Cyclin B1 scaffolds MAD1 at the kinetochore corona to activate the mitotic checkpoint. *The EMBO journal*, 39 (12):e103180, 2020. doi: 10.15252/embj.2019103180.

Anderson, D. and Hetzer, N. Nuclear envelope formation by chromatin-mediated reorganization of the endoplasmic reticulum. *Nature cell biology*, 9:1160–6, 11 2007. doi: 10.1038/ncb1636.

Antonio, C., Ferby, I., Wilhelm, H., Jones, M., Karsenti, E., Nebreda, A. R., and Vernos, I. Xkid, a chromokinesin required for chromosome alignment on the metaphase plate. *Cell*, 102(4):425–435, 2000. ISSN 0092-8674. doi: 10.1016/S0092-8674(00)00048-9.

Arquint, C. and Nigg, E. A. The PLK4-STIL-SAS-6 module at the core of centriole duplication. *Biochemical Society Transactions*, 44(5):1253–1263, 2016. doi: 10.1042/BST20160116.

Ashery-Padan, R., Ulitzur, N., Arbel, A., Goldberg, M., Weiss, A., Maus, N., Fisher, P., and Gruenbaum, Y. Localization and posttranslational modifications of otefin, a protein required for vesicle attachment to chromatin, during *Drosophila melanogaster development.* Molecular and cellular biology, *17:4114–23, 08 1997. doi: 10.1128/MCB.17.7.4114*.

Bae, J.-A., Moon, D., and Yoon, J. Nup211, the fission yeast homolog of Mlp1/Tpr, is involved in mRNA export. Journal of microbiology (Seoul, Korea), *47:337–43, 07 2009. doi: 10.1007/s12275-009-0125-7*.

Bairati, A. Struttura ed ultrastruttura dell'apparato genitale maschile di Drosophila melanogaster meig. Cell and Tissue Research, *76:56–99, 01 1967. doi: 10.1007/BF00337033*.

Bangs, P., Burke, B., Powers, C., Craig, R., Purohit, A., and Doxsey, S. Functional Analysis of Tpr: Identification of Nuclear Pore Complex Association and Nuclear Localization Domains and a Role in mRNA Export . Journal of Cell Biology, *143 (7):1801–1812, 12 1998. ISSN 0021-9525. doi: 10.1083/jcb.143.7.1801*.

Battaglia, D. E., Goodwin, P., Klein, N. A., and Soules, M. R. Fertilization and early embryology: Influence of maternal age on meiotic spindle assembly in oocytes from naturally cycling women. Human reproduction, *11:2217–2222, 11 1996. doi: 10.1093/oxfordjournals.humrep.a019080*.

Ben-Efraim, I., Frosst, P., and Gerace, L. Karyopherin binding interactions and nuclear import mechanism of Nuclear Pore Complex protein Tpr. BMC cell biology*, 10:74, 10 2009. doi: 10.1186/1471-2121-10-74.*

Blachon, S., Gopalakrishnan, J., Omori, Y., Polyanovsky, A., Church, A., Nicastro, D., Malicki, J., and Avidor-Reiss, T. Drosophila asterless and vertebrate Cep152 are orthologs essential for centriole duplication. Genetics*, 180(4):2081–2094, 2008. doi: 10.1534/genetics.108.095141.*

Bond, D. J. Mechanisms of aneuploid induction. Mutation Research/Fundamental and Molecular Mechanisms of Mutagenesis*, 181(2):257–266, 1987. ISSN 0027-5107. doi: 10.1016/0027-5107(87)90103-5.*

Bonilla, E. and Xu, E. Y. Identification and characterization of novel mammalian spermatogenic genes conserved from fly to human. Molecular Human Reproduction*, 14(3):137–142, 02 2008. ISSN 1360-9947. doi: 10.1093/molehr/gan002.*

Bornens, M. and Azimzadeh, J. Origin and evolution of the centrosome. Eukaryotic Membranes and Cytoskeleton*, pages 119–129, 2007. doi: 10.1007/978-0-387-74021-8_10.*

Boveri, T. Über mehrpolige mitosen als mittle zur analyse des zellkerns. Verhandl. Phys.-Med. Ges. Würzburg*, 35:67–90, 1902.*

Brand, A. H. and Perrimon, N. Targeted gene expression as a means of altering cell fates and generating dominant phenotypes. Development*, 118(2):401–415, 07 1993. doi: 10.1242/dev.118.2.401.*

Brickner, J. H. and Walter, P. Gene recruitment of the activated ino1 locus to the nuclear membrane. PLOS Biology*, 2(11):e342, 09 2004. doi: 10.1371/journal.pbio.0020342.*

Brouhard, G. J., Stear, J. H., Noetzel, T. L., Al-Bassam, J., Kinoshita, K., Harrison,

K. C., Howard, J., and Hyman, A. A. XMAP215 is a processive microtubule polymerase. Cell, *132(1):79–88, 2008. ISSN 0092-8674. doi: 10.1016/j.cell.2007.11.043.*

Buffin, E., Emre, D., and Karess, R. Flies without a spindle checkpoint. Nature cell biology, *9:565–572, 06 2007. doi: 10.1038/ncb1570.*

Bunt, S. M., Monk, A. C., Siddall, N. A., Johnston, N. L., and Hime, G. R. GAL4 enhancer traps that can be used to drive gene expression in developing Drosophila spermatocytes. Genesis, *50(12):914–920, 2012. doi: 10.1002/dvg.22341.*

Buonomo, S. B. C., Clyne, R. K., Fuchs, J., Loidl, J., Uhlmann, F., and Nasmyth, K. Disjunction of homologous chromosomes in meiosis i depends on proteolytic cleavage of the meiotic cohesin Rec8 by separin. Cell, *103(3):387–398, 2000. doi: 10.1016/s0092-8674(00)00131-8.*

Burns, L. H. Psychiatric aspects of infertility and infertility treatments. Psychiatric Clinics of North America, *30(4):689–716, 2007. ISSN 0193-953X. doi: 10.1016/j.psc.2007.08.001. Psychosomatic Medicine.*

Byrd, D. A., Sweet, D. J., and Panté, N. Tpr, a large coiled coil protein whose amino terminus is involved in activation of oncogenic kinases, is localized to the cytoplasmic surface of the Nuclear Pore Complex. J Cell Biol, *127(6):1515–1526, 1994. doi: 10.1083/jcb.127.6.1515.*

Cai, S., O'connell, C. B., Khodjakov, A., and Walczak, C. E. Chromosome congression in the absence of kinetochore fibres. Nature cell biology, *11(7):832–838, 2009. doi: 10.1038/ncb1890.*

Cassimeris, L. U., Walker, R. A., Pryer, N. K., and Salmon, E. D. Dynamic instability of microtubules. BioEssays, *7(4):149–154, 1987. doi: 10.1002/bies.950070403.*

Cenci, G., Bonaccorsi, S., Pisano, C., Verni, F., and Gatti, M. Chromatin and microtubule organization during premeiotic, meiotic and early postmeiotic stages of

Drosophila Melanogaster spermatogenesis. Journal of Cell Science, *107(12):3521–3534, 1994. doi: 10.1242/jcs.107.12.3521.*

Chang, P., Jacobson, M., and Mitchison, T. Poly(ADP-ribose) is required for spindle assembly and structure. Nature, *432:645–9, 01 2005. doi: 10.1038/nature03061.*

Chaurasia, S. and Lehner, C. F. Dynamics and control of sister kinetochore behavior during the meiotic divisions in Drosophila spermatocytes. PLoS genetics, *14(5): e1007372, 2018. doi: 10.1371/journal.pgen.1007372.*

Cheeseman, I. M., Chappie, J. S., Wilson-Kubalek, E. M., and Desai, A. The conserved KMN network constitutes the core microtubule-binding site of the kinetochore. Cell, *127(5):983–997, 2006. doi: 10.1016/j.cell.2006.09.039.*

Chen, D. and Mckearin, D. A discrete transcriptional silencer in the bam gene determines asymmetric division of the Drosophila germline stem cell. Development (Cambridge, England), *130:1159–70, 04 2003. doi: 10.1242/dev.00325.*

Church, K. A. and Lin, H. P. Drosophila: a model for the study of aneuploidy. Aneuploidy Part B: Induction and Test Systems, *pages 227–255, 1988.*

Cimini, D., Howell, B., Maddox, P., Khodjakov, A., Degrassi, F., and Salmon, E. D. Merotelic kinetochore orientation is a major mechanism of aneuploidy in mitotic mammalian tissue cells. The Journal of Cell Biology, *153(3):517–527, 2001. ISSN 0021-9525 1540-8140. doi: 10.1083/jcb.153.3.517.*

Cimini, D., Fioravanti, D., Salmon, E. D., and Degrassi, F. Merotelic kinetochore orientation versus chromosome mono-orientation in the origin of lagging chromosomes in human primary cells. Journal of cell science, *115(3):507–515, 2002. doi: 10.1242/jcs.115.3.507.*

Corbett, K. D., Yip, C. K., Ee, L.-S., Walz, T., Amon, A., and Harrison, S. C.

The monopolin complex crosslinks kinetochore components to regulate chromosome-microtubule attachments. Cell, *142(4):556–567, 2010. doi: 10.1016/j.cell.2010.07.017.*

Cordes, V. C., Reidenbach, S., Rackwitz, H. R., and Franke, W. W. Identification of protein p270/Tpr as a constitutive component of the Nuclear Pore Complex-attached intranuclear filaments. The Journal of Cell Biology, *136(3):515–529, 1997. ISSN 0021-9525 1540-8140. doi: 10.1083/jcb.136.3.515.*

Cordes, V. C., Hase, M. E., and Müller, L. Molecular segments of protein Tpr that confer nuclear targeting and association with the Nuclear Pore Complex. Experimental cell research, *245:43–56, 12 1998. doi: 10.1006/excr.1998.4246.*

Coyle, J. H., Bor, Y.-C., Rekosh, D., and Hammarskjold, M.-L. The Tpr protein regulates export of mRNAs with retained introns that traffic through the Nxf1 pathway. RNA, *17(7):1344–1356, 2011. doi: 10.1261/rna.2616111.*

Cuevas, M. and Matunis, E. The stem cell niche: Lessons from the Drosophila testis. Development, *138:2861–9, 07 2011. doi: 10.1242/dev.056242.*

Cunha-Silva, S., Osswald, M., Goemann, J., Barbosa, J., Santos, L. M., Resende, P., Bange, T., Ferrás, C., Sunkel, C. E., and Conde, C. Mps1-mediated release of Mad1 from nuclear pores ensures the fidelity of chromosome segregation. Journal of Cell Biology, *219(3), 01 2020. ISSN 0021-9525. doi: 10.1083/jcb.201906039.*

De Simone, A., Kitchen, C., Kwan, A., Sunde, M., Dobson, C., and Frenkel, D. Intrinsic disorder modulates protein self-assembly and aggregation. Proceedings of the National Academy of Sciences of the United States of America, *109:6951–6, 04 2012. doi: 10.1073/pnas.1118048109.*

De Souza, C. P. and Osmani, S. A. Double duty for nuclear proteins: the price of more open forms of mitosis. Trends in genetics, *25(12):545–554, 2009. ISSN 0168-9525. doi: 10.1016/j.tig.2009.10.005.*

De Souza, C. P., Hashmi, S. B., Nayak, T., Oakley, B., and Osmani, S. A. Mlp1 acts as a mitotic scaffold to spatially regulate spindle assembly checkpoint proteins in aspergillus nidulans. Molecular Biology of the Cell*, 20(8):2146–2159, 2009. ISSN 1939-4586 1059-1524. doi: 10.1091/mbc.e08-08-0878.*

De Wulf, P., McAinsh, A. D., and Sorger, P. K. Hierarchical assembly of the budding yeast kinetochore from multiple subcomplexes. Genes & development*, 17(23):2902–2921, 2003. doi: 10.1101/gad.1144403.*

DeGrasse, J., DuBois, K., Devos, D., Siegel, T., Sali, A., Field, M., Rout, M., and Chait, B. Evidence for a shared Nuclear Pore Complex architecture that is conserved from the last common eukaryotic ancestor. Molecular & cellular proteomics : MCP*, 8:2119–30, 07 2009. doi: 10.1074/mcp.M900038-MCP200.*

Desai, A., Verma, S., Mitchison, T. J., and Walczak, C. E. Kin I kinesins are microtubule-destabilizing enzymes. Cell*, 96(1):69–78, 1999. ISSN 0092-8674. doi: 10.1016/S0092-8674(00)80960-5.*

Ding, Y., Yao, C., Lince-Faria, M., Rath, U., Cai, W., Maiato, H., Girton, J., Johansen, K. M., and Johansen, J. Chromator is required for proper microtubule spindle formation and mitosis in Drosophila. Developmental Biology*, 334(1):253–263, 2009. ISSN 0012-1606. doi: 10.1016/j.ydbio.2009.07.027.*

Dumont, S. and Mitchison, T. Force and length in the mitotic spindle. Current biology: CB*, 19:R749–61, 09 2009. doi: 10.1016/j.cub.2009.07.028.*

Dura, J.-M., Preat, T., and Tully, T. Identification of linotte, a new gene affecting learning and memory in Drosophila melanogaster. Journal of neurogenetics*, 21(4):307–320, 2007. doi: 10.1080/01677060701693479.*

Earnshaw, W. C. and Rothfield, N. Identification of a family of human centromere proteins using autoimmune SERA from patients with scleroderma. Chromosoma*, 91(3):313–321, 1985. doi: 10.1007/BF00328227.*

Fabian, L. and Brill, J. A. Drosophila spermiogenesis: Big things come from little packages. Spermatogenesis*, 2(3):197–212, 2012. doi: 10.4161/spmg.21797.*

Fabian, L., Troscianczuk, J., and Forer, A. Calyculin a, an enhancer of myosin, speeds up anaphase chromosome movement. Cell & chromosome*, 6(1):1–17, 2007a. doi: 10.1186/1475-9268-6-1.*

Fabian, L., Xia, X., Venkitaramani, D., Johansen, K. M., Johansen, J., Andrew, D. J., and Forer, A. Titin in insect spermatocyte spindle fibers associates with microtubules, actin, myosin and the matrix proteins skeletor, Megator and chromator. Journal of Cell Science*, 120(13):2190–2204, 07 2007b. ISSN 0021-9533. doi: 10.1242/jcs.03465.*

Faesen, A. C., Thanasoula, M., Maffini, S., Breit, C., Müller, F., Van Gerwen, S., Bange, T., and Musacchio, A. Basis of catalytic assembly of the mitotic checkpoint complex. Nature*, 542(7642):498–502, 2017. doi: 10.1038/nature21384.*

Fang, G., Yu, H., and Kirschner, M. W. The checkpoint protein MAD2 and the mitotic regulator CDC20 form a ternary complex with the anaphase-promoting complex to control anaphase initiation. Genes & development*, 12(12):1871–1883, 1998. doi: 10.1101/gad.12.12.1871.*

Fire, A. Z., Xu, S. Q., Montgomery, M., Kostas, S., Driver, S., and Mello, C. C. Potent and specific genetic interference by double-stranded RNA in Caenorhabditis elegans. Nature*, 391:806–11, 03 1998. doi: 10.1038/35888.*

Fischer, J., Giniger, E., Maniatis, T., and Ptashne, M. GAL4 activates transcription in Drosophila. Nature*, 332:853–856, 05 1988. doi: 10.1038/332853a0.*

Fisher, D., Krasinska, L., Coudreuse, D., and Novak, B. Phosphorylation network dynamics in the control of cell cycle transitions. Journal of cell science*, 125:4703–11, 10 2012. doi: 10.1242/jcs.106351.*

Fišerová, J., Maninová, M., Sieger, T., Uhlářová, J., Šebestová, L., Efenberková, M., Čapek, M., Fišer, K., and Hozák, P. Nuclear pore protein Tpr associates with lamin B1 and affects nuclear lamina organization and nuclear pore distribution. Cellular and Molecular Life Sciences, *76(11):2199–2216, 2019. ISSN 1420-9071. doi: 10.1007/s00018-019-03037-0.*

Foley, E. A. and Kapoor, T. M. Microtubule attachment and spindle assembly checkpoint signalling at the kinetochore. Nature reviews Molecular cell biology, *14(1): 25–37, 2013. doi: 10.1038/nrm3494.*

Forer, A. and Goldman, R. Comparisons of isolated and in vivo mitotic apparatuses. Nature, *222:689–90, 06 1969. doi: 10.1038/222689a0.*

Forer, A., Spurck, T., and Pickett-Heaps, J. Ultraviolet microbeam irradiations of spindle fibres in crane-fly spermatocytes and newt epithelial cells: Resolution of previously conflicting observations. Protoplasma, *197:230–240, 09 1997. doi: 10.1007/BF01288032.*

Forer, A., Spurck, T., Pickett-Heaps, J. D., and Wilson, P. J. Structure of kinetochore fibres in crane-fly spermatocytes after irradiation with an ultraviolet microbeam: Neither microtubules nor actin filaments remain in the irradiated region. Cell Motility, *56(3):173–192, 2003. doi: 10.1002/cm.10144.*

Forer, A., Johansen, K., and Johansen, J. Movement of chromosomes with severed kinetochore microtubules. Protoplasma, *252, 01 2015. doi: 10.1007/s00709-014-0752-7.*

Forer, A., Sheykhani, R., and Berns, M. W. Anaphase chromosomes in crane-fly spermatocytes treated with taxol (paclitaxel) accelerate when their kinetochore microtubules are cut: evidence for spindle matrix involvement with spindle forces. Frontiers in Cell and Developmental Biology, *6:77, 2018. doi: 10.3389/fcell.2018.00077.*

Frosst, P., Guan., T., Subauste, C., Hahn., K., and Gerace, L. Tpr is localized within the nuclear basket of the pore complex and has a role in nuclear protein export.

Journal of Cell Biology, *156(4):617–630, 2002. ISSN 0021-9525. doi: 10.1083/jcb.200106046*.

Fuller, M. T. Spermatogenesis. In The Development of *Drosophila*, *pages 71–147. Cold Spring Harbor Laboratory Press, 1993.*

Galy, V., Gadal, O., Fromont-Racine, M., Romano, A., Jacquier, A., and Nehrbass, U. Nuclear retention of unspliced mRNAs in Yeast is mediated by perinuclear Mlp1. Cell, *116(1):63–73, 2004. ISSN 0092-8674. doi: 10.1016/S0092-8674(03)01026-2*.

Gerace, L. and Burke, B. Functional organization of the nuclear envelope. Annual review of cell biology, *4(1):335–374, 1988. doi: 10.1146/annurev.cb.04.110188.002003*.

Goldman, R. D. and Rebhun, L. I. The Structure and Some Properties of the Isolated Mitotic Apparatus. Journal of Cell Science, *4(1):179–209, 01 1969. ISSN 0021-9533. doi: 10.1242/jcs.4.1.179*.

Goldstein, L. S. B. Kinetochore structure and its role in chromosome orientation during the first meiotic division in male D. melanogaster. Cell, *25(3):591–602, 1981. doi: 10.1016/0092-8674(81)90167-7*.

Gönczy, P., Pichler, S., Kirkham, M., and Hyman, A. A. Cytoplasmic dynein is required for distinct aspects of MTOC positioning, including centrosome separation, in the one cell stage Caenorhabditis elegans embryo. The Journal of cell biology, *147(1):135–150, 1999. doi: 10.1083/jcb.147.1.135*.

González, C., Casal, J., and Ripoll, P. Relationship between chromosome content and nuclear diameter in early spermatids of Drosophila Melanogaster. Genetic Research, *54(3):205–12, 1989. ISSN 0016-6723. doi: 10.1017/s0016672300028664*.

Gorbsky, G., Sammak, P., and Borisy, G. Chromosomes move poleward in anaphase along stationary microtubules that coordinately diassemble from their kinetochore ends. The Journal of cell biology, *104:9–18, 02 1987. doi: 10.1083/jcb.104.1.9*.

Gorbsky, G. J. The spindle checkpoint and chromosome segregation in meiosis. The FEBS Journal, *282(13):2471–2487, 2015. doi: 10.1111/febs.13166*.

Gorbsky, G. J., Sammak, P. J., and Borisy, G. G. Microtubule dynamics and chromosome motion visualized in living anaphase cells. The Journal of cell biology, *106 (4):1185–1192, 1988. doi: 10.1083/jcb.106.4.1185*.

Greco, A., Pierotti, M. A., Bongarzone, I., Pagliardini, S., Lanzi, C., and Della Porta, G. TRK-T1 is a novel oncogene formed by the fusion of Tpr and TRK genes in human papillary thyroid carcinomas. Oncogene, *7(2):237—242, February 1992. ISSN 0950-9232.*

Green, D. M., Johnson, C. P., Hagan, H., and Corbett, A. H. The C-terminal domain of myosin-like protein 1 (Mlp1p) is a docking site for heterogeneous nuclear ribonucleoproteins that are required for mRNA export. Proceedings of the National Academy of Sciences, *100(3):1010–1015, 2003. ISSN 0027-8424. doi: 10.1073/pnas.0336594100*.

Grossman, E., Medalia, O., and Zwerger, M. Functional architecture of the nuclear pore complex. Annual Review of Biophysics, *41(1):557–584, 2012. doi: 10.1146/annurev-biophys-050511-102328*.

Gruneberg, U., Neef, R., Honda, R., Nigg, E. A., and Barr, F. A. Relocation of Aurora B from centromeres to the central spindle at the metaphase to anaphase transition requires MKlp2. The Journal of cell biology, *166(2):167–172, 2004. doi: 10.1083/jcb.200403084*.

Hannon, G. RNA interference. Nature, *418:244–51, 08 2002. doi: 10.1038/418244a*.

Hardwick, K. G., Li, R., Mistrot, C., Chen, R.-H., Dann, P., Rudner, A., and Murray, A. W. Lesions in Many Different Spindle Components Activate the Spindle Checkpoint in the Budding Yeast Saccharomyces cerevisiae. Genetics, *152(2):509–518, 06 1999. ISSN 1943-2631. doi: 10.1093/genetics/152.2.509*.

Hardy, R., Tokuyasu, K., Lindsley, D., and Garavito, M. The germinal proliferation centre in the testis of Drosophila. Journal of ultrastructure research, *69:180–90, 12 1979. doi: 10.1016/S0022-5320(79)90108-4.*

Hase, M. E. and Cordes, V. C. Direct interaction with Nup153 mediates binding of Tpr to the periphery of the Nuclear Pore Complex. Molecular Biology of the Cell, *14(5):1923–1940, 2003. doi: 10.1091/mbc.e02-09-0620.*

Hase, M. E., Kuznetsov, N. V., and Cordes, V. C. Amino acid substitutions of coiled-coil protein Tpr abrogate anchorage to the nuclear pore complex but not parallel, in-register homodimerization. Molecular Biology of the Cell, *12(8):2433–2452, 2001. doi: 10.1091/mbc.12.8.2433.*

Hashizume, C., Nakano, H., Yoshida, K., and Wong, R. Characterization of the role of the tumor marker Nup88 in mitosis. Molecular cancer, *9:119, 05 2010. doi: 10.1186/1476-4598-9-119.*

Hawley, R. S. Meiosis: how male flies do meiosis. Current Biology, *12(19):R660–R662, 2002. doi: 10.1016/S0960-9822(02)01161-2.*

Hayashi, D., Tanabe, K., Katsube, H., and Inoue, Y. H. B-type nuclear lamin and the Nuclear Pore Complex Nup107-160 influences maintenance of the spindle envelope required for cytokinesis in Drosophila male meiosis. Biology open, *5(8):1011–1021, 2016. doi: 10.1242/bio.017566.*

Hayden, J. H., Bowser, S. S., and Rieder, C. L. Kinetochores capture astral microtubules during chromosome attachment to the mitotic spindle: direct visualization in live newt lung cells. The Journal of cell biology, *111(3):1039–1045, 1990. doi: 10.1083/jcb.111.3.1039.*

Hayes, S. Lamin in the spindle matrix. Nature Cell Biology, *8(6):550–550, 2006. ISSN 1476-4679. doi: 10.1038/ncb0606-550.*

Holden, J. M., Koreny, L., Obado, S., Ratushny, A. V., Chen, W.-M., Chiang, J.-H., Kelly, S., Chait, B. T., Aitchison, J. D., Rout, M. P., and Field, M. Nuclear pore complex evolution: a trypanosome Mlp analogue functions in chromosomal segregation but lacks transcriptional barrier activity. Molecular Biology of the Cell*, 25(9): 1421–1436, 2014. doi: 10.1091/mbc.e13-12-0750.*

Holstein, A.-F., Schulze, W., and Davidoff, M. Understanding spermatogenesis is a prerequisite for treatment. Reproductive biology and endocrinology: RB&E*, 1:107, 12 2003. doi: 10.1186/1477-7827-1-107.*

Holy, T. E. and Leibler, S. Dynamic instability of microtubules as an efficient way to search in space. Proceedings of the National Academy of Sciences*, 91(12):5682–5685, 1994. doi: 10.1073/pnas.91.12.5682.*

Hoyt, M. A., Totis, L., and Roberts, B. T. S. cerevisiae genes required for cell cycle arrest in response to loss of microtubule function. Cell*, 66(3):507–517, 1991. doi: 10.1016/0092-8674(81)90014-3.*

Hüve, J., Wesselmann, R., Kahms, M., and Peters, R. 4Pi Microscopy of the Nuclear Pore Complex. Biophysical Journal*, 95(2):877–885, 2008. ISSN 0006-3495. doi: 10.1529/biophysj.107.127449.*

Inoue, Y. H., Savoian, M. S., Suzuki, T., Máthé, E., Yamamoto, M.-T., and Glover, D. M. Mutations in orbit/mast reveal that the central spindle is comprised of two microtubule populations, those that initiate cleavage and those that propagate furrow ingression. Journal of Cell Biology*, 166(1):49–60, 2004. ISSN 0021-9525. doi: 10.1083/jcb.200402052.*

Insco, M. L., Leon, A., Tam, C. H., McKearin, D. M., and Fuller, M. T. Accumulation of a differentiation regulator specifies transit amplifying division number in an adult stem cell lineage. Proceedings of the National Academy of Sciences*, 106(52):22311, 2009. doi: 10.1073/pnas.0912454106.*

International Strategic Analysis. The economic impact of falling birth rates. https://www.isa-world.com/news/?tx_ttnews%5BbackPid%5D=1&tx_ttnews%5Btt_news%5D=485&cHash=8066cd77ac69cb1e4a967f1e527fafdd, 2019.

Ishiguro, K.-I., Kim, J., Fujiyama-Nakamura, S., Kato, S., and Watanabe, Y. A new meiosis-specific cohesin complex implicated in the cohesin code for homologous pairing. EMBO reports*, 12(3):267–275, 2011. doi: 10.1038/embor.2011.2.*

Ishii, K., Arib, G., Lin, C., Van Houwe, G., and Laemmli, U. K. Chromatin boundaries in budding yeast: The nuclear pore connection. Cell*, 109(5):551–562, 2002. ISSN 0092-8674. doi: 10.1016/S0092-8674(02)00756-0.*

Jackman, M., Marcozzi, C., Barbiero, M., Pardo, M., Yu, L., Tyson, A. L., Choudhary, J. S., and Pines, J. Cyclin B1-Cdk1 facilitates MAD1 release from the nuclear pore to ensure a robust spindle checkpoint. Journal of Cell Biology*, 219(6), 2020. doi: 10.1083/jcb.201907082.*

Janmey, P., Hvidt, S., Käs, J., Lerche, D., Maggs, A., Sackmann, E., Schliwa, M., and Stossel, T. The mechanical properties of actin gels: Elastic modulus and filament motions. The Journal of biological chemistry*, 269:32503–13, 01 1995. doi: 10.1016/S0021-9258(18)31663-6.*

Jevtić, P., Schibler, A., Wesley, C., Pegoraro, G., Misteli, T., and Levy, D. The nucleoporin ELYS regulates nuclear size by controlling NPC number and nuclear import capacity. EMBO reports*, 20:e47283, 05 2019. doi: 10.15252/embr.201847283.*

Ji, Z., Gao, H., Jia, L., Li, B., and Yu, H. A sequential multi-target Mps1 phosphorylation cascade promotes spindle checkpoint signaling. Elife*, 6:e22513, 2017. doi: 10.7554/eLife.22513.*

Jiménez, M., Petit, T., Gancedo, C., and Goday, C. The alm1(+) gene from Schizosaccharomyces pombe encodes a coiled-coil protein that associates with the medial region during mitosis. Molecular & general genetics : MGG*, 262:921–30, 02 2000. doi: 10.1007/PL00008660.*

Johansen, J. and Johansen, K. M. The spindle matrix through the cell cycle in Drosophila. Fly*, 3(3):215–222, 2009. ISSN 1933-6934. doi: 10.4161/fly.3.3.9340.*

Johansen, K. M. and Johansen, J. Recent glimpses of the elusive spindle matrix. Cell Cycle*, 1(5):312–314, 2002. ISSN 1538-4101. doi: 10.4161/cc.1.5.144.*

Joseph, J. and Dasso, M. The nucleoporin Nup358 associates with and regulates interphase microtubules. FEBS Letters*, 582(2):190–196, 2008. ISSN 0014-5793. doi: 10.1016/j.febslet.2007.11.087.*

Kapoor, T. M., Lampson, M. A., Hergert, P., Cameron, L., Cimini, D., Salmon, E., McEwen, B. F., and Khodjakov, A. Chromosomes can congress to the metaphase plate before biorientation. Science*, 311(5759):388–391, 2006. doi: 10.1126/science.1122142.*

Katsani, K. R., Karess, R. E., Dostatni, N., and Doye, V. In vivo dynamics of Drosophila nuclear envelope components. Molecular Biology of the Cell*, 19(9):3652–3666, 2008. doi: 10.1091/mbc.e07-11-1162.*

Kelley, J. B., Datta, S., Snow, C. J., Chatterjee, M., Ni, L., Spencer, A., Yang, C.-S., Cubeñas Potts, C., Matunis, M. J., and Paschal, B. M. The defective nuclear Lamina in Hutchinson-Gilford Progeria Syndrome disrupts the nucleocytoplasmic ran gradient and inhibits nuclear localization of Ubc9. Molecular and Cellular Biology*, 31(16):3378–3395, 2011. doi: 10.1128/MCB.05087-11.*

Khodjakov, A., Copenagle, L., Gordon, M. B., Compton, D. A., and Kapoor, T. M. Minus-end capture of preformed kinetochore fibers contributes to spindle morphogenesis. The Journal of cell biology*, 160(5):671–683, 2003. doi: 10.1083/jcb.200208143.*

Kidd, S., Eskenazi, B., and Wyrobek, A. Effects of male age on semen quality and fertility: A review of the literature. Fertility and sterility*, 75:237–248, 03 2001. doi: 10.1016/S0015-0282(00)01679-4.*

Kim, T.-S., Park, J.-E., Shukla, A., Choi, S., Murugan, R. N., Lee, J. H., Ahn, M., Rhee, K., Bang, J. K., Kim, B. Y., et al. Hierarchical recruitment of Plk4 and regulation of centriole biogenesis by two centrosomal scaffolds, Cep192 and Cep152. Proceedings of the National Academy of Sciences*, 110(50):E4849–E4857, 2013. doi: 10.1073/pnas.1319656110.*

Kirschner, M. and Mitchison, T. Beyond self-assembly: from microtubules to morphogenesis. Cell*, 45(3):329–342, 1986. doi: 10.1016/0092-8674(86)90318-1.*

Kölling, R., Nguyen, T., Chen, E., and Botstein, D. A new gene with a myosin-like heptad repeat structure. Molecular & general genetics : MGG*, 237:359–69, 04 1993. doi: 10.1007/BF00279439.*

Kops, G. J. P. L., Snel, B., and Tromer, E. C. Evolutionary dynamics of the spindle assembly checkpoint in eukaryotes. Current Biology*, 30(10):R589–R602, 2020. doi: 10.1016/j.cub.2020.02.021.*

Krull, S., Thyberg, J., Björkroth, B., Rackwitz, H.-R., and Cordes, V. C. Nucleoporins as components of the nuclear pore complex core structure and Tpr as the architectural element of the nuclear basket. Molecular Biology of the Cell*, 15(9):4261–4277, 2004. doi: 10.1091/mbc.e04-03-0165.*

Krull, S., Dörries, J., Boysen, B., Reidenbach, S., Magnius, L., Norder, H., Thyberg, J., and Cordes, V. C. Protein Tpr is required for establishing nuclear pore-associated zones of heterochromatin exclusion. The EMBO Journal*, 29(10):1659–1673, 2010. doi: 10.1038/emboj.2010.54.*

LaFountain Jr, J. R., Cohan, C. S., Siegel, A. J., and LaFountain, D. J. Direct visualization of microtubule flux during metaphase and anaphase in crane-fly spermatocytes. Molecular biology of the cell*, 15(12):5724–5732, 2004. doi: 10.1091/mbc.e04-08-0750.*

Lara-Gonzalez, P., Moyle, M. W., Budrewicz, J., Mendoza-Lopez, J., Oegema, K., and Desai, A. The G2-to-M transition is ensured by a dual mechanism that protects

Cyclin B from degradation by Cdc20-activated APC/C. Developmental Cell*, 51(3): 313–325.e10, 2019. ISSN 1534-5807. doi: 10.1016/j.devcel.2019.09.005.*

Lee, E. S., Wolf, E. J., Ihn, S. S. J., Smith, H. W., Emili, A., and Palazzo, A. F. Tpr is required for the efficient nuclear export of mRNAs and lncRNAs from short and intron-poor genes. Nucleic Acids Research*, 48(20):11645–11663, 10 2020. ISSN 0305-1048. doi: 10.1093/nar/gkaa919.*

Lee, J., Miyano, T., Dai, Y., Wooding, P., Yen, T. J., and Moor, R. M. Specific regulation of CENP-E and kinetochores during meiosis I/meiosis II transition in pig oocytes. Molecular Reproduction and Development: Incorporating Gamete Research*, 56(1):51–62, 2000. doi: 10.1002/(SICI)1098-2795(200005)56:1⟨51::AID-MRD7⟩3.0.CO;2-N.*

Lee, S. H., Sterling, H., Burlingame, A., and McCormick, F. Tpr directly binds to Mad1 and Mad2 and is important for the mad1-mad2-mediated mitotic spindle checkpoint. Genes & Development*, 22(21):2926–2931, 2008. ISSN 0890-9369 1549-5477. doi: 10.1101/gad.1677208.*

Leslie, R. J., Hird, R. B., Wilson, L., McIntosh, J. R., and Scholey, J. M. Kinesin is associated with a nonmicrotubule component of sea urchin mitotic spindles. Proceedings of the National Academy of Sciences*, 84(9):2771–2775, 1987. ISSN 0027-8424. doi: 10.1073/pnas.84.9.2771.*

Li, X. and Nicklas, R. B. Mitotic forces control a cell-cycle checkpoint. Nature*, 373 (6515):630–632, 1995. doi: 10.1038/373630a0.*

Li, X. and Nicklas, R. B. Tension-sensitive kinetochore phosphorylation and the chromosome distribution checkpoint in praying mantid spermatocytes. Journal of cell science*, 110(5):537–545, 1997. doi: 10.1242/jcs.110.5.537.*

Li, Y., Yu, W., Liang, Y., and Zhu, X. Kinetochore dynein generates a poleward pulling force to facilitate congression and full chromosome alignment. Cell research*, 17:701–12, 09 2007. doi: 10.1038/cr.2007.65.*

Lince-Faria, M., Maffini, S., and Orr, B. Spatiotemporal control of mitosis by the conserved spindle matrix protein Megator. Journal of Cell Biology*, 184(5):647–657, 2009. doi: 10.1083/jcb.200811012.*

Liu, D., Vader, G., Vromans, M. J. M., Lampson, M. A., and Lens, S. M. A. Sensing chromosome bi-orientation by spatial separation of Aurora B kinase from kinetochore substrates. Science*, 323(5919):1350–1353, 2009. doi: 10.1126/science.1167000.*

Liu, J., Lin, H., Lopez, J. M., and Wolfner, M. F. Formation of the male pronuclear lamina in Drosophila melanogaster. Developmental biology*, 184(2):187–196, 1997. doi: 10.1006/dbio.1997.8523.*

Liu, Y., Singh, S. R., Zeng, X. andD Zhao, J., and Hou, S. X. The nuclear matrix protein megator regulates stem cell asymmetric division through the mitotic checkpoint complex in Drosophila testes. PLOS Genetics*, 11(12):1–20, 12 2016. doi: 10.1371/journal.pgen.1005750.*

Lussi, Y. C., Shumaker, D. K., Shimi, T., and Fahrenkrog, B. The nucleoporin Nup153 affects spindle checkpoint activity due to an association with Mad1. Nucleus*, 1(1): 71–84, 2010. doi: 10.4161/nucl.1.1.10244.*

Ma, L., Tsai, M.-Y., Wang, S., Lu, B., Chen, R., Zhu, X., Zheng, Y., et al. Requirement for nudel and dynein for assembly of the lamin b spindle matrix. Nature cell biology*, 11(3):247–256, 2009. doi: 10.1038/ncb1832.*

Maiato, H., DeLuca, J., Salmon, E. D., and Earnshaw, W. C. The dynamic kinetochore-microtubule interface. Journal of Cell Science*, 117(23):5461–5477, 2004. doi: 10.1242/jcs.01536.*

Malmanche, N., Maia, A., and Sunkel, C. E. The spindle assembly checkpoint: Preventing chromosome mis-segregation during mitosis and meiosis. FEBS Letters*, 580 (12):2888–2895, 2006. ISSN 0014-5793. doi: 10.1016/j.febslet.2006.03.081. Istanbul Special Issue.*

Manning, A., Ganem, N., Bakhoum, S., Wagenbach, M., Wordeman, L., and Compton, D. The kinesin-13 proteins Kif2a, Kif2b, and Kif2c/MCAK have distinct roles during mitosis in human cells. Molecular biology of the cell, *18:2970–9, 09 2007. doi: 10.1091/mbc.E07-02-0110.*

Mapelli, M. and Musacchio, A. MAD contortions: conformational dimerization boosts spindle checkpoint signaling. Current Opinion in Structural Biology, *17(6):716–725, 2007. ISSN 0959-440X. doi: 10.1016/j.sbi.2007.08.011.*

March, D., Bianco, V., and Franzese, G. Protein unfolding and aggregation near a hydrophobic interface. Polymers, *13:156, 01 2021. doi: 10.3390/polym13010156.*

Mascarenhas, M., Flaxman, S., Ties, B., Vanderpoel, S., and Stevens, G. National, regional, and global trends in infertility prevalence since 1990: A systematic analysis of 277 health surveys. PLoS medicine, *9(12):e1001356, 2012. doi: 10.1371/journal.pmed.1001356.*

Matsumura, F. Regulation of myosin II during cytokinesis in higher eukaryotes. Trends in cell biology, *15(7):371–377, 2005. doi: 10.1016/j.tcb.2005.05.004.*

McCloskey, A., Ibarra, A., and Hetzer, M. W. Tpr regulates the total number of Nuclear Pore Complexes per cell nucleus. Genes & Development, *32(19-20):1321–1331, 2018. doi: 10.1101/gad.315523.118.*

McKee, B. D., Yan, R., and Tsai, J.-H. Meiosis in male Drosophila. Spermatogenesis, *2(3):167–184, 2012. doi: 10.4161/spmg.21800.*

Mellone, B. G., Grive, K. J., Shteyn, V., Bowers, S. R., Oderberg, I., and Karpen, G. H. Assembly of Drosophila centromeric chromatin proteins during mitosis. PLoS genetics, *7(5):e1002068, 2011. doi: 10.1371/journal.pgen.1002068.*

Mendjan, S., Taipale, M., Kind, J., Holz, H., Gebhardt, P., Schelder, M., Vermeulen, M., Buscaino, A., Duncan, K., Mueller, J., Wilm, M., Stunnenberg, H. G., Saumweber, H., and Akhtar, A. Nuclear Pore Components are involved in the transcriptional

regulation of dosage compensation in Drosophila. Molecular Cell, *21(6):811–823, 2006. ISSN 1097-2765. doi: 10.1016/j.molcel.2006.02.007.*

Merdes, A. and De Mey, J. The mechanism of kinetochore-spindle attachment and polewards movement analyzed in Ptk2 cells at the prophase-prometaphase transition. European journal of cell biology, *53(2):313–325, 1990.*

Mimori-Kiyosue, Y., Grigoriev, I., Lansbergen, G., Sasaki, H., Matsui, C., Severin, F., Galjart, N., Grosveld, F., Vorobjev, I., Tsukita, S., and Akhmanova, A. CLASP1 and CLASP2 bind to EB1 and regulate microtubule plus-end dynamics at the cell cortex. Journal of Cell Biology, *168(1):141–153, 01 2005. ISSN 0021-9525. doi: 10.1083/jcb.200405094.*

Mishra, R. K., Chakraborty, P., Arnaoutov, A., Fontoura, B. M., and Dasso, M. The Nup107-160 complex and gamma-TuRC regulate microtubule polymerization at kinetochores. Nat Cell Biol, *12(2):164–169, 2010. doi: 10.1038/ncb2016.*

Mitchell, P. J. and Cooper, C. S. The human Tpr gene encodes a protein of 2094 amino acids that has extensive coiled-coil regions and an acidic c-terminal domain. Oncogene, *7(11):2329—2333, November 1992. ISSN 0950-9232.*

Mitchison, T. J. Polewards microtubule flux in the mitotic spindle: evidence from photoactivation of fluorescence. The Journal of cell biology, *109(2):637–652, 1989. doi: 10.1083/jcb.109.2.637.*

Mitchison, T. J., Maddox, P., Gaetz, J., Groen, A., Shirasu, M., Desai, A., Salmon, E. D., and Kapoor, T. M. Roles of polymerization dynamics, opposed motors, and a tensile element in governing the length of xenopus extract meiotic spindles. Molecular biology of the cell, *16(6):3064–3076, 2005.*

Mohri, H., Inaba, K., Ishijima, S., and Baba, S. A. Tubulin-dynein system in flagellar and ciliary movement. Proceedings of the Japan Academy, Series B, *88(8):397–415, 2012. doi: 10.2183/pjab.88.397.*

Moir, R., Yoon, M., Khuon, S., and Goldman, R. Nuclear lamins A and B1: different pathways of assembly during nuclear envelope formation in living cells. The Journal of cell biology, *151:1155–68, 01 2001. doi: 10.1083/jcb.151.6.1155.*

Morgan, T. H. No crossing over in the male of Drosophila of genes in the second and third pairs of chromosomes. The Biological Bulletin, *26(4):195–204, 1914. doi: 10.2307/1536193.*

Morin, V., Prieto, S., Melines, S., Hem, S., Rossignol, M., Lorca, T., Espeut, J., Morin, N., and Abrieu, A. CDK-dependent potentiation of MPS1 kinase activity is essential to the mitotic checkpoint. Current Biology, *22(4):289–295, 2012. doi: 10.1016/j.cub.2011.12.048.*

Morrow, C. J., Tighe, A., Johnson, V. L., Scott, M. I. F., Ditchfield, C., and Taylor, S. S. Bub1 and Aurora B cooperate to maintain BubR1-mediated inhibition of APC/CCdc20. Journal of cell science, *118(16):3639–3652, 2005. doi: 10.1242/jcs.02487.*

Musacchio, A. and Desai, A. A molecular view of kinetochore assembly and function. Biology, *6(1):5, 2017. doi: 10.3390/biology6010005.*

Musacchio, A. and Hardwick, A. The spindle checkpoint: Structural insights into dynamic signalling. Nature reviews. Molecular cell biology, *3:731–41, 11 2002. doi: 10.1038/nrm929.*

Musacchio, A. and Salmon, E. D. The spindle-assembly checkpoint in space and time. Nature Reviews Molecular Cell Biology, *8:268–275, 2007. doi: 10.1038/nrm2163.*

Nagaoka, S., Hassold, T., and Hunt, P. Human aneuploidy: Mechanisms and new insights into an age-old problem. Nature reviews. Genetics, *13:493–504, 06 2012. doi: 10.1038/nrg3245.*

Nakano, H., Funasaka, T., Hashizume, C., and Wong, R. W. Nucleoporin translocated promoter region (Tpr) associates with dynein complex, preventing chromosome

lagging formation during mitosis. The Journal of Biological Chemistry, *285(14): 10841–10849, 2010. doi: 10.1074/jbc.M110.105890*.

Nasmyth, K. and Haering, C. H. Cohesin: its roles and mechanisms. Annual review of genetics, *43:525–558, 2009. doi: 10.1146/annurev-genet-102108-134233*.

Newport, J. A lamin-independent pathway for nuclear envelope assembly. The Journal of Cell Biology, *111:2247–2259, 12 1990. doi: 10.1083/jcb.111.6.2247*.

Niepel, M., Strambio-de Castillia, C., Fasolo, J., Chait, B. T., and Rout, M. P. The Nuclear Pore Complex–associated protein, Mlp2p, binds to the yeast spindle pole body and promotes its efficient assembly . Journal of Cell Biology, *170(2):225–235, 07 2005. ISSN 0021-9525. doi: 10.1083/jcb.200504140*.

Ombelet, W., Cooke, I., Dyer, S., Serour, G., and Devroey, P. Infertility and provision of infertility medical services in developing countries. Human reproduction update, *14(6):605–21, 10 2008. doi: 10.1093/humupd/dmn042*.

Paddison, P. J., Caudy, A. A., Bernstein, E., Hannon, G. J., and Conklin, D. S. Short hairpin RNAs (shRNAs) induce sequence-specific silencing in mammalian cells. Genes & development, *16:948–58, 05 2002. doi: 10.1101/gad.981002*.

Park, M., Dean, M., Cooper, C. S., Schmidt, M., O'Brien, S. J., Blair, D. G., and Vande Woude, G. F. Mechanism of met oncogene activation. Cell, *45(6):895–904, 1986. ISSN 0092-8674. doi: 10.1016/0092-8674(86)90564-7*.

Perrimon, N., Ni, J.-Q., and Perkins, L. In vivo RNAi: Today and tomorrow. Cold Spring Harbor perspectives in biology, *2:a003640, 08 2010. doi: 10.1101/cshperspect.a003640*.

Petronczki, M., Siomos, M. F., and Nasmyth, K. Un ménage à quatre: The molecular biology of chromosome segregation in meiosis. Cell, *112(4):423–440, 2003. ISSN 0092-8674. doi: 10.1016/S0092-8674(03)00083-7*.

Pfarr, C., Coue, M., Grissom, P. M., Hays, T., Porter, M., and McIntosh, R. Cytoplasmic dynein is localized to kinetochores during mitosis. Nature*, 345:263–5, 06 1990. doi: 10.1038/345263a0.*

Pickett-Heaps, J. and Forer, A. Mitosis: Spindle evolution and the matrix model. Protoplasma*, 235:91–9, 04 2009. doi: 10.1007/s00709-009-0030-2.*

Pickett-Heaps, J., Tippit, D., and Porter, K. Rethinking mitosis. Cell*, 29:729–44, 08 1982. doi: 10.1016/0092-8674(82)90435-4.*

Pickett-Heaps, J., Forer, A., and Spurck, T. Rethinking anaphase: Where "PAC-MAN" fails and why a role for the spindle matrix is likely. Protoplasma*, 192:1–10, 03 1996. doi: 10.1007/BF01273239.*

Pickett-Heaps, J. D., Tippit, D. H., and Leslie, R. Light and electron microscopic observations on cell division in two large pennate diatoms, hantzschia and nitzschia. i. mitosis in vivo. European journal of cell biology*, 21(1):1—11, April 1980. ISSN 0171-9335.*

Pickett-Heaps, J. D., Spurck, T., and Tippit, D. Chromosome motion and the spindle matrix. The Journal of cell biology*, 99(1 Pt 2):137s, 1984. doi: 10.1083/jcb.99.1.137s.*

Pickett-Heaps, J. D., Forer, A., and Spurck, T. Traction fibre: Toward a "tensegral" model of the spindle. Cell Motility*, 37(1):1–6, 1997. doi: 10.1002/(SICI)1097-0169(1997)37:1⟨1::AID-CM1⟩3.0.CO;2-D.*

Pisano, C., Bonaccorsi, S., and Gatti, M. The kl-3 loop of the Y chromosome of Drosophila Melanogaster binds a tektin-like protein. Genetics*, 133(3):569–579, 1993. ISSN 0016-6731. doi: 10.1093/genetics/133.3.569.*

Preston, C. C., Storm, E. C., Leonard, R. J., and Faustino, R. S. Emerging roles for nucleoporins in reproductive cellular physiology. Canadian Journal of Physiology and Pharmacology*, 97(4):257–264, 2019. doi: 10.1139/cjpp-2018-0436.*

Przewloka, M. R. and Glover, D. M. The kinetochore and the centromere: a working long distance relationship. Annual review of genetics, *43:439–465, 2009. doi: 10.1146/annurev-genet-102108-134310.*

Qi, H., Rath, U., Wang, D., Xu, Y.-Z., Ding, Y., Zhang, W., Blacketer, M. J., Paddy, M. R., Girton, J., Johansen, J., and Johansen, K. M. Megator, an essential coiled-coil protein that localizes to the putative spindle matrix during mitosis in Drosophila. Molecular Biology of the Cell, *15(11):4854–4865, 2004. doi: 10.1091/mbc.e04-07-0579.*

Qi, H., Rath, U., Ding, Y., Ji, Y., Blacketer, M. J., Girton, J., Johansen, J., and Johansen, K. M. EAST interacts with Megator and localizes to the putative spindle matrix during mitosis in Drosophila. Journal of Cellular Biochemistry, *95(6):1284–1291, 2005. ISSN 0730-2312. doi: 10.1002/jcb.20495.*

Qi, H., Yao, C., Cai, W., Girton, J., Johansen, K. M., and Johansen, J. Asator, a tau-tubulin kinase homolog in Drosophila localizes to the mitotic spindle. Developmental Dynamics, *238(12):3248–3256, 2009. doi: 10.1002/dvdy.22150.*

R Core Team. R: A Language and Environment for Statistical Computing. *R Foundation for Statistical Computing, Vienna, Austria, 2017. URL https://www.R-project.org/.*

Rajanala, K. and Nandicoori, V. K. Localization of nucleoporin Tpr to the nuclear pore complex is essential for Tpr mediated regulation of the export of unspliced RNA. PLOS ONE, *7:1–17, 01 2012. doi: 10.1371/journal.pone.0029921.*

Rajanala, K., Sarkar, A., Jhingan, G. D., Priyadarshini, R., Jalan, M., Sengupta, S., and Nandicoori, V. K. Phosphorylation of nucleoporin Tpr governs its differential localization and is required for its mitotic function. Journal of Cell Science, *127(16):3505–3520, 08 2014. ISSN 0021-9533. doi: 10.1242/jcs.149112.*

Rath, U., Wang, D., Ding, Y., Xu, Y.-Z., Qi, H., Blacketer, M. J., Girton, J.,

Johansen, J., and Johansen, K. M. Chromator, a novel and essential chromodomain protein interacts directly with the putative spindle matrix protein skeletor. Journal of Cellular Biochemistry, *93(5):1033–1047, 2004. ISSN 0730-2312. doi: 10.1002/jcb.20243.*

Rebollo, E. and González, C. Visualizing the spindle checkpoint in Drosophila spermatocytes. EMBO reports, *1(1):65–70, 2000. ISSN 1469-221X 1469-3178. doi: 10.1093/embo-reports/kvd011.*

Rieder, C. L. and Alexander, S. P. Kinetochores are transported poleward along a single astral microtubule during chromosome attachment to the spindle in newt lung cells. The Journal of cell biology, *110(1):81–95, 1990. doi: 10.1083/jcb.110.1.81.*

Rieder, C. L. and Khodjakov, A. Mitosis through the microscope: advances in seeing inside live dividing cells. Science, *300(5616):91–96, 2003. doi: 10.1126/science.1082177.*

Rieder, C. L. and Maiato, H. Stuck in division or passing through: what happens when cells cannot satisfy the spindle assembly checkpoint. Developmental cell, *7(5):637–651, 2004. doi: 10.1016/j.devcel.2004.09.002.*

Rieder, C. L. and Salmon, E. D. The vertebrate cell kinetochore and its roles during mitosis. Trends in cell biology, *8(8):310–318, 1998. doi: 10.1016/s0962-8924(98)01299-9.*

Rieder, C. L., Cole, R. W., Khodjakov, A., and Sluder, G. The checkpoint delaying anaphase in response to chromosome monoorientation is mediated by an inhibitory signal produced by unattached kinetochores. Journal of Cell Biology, *130(4):941–948, 08 1995. doi: 10.1083/jcb.130.4.941.*

Robinson, J. T., Wojcik, E. J., Sanders, M. A., McGrail, M., and Hays, T. S. Cytoplasmic dynein is required for the nuclear attachment and migration of centrosomes during mitosis in Drosophila. The Journal of cell biology, *146(3):597–608, 1999. doi: 10.1083/jcb.146.3.597.*

Rodriguez-Bravo, V., Maciejowski, J., Corona, J., Buch, H. K., Collin, P., Kanemaki, M. T., Shah, J. V., and Jallepalli, P. V. Nuclear pores protect genome integrity by assembling a premitotic and Mad1-dependent anaphase inhibitor. Cell, *156(5): 1017–1031, 2014. ISSN 0092-8674. doi: 10.1016/j.cell.2014.01.010.*

Rogers, G., Rogers, S., Schwimmer, T., Ems-McClung, S., Walczak, C., Scholey, J., and Sharp, D. Two mitotic kinesins cooperate to drive sister chromatid separation during anaphase. Nature, *427:364–70, 02 2004. doi: 10.1038/nature02256.*

Roser, M. Fertility rate. https://ourworldindata.org/fertility-rate, 2014. Our World in Data.

Sacristan, C. and Kops, G. J. P. L. Joined at the hip: kinetochores, microtubules, and spindle assembly checkpoint signaling. Trends in cell biology, *25(1):21–28, 2015. doi: 10.1016/j.tcb.2014.08.006.*

Salsi, V., Ferrari, S., Gorello, P., Fantini, S., Chiavolelli, F., Mecucci, C., and Zappavigna, V. Nup98 fusion oncoproteins promote aneuploidy by attenuating the mitotic spindle checkpoint. Cancer Research, *74(4):1079–1090, 2014. ISSN 0008-5472. doi: 10.1158/0008-5472.CAN-13-0912.*

Sauer, G., Körner, R., Hanisch, A., Ries, A., Nigg, E., and Silljé, H. Proteome analysis of the human spindle. Molecular & cellular proteomics : MCP, *4:35–43, 02 2005. doi: 10.1074/mcp.M400158-MCP200.*

Saurin, A., Waal, M., Medema, R., Lens, S., and Kops, G. Aurora B potentiates Mps1 activation to ensure rapid checkpoint establishment at the onset of mitosis. Nature communications, *2:316, 05 2011. doi: 10.1038/ncomms1319.*

Savoian, M. S. Using photobleaching to measure spindle microtubule dynamics in primary cultures of dividing Drosophila meiotic spermatocytes. Journal of biomolecular techniques : JBT, *26:66–73, 03 2015. doi: 10.7171/jbt.15-2602-004.*

Savoian, M. S., Goldberg, M. L., and Rieder, C. L. The rate of poleward chromosome motion is attenuated in Drosophila zw10 and rod mutants. Nature Cell Biology, *2 (12):948–952, 2000. ISSN 1476-4679. doi: 10.1038/35046605.*

Savoian, M. S., Gatt, M. K., Riparbelli, M. G., Callaini, G., and Glover, D. M. Drosophila Klp67A is required for proper chromosome congression and segregation during meiosis i. Journal of Cell Science, *117(16):3669–3677, 2004. doi: 10.1242/jcs.01213.*

Schneider, C. A., Rasband, W. S., and Eliceiri, K. W. NIH Image to ImageJ: 25 years of image analysis. Nature Methods, *9(7):671–675, 2012. ISSN 1548-7105. doi: 10.1038/nmeth.2089.*

Schweizer, N., Ferrás, C., Kern, D. M., Logarinho, E., Cheeseman, I. M., and Maiato, H. Spindle assembly checkpoint robustness requires Tpr-mediated regulation of Mad1/Mad2 proteostasis. Journal of Cell Biology, *203(6):883–893, 2013. ISSN 0021-9525. doi: 10.1083/jcb.201309076.*

Sharp, D. J., Yu, K. R., Sisson, J. C., Sullivan, W., and Scholey, J. M. Antagonistic microtubule-sliding motors position mitotic centrosomes in Drosophila early embryos. Nature cell biology, *1(1):51–54, 1999. doi: 10.1038/9025.*

Sharp, D. J., Brown, H. M., Kwon, M., Rogers, G. C., Holland, G., and Scholey, J. M. Functional coordination of three mitotic motors in Drosophila embryos. Molecular Biology of the Cell, *11(1):241–253, 2000. doi: 10.1091/mbc.11.1.241.*

Shi, C., Channels, W. E., Zheng, Y., and Iglesias, P. A. A computational model for the formation of lamin-b mitotic spindle envelope and matrix. Interface Focus, *4(3): 20130063, 2014. doi: 10.1098/rsfs.2013.0063.*

Shibata, S., Matsuoka, Y., and Yoneda, Y. Nucleocytoplasmic transport of proteins and poly(A)+ RNA in reconstituted Tpr-less nuclei in living mammalian cells. Genes to Cells, *7(4):421–434, 2002. doi: 10.1046/j.1365-2443.2002.00525.x.*

Shonn, M. A., Murray, A. L., and Murray, A. W. Spindle checkpoint component mad2 contributes to biorientation of homologous chromosomes. Curr Biol, *13(22): 1979–1984, 2003. doi: 10.1016/j.cub.2003.10.057.*

Sikirzhytski, V., Magidson, V., Steinman, J. B., He, J., Le Berre, M., Tikhonenko, I., Ault, J. G., McEwen, B. F., Chen, J. K., Sui, H., Piel, M., Kapoor, T. M., and Khodjakov, A. Direct kinetochore–spindle pole connections are not required for chromosome segregation. Journal of Cell Biology, *206(2):231–243, 07 2014. ISSN 0021-9525. doi: 10.1083/jcb.201401090.*

Sillers, P. J. and Forer, A. Action spectrum for changes in spindle fibre birefringence after ultraviolet microbeam irradiations of single chromosomal spindle fibres in crane-fly spermatocytes. Journal of Cell Science, *62(1):1–25, 07 1983. ISSN 0021-9533. doi: 10.1242/jcs.62.1.1.*

Singleton, M. R. Getting to the heart of an unusual kinetochore. Open Biology, *6(4): 160040, 2016.*

Skaggs, H., Xing, H., Wilkerson, D., Murphy, L., Hong, Y., Mayhew, C., and Sarge, K. HSF1-TPR interaction facilitates export of stress-induced HSP70 mRNA. The Journal of biological chemistry, *282:33902–7, 12 2007. doi: 10.1074/jbc.M704054200.*

Snow, C. J. and Paschal, B. M. Roles of the Nucleoporin Tpr in Cancer and Aging, *pages 309–322. Springer New York, New York, NY, 2014. ISBN 978-1-4899-8032-8. doi: 10.1007/978-1-4899-8032-8_14.*

Snow, C. J., Dar, A., Dutta, A., Kehlenbach, R. H., and Paschal, B. M. Defective nuclear import of Tpr in Progeria reflects the Ran sensitivity of large cargo transport. Journal of Cell Biology, *201(4):541–557, 05 2013. ISSN 0021-9525. doi: 10.1083/jcb.201212117.*

Soman, N. R., Correa, P., Ruiz, B. A., and Wogan, G. N. The TPR-MET oncogenic rearrangement is present and expressed in human gastric carcinoma and precursor

lesions. Proceedings of the National Academy of Sciences, *88(11):4892–4896, 1991. ISSN 0027-8424. doi: 10.1073/pnas.88.11.4892.*

Sorokin, A., Kim, E., and Ovchinnikov, L. Nucleocytoplasmic transport of proteins. Biochemistry (Moscow), *72:1439–1457, 01 2007. doi: 10.1134/s0006297907130032.*

Spurck, T., Forer, A., and Pickett-Heaps, J. Ultraviolet microbeam irradiations of epithelial and spermatocyte spindles suggest that forces act on the kinetochore fibre and are not generated by its disassembly. Cell Motility, *36(2):136–148, 1997. doi: 10.1002/(SICI)1097-0169(1997)36:2⟨136::AID-CM4⟩3.0.CO;2-7.*

StatsNz. New Zealand's birth rate lowest on record, deaths drop in 2020. https://www.stats.govt.nz/news/new-zealands-birth-rate-lowest-on-record-deaths-drop-in-2020, 2021.

Steuer, E. R., Wordeman, L., Schroer, T., and Sheetz, M. Localization of cytoplasmic dynein to mitotic spindles and kinetochores. Nature, *345:266–268, 06 1990. doi: 10.1038/345266a0.*

Strambio-de Castillia, C., Blobel, G., and Rout, M. P. Proteins connecting the Nuclear Pore Complex with the nuclear interior. The Journal of Cell Biology, *144(5):839–855, 1999. ISSN 0021-9525 1540-8140. doi: 10.1083/jcb.144.5.839.*

Sudakin, V., Chan, G. K. T., and Yen, T. J. Checkpoint inhibition of the APC/C in HeLa cells is mediated by a complex of BUBR1, BUB3, CDC20, and MAD2 . Journal of Cell Biology, *154(5):925–936, 09 2001. doi: 10.1083/jcb.200102093.*

Taddei, A., Houwe, G., Hediger, F., Kalck, V., Cubizolles, F., Schober, H., and Gasser, S. Nuclear pore association confers optimal expression levels for an inducible yeast gene. Nature, *441:774–8, 07 2006. doi: 10.1038/nature04845.*

Tanaka, K., Mukae, N., Dewar, H., Van Breugel, M., James, E. K., Prescott, A. R., Antony, C., and Tanaka, T. U. Molecular mechanisms of kinetochore capture by spindle microtubules. Nature, *434(7036):987–994, 2005. doi: 10.1038/nature03483.*

Tanaka, T. U., Rachidi, N., Janke, C., Pereira, G., Galova, M., Schiebel, E., Stark, M. J. R., and Nasmyth, K. Evidence that the ipl1-sli15 (Aurora kinase-INCENP) complex promotes chromosome bi-orientation by altering kinetochore-spindle pole connections. Cell, *108(3):317–329, 2002. doi: 10.1016/s0092-8674(02)00633-5.*

Tates, A. D. Cytodifferentiation during spermatogenesis in Drosophila Melanogaster : an electron microscope study. Ph.D. Thesis. Rijksuniversiteit, Leiden, *01 1971.*

Team, T. G. D. GIMP. https://www.gimp.org, 2021.

Thomas, S. E., Soltani-Bejnood, M., Roth, P., Dorn, R., Logsdon Jr, J. M., and McKee, B. D. Identification of two proteins required for conjunction and regular segregation of achiasmate homologs in Drosophila male meiosis. Cell, *123(4):555–568, 2005. doi: 10.1016/j.cell.2005.08.043.*

Thornton, B. and Toczyski, D. Securin and b-cyclin/cdk are the only essential targets of the apc. Nature cell biology, *5:1090–4, 01 2004. doi: 10.1038/ncb1066.*

Tokuyasu, K., Peacock, W., and Hardy, R. Dynamics of spermiogenesis in Drosophila melanogaster. II. Coiling process. Zeitschrift für Zellforschung und mikroskopische Anatomie, *127:492–525, 02 1972a. doi: 10.1007/BF00306868.*

Tokuyasu, K., Peacock, W., and Hardy, R. Dynamics of spermiogenesis in Drosophila melanogaster. I. Individualization process. Zeitschrift für Zellforschung und mikroskopische Anatomie, *124:479–506, 02 1972b. doi: 10.1007/BF00335253.*

Tokuyasu, K., Peacock, W., and Hardy, R. Dynamics of spermiogenesis in Drosophila melanogaster. IV. Nuclear transformation. Journal of ultrastructure research, *48: 284–303, 09 1974. doi: 10.1016/S0022-5320(74)80083-3.*

Tsai, M.-Y., Wang, S., Heidinger, J. M., Shumaker, D. K., Adam, S. A., Goldman, R. D., and Zheng, Y. A mitotic lamin B matrix induced by RanGTP required for spindle assembly. Science, *311(5769):1887, 2006. doi: 10.1126/science.1122771.*

Turner, K., Rambhatla, A., Schon, S., Agarwal, A., Krawetz, S., Dupree, J., and Avidor-Reiss, T. Male infertility is a women's health issue—research and clinical evaluation of male infertility is needed. Cells*, 9:990, 04 2020. doi: 10.3390/cells9040990.*

Vander Borght, M. and Wyns, C. Fertility and infertility: Definition and epidemiology. Clinical Biochemistry*, 62:2–10, 2018. ISSN 0009-9120. doi: 10.1016/j.clinbiochem.2018.03.012. The Role of Biomarkers in Reproductive Health.*

Vazquez, J., Belmont, A. S., and Sedat, J. W. The dynamics of homologous chromosome pairing during male Drosophila meiosis. Current Biology*, 12(17):1473–1483, 2002. doi: 10.1016/s0960-9822(02)01090-4.*

Vinciguerra, P., Iglesias, N., Camblong, J., Zenklusen, D., and Stutz, F. Perinuclear Mlp proteins downregulate gene expression in response to a defect in mRNA export. The EMBO Journal*, 24(4):813–823, 2005. doi: 10.1038/sj.emboj.7600527.*

Vleugel, M., Hoogendoorn, E., Snel, B., and Kops, G. J. P. L. Evolution and function of the mitotic checkpoint. Developmental Cell*, 23(2):239–250, 2012. ISSN 1534-5807. doi: 10.1016/j.devcel.2012.06.013.*

Vollset, S., Goren, E., Yuan, C.-W., Cao, J., Smith, A., Hsiao, T., Bisignano, C., Azhar, G., Castro, E., Chalek, J., Dolgert, A., Frank, T., Fukutaki, K., Hay, S., Lozano, R., Mokdad, A., Nandakumar, V., Pierce, M., Pletcher, M., and Murray, C. Fertility, mortality, migration, and population scenarios for 195 countries and territories from 2017 to 2100: a forecasting analysis for the global burden of disease study. The Lancet*, 396:1285–1306, 07 2020. doi: 10.1016/S0140-6736(20)30677-2.*

Vomastek, T., Iwanicki, M. P., Burack, W. R., Tiwari, D., Kumar, D., Parsons, J. T., Weber, M. J., and Nandicoori, V. K. Extracellular signal-regulated Kinase 2 (ERK2) phosphorylation sites and docking domain on the Nuclear Pore Complex protein Tpr cooperatively regulate ERK2-Tpr interaction. Molecular and Cellular Biology*, 28(22):6954–6966, 2008. doi: 10.1128/MCB.00925-08.*

Von Wettstein, D. The synaptinemal complex and four-strand crossing over. Proceedings of the National Academy of Sciences, *68(4):851–855, 1971. doi: 110.1073/pnas.68.4.851.*

Vorozhko, V., Emanuele, M., Kallio, M., Stukenberg, P., and Gorbsky, G. Multiple mechanisms of chromosome movement in vertebrate cells mediated through the Ndc80 complex and dynein/dynactin. Chromosoma, *117:169–79, 05 2008. doi: 10.1007/s00412-007-0135-3.*

Waizenegger, I. C., Hauf, S., Meinke, A., and Peters, J.-M. Two distinct pathways remove mammalian cohesin from chromosome arms in prophase and from centromeres in anaphase. Cell, *103(3):399–410, 2000. doi: 10.1016/s0092-8674(00)00132-x.*

Walczak, C. E., Gayek, S., and Ohi, R. Microtubule-depolymerizing kinesins. Annual Review of Cell and Developmental Biology, *29(1):417–441, 2013. doi: 10.1146/annurev-cellbio-101512-122345.*

Walker, D. L., Wang, D., Jin, Y., Rath, U., Wang, Y., Johansen, J., and Johansen, K. M. Skeletor, a novel chromosomal protein that redistributes during mitosis provides evidence for the formation of a spindle matrix. The Journal of Cell Biology, *151(7):1401–1412, 2000. ISSN 0021-9525. doi: 10.1083/jcb.151.7.1401.*

Wasser, M., Bte Osman, Z., and Chia, W. EAST and Chromator control the destruction and remodeling of muscles during Drosophila metamorphosis. Developmental Biology, *307(2):380–393, 2007. ISSN 0012-1606. doi: 10.1016/j.ydbio.2007.05.001.*

Wassmann, K. and Benezra, R. Mad2 transiently associates with an apc/p55cdc complex during mitosis. Proceedings of the National Academy of Sciences, *95(19):11193–11198, 1998. doi: 10.1073/pnas.95.19.11193.*

Watanabe, Y. Shugoshin: guardian spirit at the centromere. Current opinion in cell biology, *17(6):590–595, 2005. doi: 10.1016/j.ceb.2005.10.003.*

Watanabe, Y. and Nurse, P. Cohesin Rec8 is required for reductional chromosome segregation at meiosis. Nature, *400(6743):461–464, 1999. doi: 10.1038/22774.*

Webber, H. A., Howard, L., and Bickel, S. E. The cohesion protein ORD is required for homologue bias during meiotic recombination. The Journal of cell biology, *164 (6):819–829, 2004. doi: 10.1083/jcb.200310077.*

Webster, K., Henke, K., Ingalls, D., Nahrin, A., Harris, M., and Siegfried, K. Cyclin-dependent kinase 21 is a novel regulator of proliferation and meiosis in the male germ line of zebrafish. Reproduction, *157, 02 2019. doi: 10.1530/REP-18-0386.*

Wente, S. R. and Rout, M. P. The nuclear pore complex and nuclear transport. Cold Spring Harbor Perspectives in Biology, *2(10), 2010. doi: 10.1101/cshperspect.a000562.*

Whitehead, C. M., Winkfein, R. J., and Rattner, J. B. The relationship of HsEg5 and the actin cytoskeleton to centrosome separation. Cell motility and the cytoskeleton, *35(4):298–308, 1996. doi: 10.1002/(SICI)1097-0169(1996)35:4⟨298::AID-CM3⟩3.0.CO;2-3.*

Wilson, R. and Doudna, J. Molecular mechanisms of RNA interference. Annual review of Biophysics, *42:217–39, 05 2013. doi: 10.1146/annurev-biophys-083012-130404.*

Wolfner, M. and Collas, P. Nuclear Envelope Dynamics in *Drosophila* Pronuclear Formation and in Embryos, *pages 131–142. Landes Bioscience, 07 2011. ISBN 978-1-4613-4937-2. doi: 10.1007/978-1-4615-0129-9_10.*

World Bank Data. World Bank Group. https://data.worldbank.org/indicator/SP.DYN.TFRT.IN?most_recent_value_desc=true&year_high_desc=true, 2019.

Wozniak, R., Burke, B., and Doye, V. Nuclear transport and the mitotic apparatus: An evolving relationship. Cellular and molecular life sciences : CMLS, *67:2215–30, 04 2010. doi: 10.1007/s00018-010-0325-7.*

Xu, X. M., Rose, A., Muthuswamy, S., Jeong, S. Y., Venkatakrishnan, S., Zhao, Q., and Meier, I. Nuclear pore anchor, the Arabidopsis homolog of Tpr/Mlp1/Mlp2/Megator, is involved in mRNA export and SUMO homeostasis and affects diverse aspects of plant development. The Plant cell, *19(5):1537–1548, 2007. ISSN 1040-4651 1532-298X. doi: 10.1105/tpc.106.049239.*

Yamashita, Y. M., Jones, D. L., and Fuller, M. T. Orientation of asymmetric stem cell division by the APC tumor suppressor and centrosome. Science, *301(5639): 1547–1550, 2003. doi: 10.1126/science.1087795.*

Yan, R. and McKee, B. D. The cohesion protein SOLO associates with SMC1 and is required for synapsis, recombination, homolog bias and cohesion and pairing of centromeres in Drosophila meiosis. PLoS genetics, *9(7):e1003637, 2013. doi: 10.1371/journal.pgen.1003637.*

Yao, C., Rath, U., Maiato, H., Sharp, D., Girton, J., Johansen, K. M., and Johansen, J. A nuclear-derived proteinaceous matrix embeds the microtubule spindle apparatus during mitosis. Molecular Biology of the Cell, *23(18):3532–3541, 2012. doi: 10.1091/mbc.e12-06-0429.*

Yao, C., Wang, C., and Li, Y. Evidence for a role of spindle matrix formation in cell cycle progression by antibody perturbation. PLoS One, *13(11):1–23, 2018. doi: 10.1371/journal.pone.0208022.*

Zegers-Hochschild, F., Adamson, G., Dyer, S., Racowsky, C., de Mouzon, J., Sokol, R., Rienzi, L., Sunde, A., Schmidt, L., Cooke, I. D., Simpson, J. L., and van der Poel, S. The international glossary on infertility and fertility care. Fertility and Sterility, *108(3):393–406, 2017. doi: 10.1016/j.fertnstert.2017.06.005.*

Zhai, Y., Kronebusch, P. J., and Borisy, G. G. Kinetochore microtubule dynamics and the metaphase-anaphase transition. The Journal of cell biology, *131(3):721–734, 1995. doi: 10.1083/jcb.131.3.721.*

Zhang, R., Mehla, R., and Chauhan, A. Perturbation of host nuclear membrane component ranBP2 impairs the nuclear import of human immunodeficiency virus -1 preintegration complex (DNA). PLOS ONE, *5(12):1–13, 12 2010. doi: 10.1371/journal.pone.0015620 .*

Zhao, X., Wu, C.-Y., and Blobel, G. Mlp-dependent anchorage and stabilization of a desumoylating enzyme is required to prevent clonal lethality . Journal of Cell Biology, *167(4):605–611, 11 2004. ISSN 0021-9525. doi: 10.1083/jcb.200405168 .*

Zimowska, G., Aris, J. P., and Paddy, M. R. A Drosophila Tpr protein homolog is localized both in the extrachromosomal channel network and to Nuclear Pore Complexes. Journal of Cell Science, *110(8):927, 1997. doi: 10.1242/jcs.110.8.927 .*

Appendix

Fly strains (Shorthand names)	Genotype	Source
w(CS10)	$[CS10]$	Dura et al. (2007)
β-tubulinEGFP;bam-GAL4	$w[CS10]; P\{\beta Tubulin56D :: EGFP\}; P\{bam\text{-}GAL4 : VP16\}$	This study
Mtor-mcherry 1M	*y1 w*; P{Mtor.mCherry}2*	Johansen, J.
Mtor-mcherry 2M	*y1 w*; P{Mtor.mCherry}2*	Johansen, J.
MtorRNAi (UAS-Mtor)	*y[1] sc[*] v[1] sev[21]; P{y[+t7.7] v[+t1.8]=TRiP.HMS00735}attP2*	VDRC #32941

Table A.1: List of genotypes and sources of *Drosophila melanogaster* fly lines used in this study *w(CS10)* is a fly line generated by out-crossing the Canton-S strain with w1118. w1118 has a mutation in the white gene (w), present on the X chromosome. The *β-tubulinEGFP//;bam-GAL4//* fly line used in this study come from two pre-existing stocks, generated by crossing flies expressing *ßtubulin56D::EGFP* for the labelling of microtubules (Inoue et al., 2004) to flies expressing the driver *bam-GAL4* for the maintenance of *Drosophila*'s germline differentiation (Chen and Mckearin, 2003). The two Mtor (Megator) m-Cherry fly lines were kindly donated by Jorgen Johansen, University of Indiana. Those strains were originally described in (Yao et al., 2018) and the Mtor m-Cherry 2M has a chromosomal insertion in the chromosome 2, while the Mtor m-Cherry 1M in the chromosome 3. VDRC indicates Vienna Drosophila Resource Centre.

Area	Mean	StdDev	Mode	Min	Max	IntDen	Median	RawIntDen	Location	Experiment
7.62	49.7	9.3	49	26	81	378.3	49	75912	Spindle	Control
7.62	4.1	2.2	3	0	16	31.2	4	6252	Cytoplasm	Control
7.62	41.2	11.7	42	8	77	313.6	41	62915	Spindle	Control
7.62	5.1	3.4	4	0	35	38.8	4	7778	Cytoplasm	Control
7.62	23.7	4.8	20	11	41	180.3	23	36172	Spindle	Control
7.62	2.5	2.3	1	0	19	19.3	2	3874	Cytoplasm	Control
7.62	30.1	5.1	27	18	50	229.2	29	45983	Spindle	Control
7.62	2.4	1.1	2	0	7	18.4	2	3690	Cytoplasm	Control
7.62	27.6	5.1	24	12	46	210.4	27	42207	Spindle	Control
7.62	2.5	1.2	2	0	9	18.9	2	3791	Cytoplasm	Control
7.62	22.0	4.8	21	11	40	167.9	22	33689	Spindle	Control
7.62	2.4	1.0	2	0	8	18.4	2	3697	Cytoplasm	Control
7.62	30.8	6.4	29	14	52	234.8	30	47105	Spindle	Control
7.62	3.2	1.8	3	0	18	24.3	3	4884	Cytoplasm	Control
7.62	32.4	6.5	31	14	57	246.6	33	49477	Spindle	Control
7.62	5.6	3.2	3	1	17	42.8	5	8596	Cytoplasm	Control
7.62	31.8	6.2	28	14	55	242.1	31	48576	Spindle	Control
7.62	2.8	1.7	2	0	15	21.3	2	4273	Cytoplasm	Control

Area	Mean	StdDev	Mode	Min	Max	IntDen	Median	RawIntDen	Location	Experiment
7.62	26.0	7.0	22	9	47	197.9	25	39707	Spindle	Control
7.62	1.9	0.9	2	0	5	14.3	2	2860	Cytoplasm	Control
7.62	28.7	6.3	26	13	55	218.2	28	43789	Spindle	Control
7.62	2.4	1.0	2	0	7	18.2	2	3648	Cytoplasm	Control
7.62	36.9	7.4	31	18	65	281.2	36	56427	Spindle	Control
7.62	3.1	1.2	3	0	8	23.3	3	4684	Cytoplasm	Control
7.62	29.0	6.5	26	11	48	220.9	29	44322	Spindle	Control
7.62	2.4	1.1	2	0	8	18.6	2	3728	Cytoplasm	Control
7.62	15.3	3.1	14	8	27	116.3	15	23330	Spindle	Control
7.62	1.6	0.9	1	0	5	12.2	1	2454	Cytoplasm	Control
7.62	14.5	4.0	14	3	32	110.5	14	22172	Spindle	Control
7.62	2.2	1.3	2	0	11	17.1	2	3426	Cytoplasm	Control
7.62	16.1	4.1	15	7	32	122.6	16	24589	Spindle	Control
7.62	2.6	1.4	2	0	13	20.0	2	4010	Cytoplasm	Control
7.62	38.3	11.3	35	9	74	291.3	38	58447	Spindle	Control
7.62	3.6	2.1	3	1	22	27.3	3	5484	Cytoplasm	Control
7.62	64.1	11.2	62	34	101	488.5	64	98014	Spindle	Control
7.62	5.1	1.5	5	1	13	39.1	5	7850	Cytoplasm	Control

Area	Mean	StdDev	Mode	Min	Max	IntDen	Median	RawIntDen	Location	Experiment
7.62	73.7	11.5	75	43	120	561.1	74	112579	Spindle	Control
7.62	5.3	2.2	5	1	14	40.0	5	8031	Cytoplasm	Control
7.62	75.9	11.9	80	43	111	578.1	77	115993	Spindle	Control
7.62	4.6	1.5	4	1	13	34.7	4	6963	Cytoplasm	Control
7.62	67.8	9.3	69	44	99	516.1	67	103553	Spindle	Control
7.62	4.2	1.9	4	0	16	32.1	4	6432	Cytoplasm	Control
7.62	56.5	11.8	58	28	94	430.1	58	86306	Spindle	Control
7.62	4.7	1.5	4	1	11	35.5	5	7131	Cytoplasm	Control
7.62	48.3	7.8	48	28	77	367.5	48	73735	Spindle	Control
7.62	6.2	2.3	5	2	16	47.4	6	9519	Cytoplasm	Control
7.62	54.0	9.0	54	26	87	411.3	54	82531	Spindle	Control
7.62	4.3	1.5	4	0	15	32.9	4	6598	Cytoplasm	Control
7.62	49.3	9.6	52	17	80	375.2	50	75284	Spindle	Control
7.62	5.8	2.4	5	2	18	43.9	5	8803	Cytoplasm	Control
7.62	48.8	16.9	37	10	105	371.7	47	74582	Spindle	Control
7.62	4.0	1.5	4	1	14	30.6	4	6136	Cytoplasm	Control
7.62	53.0	10.0	59	16	79	403.5	54	80953	Spindle	Control
7.62	4.2	1.9	3	1	16	32.1	4	6442	Cytoplasm	Control

Area	Mean	StdDev	Mode	Min	Max	IntDen	Median	RawIntDen	Location	Experiment
7.62	51.6	14.0	56	20	88	392.7	52	78798	Spindle	Control
7.62	8.8	4.7	8	1	26	67.3	8	13508	Cytoplasm	Control
7.62	8.1	2.8	8	2	20	61.5	8	12346	Spindle	Megator depleted
7.62	3.6	1.2	3	1	9	27.6	4	5539	Cytoplasm	Megator depleted
7.62	6.7	2.1	6	2	15	51.3	7	10300	Spindle	Megator depleted
7.62	4.4	1.4	4	1	10	33.8	4	6776	Cytoplasm	Megator depleted
7.62	7.0	2.7	6	1	17	53.1	7	10663	Spindle	Megator depleted
7.62	2.1	1.1	2	0	8	16.0	2	3220	Cytoplasm	Megator depleted
7.62	6.2	2.5	5	1	17	47.2	6	9472	Spindle	Megator depleted
7.62	1.7	0.8	2	0	5	13.2	2	2658	Cytoplasm	Megator depleted
7.62	5.1	2.2	4	0	13	38.5	5	7717	Spindle	Megator depleted
7.62	1.4	0.8	1	0	5	10.7	1	2144	Cytoplasm	Megator depleted
7.62	4.7	2.0	4	1	14	36.1	4	7234	Spindle	Megator depleted
7.62	1.7	0.9	1	0	6	13.0	2	2610	Cytoplasm	Megator depleted
7.62	5.6	2.1	5	1	14	42.7	5	8568	Spindle	Megator depleted
7.62	1.7	0.9	1	0	6	12.6	2	2527	Cytoplasm	Megator depleted
7.62	4.9	2.1	5	0	13	37.6	5	7539	Spindle	Megator depleted
7.62	1.5	0.9	1	0	6	11.4	1	2291	Cytoplasm	Megator depleted

Area	Mean	StdDev	Mode	Min	Max	IntDen	Median	RawIntDen	Location	Experiment
7.62	5.2	2.9	4	0	17	39.3	5	7878	Spindle	Megator depleted
7.62	2.9	2.1	2	0	12	22.0	3	4418	Cytoplasm	Megator depleted
7.62	12.7	8.8	5	0	53	97.0	11	19459	Spindle	Megator depleted
7.62	3.6	2.4	2	0	15	27.7	3	5561	Cytoplasm	Megator depleted
7.62	5.7	5.8	2	0	51	43.4	4	8708	Spindle	Megator depleted
7.62	2.4	1.8	1	0	10	18.6	2	3722	Cytoplasm	Megator depleted
7.62	6.5	2.6	6	1	19	49.2	6	9878	Spindle	Megator depleted
7.62	1.7	0.9	2	0	5	12.9	2	2597	Cytoplasm	Megator depleted
7.62	7.2	2.4	6	2	16	54.5	7	10934	Spindle	Megator depleted
7.62	1.8	0.9	2	0	6	13.4	2	2694	Cytoplasm	Megator depleted
7.62	7.1	2.7	7	0	21	54.0	7	10826	Spindle	Megator depleted
7.62	2.2	1.1	2	0	8	16.8	2	3363	Cytoplasm	Megator depleted
7.62	7.1	3.6	6	1	26	53.7	6	10783	Spindle	Megator depleted
7.62	1.9	0.9	2	0	6	14.2	2	2841	Cytoplasm	Megator depleted
7.62	7.8	3.4	8	1	25	59.4	7	11912	Spindle	Megator depleted
7.62	2.0	1.1	2	0	7	15.0	2	3001	Cytoplasm	Megator depleted
7.62	7.4	2.8	7	2	20	56.7	7	11367	Spindle	Megator depleted
7.62	2.0	0.9	2	0	6	14.9	2	2991	Cytoplasm	Megator depleted

Area	Mean	StdDev	Mode	Min	Max	IntDen	Median	RawIntDen	Location	Experiment
7.62	8.4	2.8	7	2	19	63.9	8	12819	Spindle	Megator depleted
7.62	1.6	0.9	1	0	6	12.3	2	2465	Cytoplasm	Megator depleted
7.62	7.2	2.7	7	1	23	54.9	7	11018	Spindle	Megator depleted
7.62	1.7	1.0	1	0	7	13.2	2	2650	Cytoplasm	Megator depleted
7.62	9.6	3.6	9	2	29	73.2	9	14684	Spindle	Megator depleted
7.62	1.5	0.9	1	0	5	11.7	1	2347	Cytoplasm	Megator depleted
7.62	6.2	2.3	6	0	15	46.9	6	9411	Spindle	Megator depleted
7.62	1.4	0.8	1	0	5	10.7	1	2138	Cytoplasm	Megator depleted
7.62	6.4	2.6	6	1	16	48.9	6	9816	Spindle	Megator depleted
7.62	1.8	0.9	2	0	5	13.9	2	2798	Cytoplasm	Megator depleted
7.62	6.4	2.2	6	1	16	48.7	6	9766	Spindle	Megator depleted
7.62	1.8	0.9	2	0	5	13.5	2	2709	Cytoplasm	Megator depleted
7.62	5.3	2.1	5	1	15	40.2	5	8074	Spindle	Megator depleted
7.62	1.5	0.8	1	0	5	11.6	1	2332	Cytoplasm	Megator depleted

Table A.2: Total fluorescence counting in the spindle/cytoplasm regions of control and Megator depleted cells. Mean values of fluorescence intensity counting of circle area (region of interest or ROI) of $7.62\mu m^2$ positioned in the largest areas of the spindle (chromosomes and microtubules excluded) and cytoplasm of control (n=28) and Megator depleted cells (n=24) during prometaphase I.

Shortened genotype name	Slide	Nebenkern Nuclei Ratio								Total	result
		1:1	1:2	2:1	0:1	1:0	2:0	0:2	Other		
$+;\beta\text{-}tubulinEGFP//;bam\text{-}GAL4//;+$	1	90	0	0	0	0	0	0	0	90	0
$+;\beta\text{-}tubulinEGFP//;bam\text{-}GAL4//;+$	2	606	1	5	0	0	0	0	0	612	0.010
$+;\beta\text{-}tubulinEGFP//;bam\text{-}GAL4//;+$	3	497	1	0	0	3	0	0	0	501	0.008
$+;\frac{\beta\text{-}tubulinEGFP}{+};\frac{bam\text{-}GAL4}{UAS-Mtor};+$	1	130	1	2	2	12	3	0	4	154	0.156
$+;\frac{\beta\text{-}tubulinEGFP}{+};\frac{bam\text{-}GAL4}{UAS-Mtor};+$	2	122	0	6	0	83	4	7	9	231	0.472
$+;\frac{\beta\text{-}tubulinEGFP}{+};\frac{bam\text{-}GAL4}{UAS-Mtor};+$	3	134	2	4	6	124	5	1	9	285	0.530
$+;\frac{\beta\text{-}tubulinEGFP}{+};\frac{bam\text{-}GAL4}{UAS-Mtor};+$	4	220	0	4	0	12	7	0	0	243	0.095
$+;\frac{\beta\text{-}tubulinEGFP}{+};\frac{bam\text{-}GAL4}{UAS-Mtor};+$	5	70	0	4	2	10	6	0	3	95	0.263
$+;\frac{\beta\text{-}tubulinEGFP}{+};\frac{bam\text{-}GAL4}{UAS-Mtor};+$	6	73	1	1	4	9	3	0	2	93	0.215

Shortened genotype name	Slide	Nebenkern Nuclei Ratio									
		1:1	1:2	2:1	0:1	1:0	2:0	0:2	Other	Total	result
$+;\frac{\beta\text{-}tubulinEGFP}{+};\frac{bam\text{-}GAL4}{UAS-Mtor};+$	7	225	1	8	4	18	18	0	13	287	0.216
$w(CS10)//;+;+;+$	1	619	1	2	0	0	0	0	0	622	0.005
$w(CS10)//;+;+;+$	2	310	0	1	0	0	5	0	2	318	0.025
$w(CS10)//;+;+;+$	3	291	0	0	0	0	0	0	1	292	0.003
$w(CS10)//;+;+;+$	4	238	0	0	0	1	0	0	0	239	0.004
$+;+;UAS\text{-}Mtor//;+$	1	177	1	0	0	0	0	0	1	179	0.011
$+;+;UAS\text{-}Mtor//;+$	2	581	0	0	0	3	1	0	2	587	0.010
$+;+;UAS\text{-}Mtor//;+$	3	96	0	0	0	2	0	0	0	98	0.020
$+;+;UAS\text{-}Mtor//;+$	4	236	2	2	1	1	1	1	1	245	0.037

Shortened genotype name	Slide	Nebenkern Nuclei Ratio									
		1:1	1:2	2:1	0:1	1:0	2:0	0:2	Other	Total	result
$+;+;UAS\text{-}Mtor//;+$	1	224	3	0	2	2	2	0	0	233	0.039
$+;+;UAS\text{-}Mtor//;+$	2	199	2	1	0	1	2	2	1	208	0.043
$+;+;UAS\text{-}Mtor//;+$	3	236	2	1	2	1	2	0	1	245	0.037
$\frac{w(CS10)}{+};\frac{\beta\text{-}tubulinEGFP}{+};\frac{bam\text{-}GAL4}{+};+$	1	487	1	0	0	2	1	0	0	491	0.010
$\frac{w(CS10)}{+};\frac{\beta\text{-}tubulinEGFP}{+};\frac{bam\text{-}GAL4}{+};+$	2	359	0	0	1	0	0	2	3	362	0.010
$\frac{w(CS10)}{+};\frac{\beta\text{-}tubulinEGFP}{+};\frac{bam\text{-}GAL4}{+};+$	3	270	0	1	0	1	0	0	1	273	0.010

Table A.3: Total counting of nebenkern to nuclei ratio in the onion stage spermatids in the homozygous parental lines and progeny.